# Inter- cell Interference Coordination in 5G Ultra-Dense networks




BY

Oladele felix Afolalu

A thesis submitted for the degree of
***Doctor of Philosophy***
in the Department of Electrical Engineering,
Faculty of Engineering and the Built Environment, University of Cape Town
February 2020

Supervisor: Neco Ventura

As the candidate's supervisor, I have approved this dissertation for submission.

Supervisor: Neco Ventura

Sign: _____

Date: 15 February 2020

# Declaration

I hereby declare that: (1) the above thesis is my own unaided work, both in conception and execution, and that apart from the normal guidance of my supervisor, I have received no assistance apart from that stated below; (2) except as stated below, neither the substance nor any part of the thesis, has been submitted in the past, or is being, or is to be submitted for a degree in the University, or any other University.

I am now presenting the thesis for examination for the Degree of PhD in Electrical Engineering. I also grant the University free license to reproduce the above thesis in whole or in part, for the purpose of research.

Signed by candidate

| Oladele felix Afolalu | 15 February 2020 |
| --- | --- |
| Name | Date |

# Dedication

*Dedicated to Late Mrs Margaret Bolanle OLUFEMI.*

*(1956-2017)*

# Acknowledgements

I fall short of words to thank everyone who has, in one way or other, inspired, aided and contributed immensely to bringing my PhD to completion.

First and foremost, my utmost gratitude goes to Almighty God, the giver of wisdom, for bestowing on me the wisdom, courage and strength to navigate the rough, but interesting journey of research. May HIS name be continually praised.

I would also like to thank my amiable supervisor, more like a father, Neco Ventura, head, Centre for Broadband Networks and Applications, for his mentorship and for providing me the opportunity to carry out research into the exciting and exhilarating area of communications in his lab, Communication Research Group (CRG). I have indeed gathered a great amount of life and working experiences during my doctoral time in the lab. To say the least, I am profoundly grateful for his great supervision, constructive ideas and unreserved full support during this thesis process.

Special thanks to all reviewers and examiners for their expertise effort and timely response to my submitted papers throughout the PhD study.

I would like to thank all my CRG colleagues, past and present, Mary, Uwa, Bessie, Elisha, Uyoata, Joseph, Paul, Steven and Sunday, for their fruitful discussions, air of optimism and

constructive comments.

My appreciation goes to the Government of the Federal Republic of Nigeria through the Tertiary Education Trust Fund (TETFUND) for funding this PhD study.

I would also like to express my deepest gratitude towards my parents who solely took up the herculean responsibility of taking care of the kids in the first two years of my study. Your everlasting care, support, motivation and constant prayers are the ingredients that helped me to complete my study successfully.

In a special way, I extend my heartiest appreciation to my family, for their love, encouragement and support both financially and physically.

Last but not least, all thanks to my lovely children, Scholastica and Benedict, for enduring with the grannies in 'our' first two years of absence, and to Oliver, for coming in the final year of my study to weather the storm a bit. My thanks know no bounds to my dear wife, the rock and motivator per excellence, whose understanding and unalloyed love has made life easy for me since our paths crossed.

# Contents

# Abstract

The exponentially increasing demand for mobile broadband communications has led to the dense deployment of cellular networks with aggressive frequency reuse patterns. The future Fifth Generation (5G) networks are expected to overcome capacity and throughput challenges by adopting a multi-tier architecture where several low-power Base Stations (BSs) are deployed within the coverage area of the macro cell. Hence, Inter-Cell Interference (ICI) caused by the simultaneous usage of the same spectrum in different cells creates severe problems. ICI reduces system throughput and network capacity, and has a negative impact on cell-edge users and overall system performance. Therefore, effective interference coordination techniques are required, especially, for user-to-cell association and resource allocation to mitigate severe impact of ICI on system performance in 5G heterogeneous networks (HetNets). This is to improve Quality of Service (QoS) and maximize system throughput arising from the deployment of small cell overlay on macro BSs in heterogeneous cellular networks, which creates traffic load imbalance due to varying transmit power of different BSs in the downlink. In this research, a cell association scheme based on Cell Range Expansion (CRE), integrated with power control techniques is proposed. Simulation results are presented to show the ability of this technique to protect offloaded users from severe ICI and maximize throughput while achieving desirable QoS and load balancing for users of different tiers. With the advancement of information and computer technology, the envisioned 5G wireless communication is expected to encompass an unprecedented heterogeneous and ultra-dense communication environment. Vehicular communications play a vital role in 5G wireless network and have been widely studied recently due to its great

potential to ensure reliability and support intelligent transportation and various safety applications. This research therefore exploits the tractability of stochastic geometry to analyze the coverage of urban vehicular networks, by deriving a closed-form expression to maximize the ergodic capacity of cellular users (CUEs) and mitigate interference, taking into consideration the QoS requirements of both vehicle-to-vehicle (V2V) and vehicle-to-infrastructure (V2I) links. Consequently, the latency and reliability requirements of V2V/V2I links are formulated as optimization constraints, involving joint power allocation and spectrum sharing (PASS), taking into account the slow varying and large scale channel state information (CSI) measurements. Due to non-convex nature of the problem, the optimization is transformed into sub-optimal convex equivalence, while a low complexity Algorithm that yields optimal resource allocation is then designed to solve it. Simulation results are used to show enhanced performance in our approach compared to related works. Finally, the upsurge in the number of connected devices, such as smart cars, to the envisioned 5G technology is expected to pose high capacity and data rate demands on the network. The conventional access techniques (i.e., CDMA, TDMA and OFDMA) may not meet stringent requirements, such as ultra-low latency, high reliability, improved spectral efficiency and massive device connectivity. This work further investigates non-orthogonal multiple access (NOMA) technique as promising solution to improve spectral efficiency and reduce interference in 5G Ultra Dense Network (UDN). The NOMA scheme is combined with two promising capacity and bandwidth enhancement techniques - massive multiple input and multiple output (MIMO) and carrier aggregation (CA), for overall network performance. In particular, for the proposed novel NOMA-CA approach, we justify the importance of

maintaining green communication as a key requirement for 5G with Energy Efficiency (EE) analysis. Firstly, a proportional fairness scheduler is used to perform resource allocation and maintain fairness among users based on their channel condition. Secondly, an optimization problem to maximize the EE weighted-sum under joint power and bandwidth allocation on each aggregated component carrier (CC) is formulated. Conventionally, the formulated optimization is transformed from non-convex to convex problem. An iteratively adaptive Algorithm is then developed to find optimal solution for the problem. Simulation results show better improvement in EE and sum rate compared to the traditional OMA scheme.

# List of Abbreviations

| | |
|---|---|
| **3GPP** | Third Generation Partnership Project |
| **4G** | Fourth Generation |
| **5G** | Fifth Generation |
| **AMC** | Adaptive and Modulation Coding |
| **AWGN** | Additive White Gaussian Noise |
| **BE** | Best Effort |
| **BER** | Bit-Error-Rate |
| **BnB** | Branch and Bound |
| **BPSK** | Binary Phase Shift Keying |
| **BS** | Base Station |
| **C** | Constraint |
| **CA** | Carrier Aggregation |
| **CAC** | Call Admission Control |
| **CAGR** | Compound Annual Growth Rate |
| **CAPEX** | Capital Expenditure |
| **CC** | Component Carrier |
| **CCC** | Common Control Channel |
| **CFN** | Cognitive Femtocell Network |
| **CN** | Core Network |
| **CQI** | Channel Quality Indicator |
| **CR** | Cognitive radio |
| **CRRM** | Cognitive Radio Resource management |
| **CSG** | Closed Subscriber Group |
| **CSI** | Channel State Information |
| **DL** | Downlink |
| **D2D** | Device-to-Device |
| **DSA** | Dynamic Spectrum Access |
| **DSL** | Digital Subscriber Line |
| **E2E** | End-to-End |
| **EE** | Energy Efficiency |
| **EE-SET** | Energy Efficiency and Spectrum Efficiency Trade-off |
| **eNB** | evolve Node-B |
| **EPA** | Equal Power Allocation |
| **EPC** | Evolved Packet Core |

| | |
|---|---|
| **E-UTRAN** | Evolved Universal Terrestrial Radio Access network |
| **FAP** | Femto Access Point |
| **FAP-GW** | Femto Access Point Gateway |
| **FD** | Full Duplexing |
| **FDD** | Frequency Division Duplexing |
| **FGWNs** | Future Generation Wireless Networks |
| **FSMM** | Finite State Markov Model |
| **FTP** | File Transfer Protocol |
| **FUE** | Femtocell User Equipment |
| **GA** | Genetic Algorithm |
| **Gbps** | Giga bits per second |
| **GHz** | Giga Hertz |
| **HeNB** | Home evolve Node-B |
| **HetNet** | Heterogeneous Network |
| **HSDPA** | High-Speed Data Packet Access |
| **HWNs** | Heterogeneous Wireless Networks |
| **ICI** | Inter Cell Interference |
| **IEEE** | Institute of Electrical and Electronic Engineers |
| **IoT** | Internet of Things |
| **IP** | Internet Protocol |
| **IPsec** | Internet Protocol Security |
| **J** | Joule |
| **JRRA** | Joint Radio Resource Allocation |
| **LDD** | Lagrangian Dual Decomposition |
| **LTE** | Long Term Evolution |
| **LTE-A** | Long Term Evolution-Advanced |
| **M2M** | Machine-to-Machine |
| **MAC** | Medium Access Control |
| **MATLAB** | Matrix Laboratory |
| **Max** | Maximum |
| **MBS** | Macro Base Station |
| **MCS** | Modulation and Coding Scheme |
| **MHz** | Mega Hertz |
| **MIMO** | Multiple Input Multiple Output |
| **Min** | Minimum |
| **MINLP** | Mixed Integer Non-Linear Programming |
| **MILP** | Mixed Integer Linear Programming |
| **MME** | Mobility Management Entity |
| **mmWave** | Millimetre Wave |
| **NE** | Nash Equilibrium |
| **NOMA** | Non-Orthogonal Multiple Access |
| **NP** | Non-deterministic Polynomial time |
| **NRT** | Non-Real Time |
| **NSGA** | Non-dominated Sorting Genetic Algorithm |

| | |
|---|---|
| **OFDM** | Orthogonal Frequency Division Multiplexing |
| **OFDMA** | Orthogonal Frequency Division Multiple Access |
| **OMA** | Orthogonal Multiple Access |
| **OOB** | Out-of-Band |
| **OPEX** | Operating Expenditure |
| **PAPR** | Peak to Average Power Ratio |
| **PHY** | Physical |
| **PRB** | Physical Resource Block |
| **PU** | Primary User |
| **QAM** | Quadrature Amplitude Modulation |
| **QoE** | Quality of Experience |
| **QoS** | Quality of Service |
| **QPSK** | Quadrature Phase Shift Keying |
| **RAN** | Radio Access Network |
| **RATs** | Radio Access Technologies |
| **RB** | Radio Block |
| **RF** | Radio Frequency |
| **RLC** | Radio Link Control |
| **RNC** | Radio Network Controller |
| **RRA** | Radio Resource Allocation |
| **RRAO** | Radio Resource Allocation Optimization |
| **RRM** | Radio Resource Management |
| **RT** | Real Time |
| **SAE** | System Architecture Evolution |
| **SC-OFDMA** | Single Carrier Orthogonal Frequency Multiple Access |
| **SE** | Spectrum Efficiency |
| **Se GW** | Security Gateway |
| **S-GW** | Serving Gate Way |
| **SINR** | Signal-to-Interference-plus-Noise Ratio |
| **SNR** | Signal-to-Noise Ratio |
| **SOHO** | Small Office/Home Office |
| **SON** | Self Organized Network |
| **SORRM** | Self-Organizing Radio Resource Management |
| **SQP** | Sequential Quadratic Programming |
| **SU** | Secondary User |
| **TDD** | Time Division Duplexing |
| **TTI** | Transmission Time Interval |
| **UE** | User Equipment |
| **UL** | Uplink |
| **UMTS** | Universal Mobile Telecommunications System |
| **VoIP** | Voice over Internet Protocol |
| **WiFi** | Wireless Fidelity |
| **WiMAX** | Worldwide Interoperability for Microwave Access |
| **WLANs** | Wireless Local Area Networks |
| **WMAN** | Wireless Metropolitan Area Networks |

# List of Tables

# List of Figures

# List of Publications

The research described in this thesis has generated ideas that have resulted in the following research outputs:

**Conference Publications:**

1. O. Afolalu and N. Ventura, *Dynamic Cell Selection Technique for Interference Coordination in 5G Heterogeneous Networks*, pp. 26-31, SATNAC, 2017.

2. O. Afolalu and N. Ventura, *Robust Power Allocation for Capacity Maximization in 5G Ultra-Dense Vehicular Communication Networks*, pp. 2-7, SATNAC, 2018.

3. O. Afolalu and N. Ventura, *Joint Implementation of Massive MIMO and NOMA Techniques for Improved Capacity in 5G Networks*, pp. 26-31, SATNAC, 2019. **(Best Paper Award)**.

**Journal Papers:**

1. O. Afolalu and N. Ventura, *A Novel Approach on NOMA Scheme Integrated with Carrier Aggregation for Improved Network Performance in 5G Systems*, International Journal of Communication Systems, 2020; e4701. https://doi.org/10.1002/dac.4701

# Chapter 1

# Introduction

## 1.1 Research Background

In recent years, the exponential growth of mobile users and an ever increasing demand for data has imposed a lot of challenges on the current mobile and wireless communication networks, particularly the future Heterogeneous networks (HetNets)/Ultra dense Network (UDN) [1]. Wireless communication networks are perhaps the most critical element in the global ICT world, known to be the most dynamic and fastest growing sectors. The next generation wireless network will become heterogeneous, possessing smart devices that can handle various mix of technologies such as cooperative, green and massive MIMO communications, to support high energy efficiency and spectral efficiency. This paradigm shift will enable the envisioned fifth generation network (5G) to support a plethora of devices expected to meet the expected increase in data volumes, coupled with broadening range of application domains [2]. Expectedly, 5G will build upon the evolution of existing

technologies, in addition to new framework designed to meet the new and challenging needs. In the same vein, important applications such as e-health, e-learning and e-banking will continue to increase rapidly and become popular. As research into 5G technologies gradually emerges, increased growth in internet traffic is anticipated due to large number of heterogeneous and smart devices that are expected to simultaneously access the technology. Therefore, 5G is required to meet a significantly higher rate requirements than the existing 4G technology in order to meet the aforementioned functionalities.

According to the latest Cisco Visual Networking Index (VNI) report, annual global IP traffiic will reach 3.3 ZB per year (278 EB per month) by 2021, compared to 1.2 ZB growth per year in 2016 (96 EB per month) [3]. In addition, Cisco predicted a shortfall of 21% in PCs' total IP traffic composition from 2016 to 2021, as compared to 20% increase in IP trafic composition for smartphones within the same duration. In the same manner, a 10% Compound Annual Growth Rate (CAGR) is expected from all traffics originating from PCs, while smart phones, tablets, TVs and Machine-to-Machine (M2M) enabled devices will account for traffic growth rate of 49%, 29%, 21% and 49%, respectively. Furthermore, the report estimated that wired devices accounted for 51% bulk of IP traffic in 2016, contrary to 37% and 63% expected to be separately accounted for by wired and both Wi-Fi and mobile devices in 2021.

Similarly, Ericsson Mobility Report attributed increase in average data volume per subscription and rise in the number of smartphone subscriptions as factors responsible for the growth in mobile data volume [4]. The paper reported an addition of 53 million new mobile subscriptions during the last quarter of 2017, which resulted in 7.8 billion total number

of mobile subscriptions. In the review period, there was a reported 150 million decline in subscriptions resulting from the use of GSM/EDGE technologies, while WCDMA/HSPA and LTE subscriptions grew by approximately 30 and 180 million, respectively, with the latter reaching a total of 2.7 billion.

The International Mobile Telecommunications-Advanced (IMT-A) designed 4G LTE/LTE-A wireless systems to utilize IP for all operations. Some of the requirements of 4G systems are the use of advanced radio interface in conjunction with technologies like link adaptation, multiple-input multiple-output (MIMO) and orthogonal frequency division multiplexing (OFDM) [5]. However, 5G networks (Figure 1.1), whose use cases have started to be

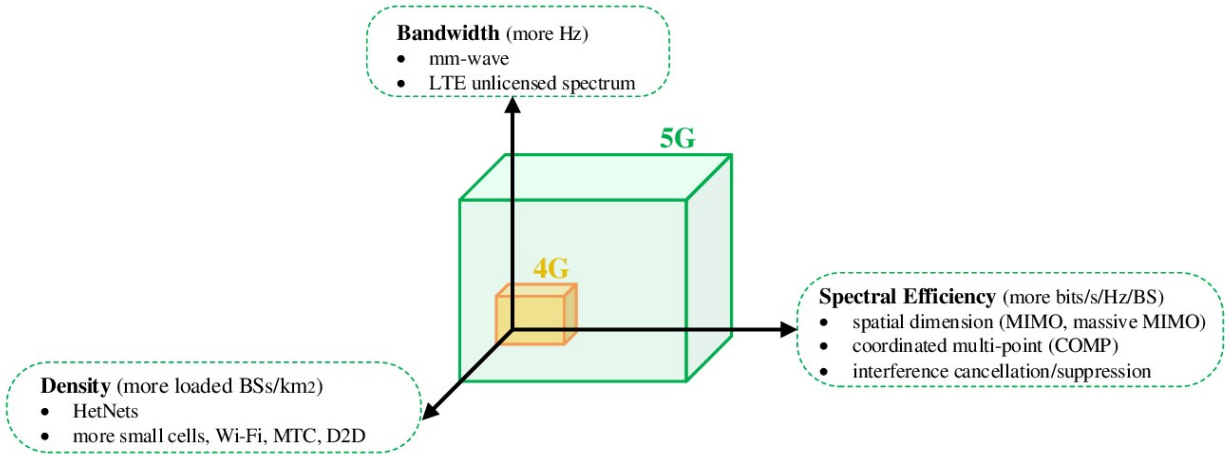


**Figure 1.1:** Key drivers for Wireless evolution

implemented by the fifth Generation Public Private Partnership 5GPPP, is expected to be standardized around 2020 and aims to achieve 10 Gb/s peak data rate for low mobility and 1 Gb/s for high mobility users. In addition, 5G will, among other things, attain 10 times spectral and energy efficiency, 1/1000 times end-to-end latency, e.g., Vehicle to Vehicle communication, 25 times the average cell throughput and 1000 times the system capacity

[6–9]. Others are support for emerging IoT and green communication through large number of connected devices and almost 90% reduction in energy usage, respectively, longer battery life due to reduction in power consumption, and approximately 100% connectivity coverage.

In addition, the 5GPPP identified the under-listed key use cases to be synthesized with the aforementioned supported requirements [9]:

- Urban dense: this entails usage in both indoor and outdoor environments, taking into account smart homes, hotspots and cloud services.
- Connected vehicles: grouped under this use case are vehicular communication with particular attention to road safety for V2V and V2I, vehicle mobility for Dynamic Mobility Applications (DMAs) and environmental impact for Road Weather Applications (RWAs).
- Ubiquitous Broadband: service provision in rural, suburban and high speed trains with data rate higher than 50Mbps.
- Limited Bandwidth Internet of Things (IoT): this group encompasses interconnection of large objects like sensors and smart cities.
- Future smart offices: this group involves indoor communications like smart offices or virtual reality which require low latency and high capacity.
- Tactile internet: this is a group that attaches high importance to reliability as in the case of e-health and V2V communications.

One key feature of 5G is the capability to achieve seamless and ubiquitous communication and ensure continuity of user experience in challenging circumstances through whatever networks, services or devices they desire, regardless of user's location (e.g., village, city center, airplane or high speed train) [10]. With the significant role played by network performance on emerging mobile networks, a user will have the opportunity to make a transparent choice from the best performing 5G technologies like new radio interfaces, 4G and WiFi. The nature of a particular choice will depend on relevant performance metrics so much that latency, for example, may be of more importance than throughput for services like V2V communications, an online game or e-health. Therefore, to realize the goal of 5G for improved energy consumption, ultra-reliability, extended coverage, low latency and high capacity, the 5G architecture is anticipated to embrace sorphisticated services such as backhaul and fronthaul schemes, converged network access infrastructure and intelligent intra-system utilization [11].

Consequently, increased capacity for the next generation wireless networks will be achieved through a multi-tier network architecture, which involves deployment of massive number of low power nodes such as femtocells, picocells, D2D links and relays in the coverage of macrocells [12], [13]. In addition, coverage and capacity will be enhanced by integrating different air interfaces, coupled with coexistence of low and high band frequencies [14]. In the latter case, low band macro and small cell base stations on frequencies below 6 GHz will coexist with 4G LTE/LTE-A and legacy 2G/3G technologies [15], while small cells on high band frequencies above 6 GHz will be co-located with WIFI and earlier versions of 3GPP technologies. Moreover, 5G architecture will integrate small cells with UDN, as part of

requirement for some specialized access network models involving non-operator deployment and maintenance.

However, the major challenge to base station densification is interference. Specifically, so many factors are responsible for the interference dynamics in multi-tier network. Some of the factors are: (1) heterogeneous and ultra dense deployment of wireless devices, (2) restricted access mode of some tiers, e.g., femtocell, deployed in closed subscriber group (CSG) mode, (3) downlink and uplink asymmetry due to varying transmission power of base stations, and (4) access priorities of allocated resources and different channels with different frequencies. Furthermore, the introduction of coordinated multi-point transmission(CoMP), carrier aggregation and Device-to-Device communication in release 13, may worsen the interference dynamics.

There are so many approaches that can be used to mitigate interference in multi-tier cellular networks based on the identified factors above. One of such is to design an optimized cell association and power control (OCAPC) techniques for users in the uplink and BSs in the downlink, that can reduce power consumption, mitigitate interference and maximize throughput. Another efficient method is to design intelligent algorithms capable of synchronizing connection to multiple base stations for uplink and downlink association to reduce outage ratio and improve the entire network throughput. Lastly, 5G UDN will also benefit from coordination and cooperation among multiple tiers as a major requirement for interference mitigation, and spectral and energy efficiency maximization. However, proper tuning of the user location and channel conditions, coupled with the use of low latency backhaul are very important for integrating small cells into the network.

Thus, future 5G UDN promises to provide improvement in the spectrum efficiency and entire network capacity through BS densification (i.e., dense deployment of small cells, e.g., pico and femto cells) and heterogenous nodes such as M2M sensors, Device to Device (D2D), RRH and low power access points [16]. However, this comes with the great challenge of strong interference as a result of complicated and assymetric nature of the network topology which renders existing management techniques insufficient. Therefore, this thesis aims to develop a novel distributed interference coordination schemes that solves technical challenges in 5G UDN architecture. The choice of decentralized approach is the offered benefit of low computational complexity for the envisioned 5G UDN archictecture, where resource allocation is performed independently or, at the least, with minimal assistance of macro BS, serving as the central controller.

## 1.2 Research Motivation

Beside the advantages of increased coverage, spectral efficiency and traffic offloading offered by ultra dense deployment of small cells, there is also the challenge of severe interference due to the integration of macrocell with other low power nodes as depicted in Figure 1.2. In addition to this, integration of small cell also introduces challenge of cell selection. This leads to maximum utilization problem where the number of satisfied users are drastically reduced, thereby impacting on the overall network performance. Hence, network operators need to devise a new technique to prevent under-utilization of small cell underlaid in a macrocellular network. Major factors such as access control problem, self organizing nature of small cells, especially femtocells, and the short range of small cells coverage area contribute to the

severity of interference and cell selection process in 5G UDN. Self-organizing functionality in 5G can generally be categorized into self-healing, self-configuration and self-optimization [17]. These will be discussed in detail in the next chapter.

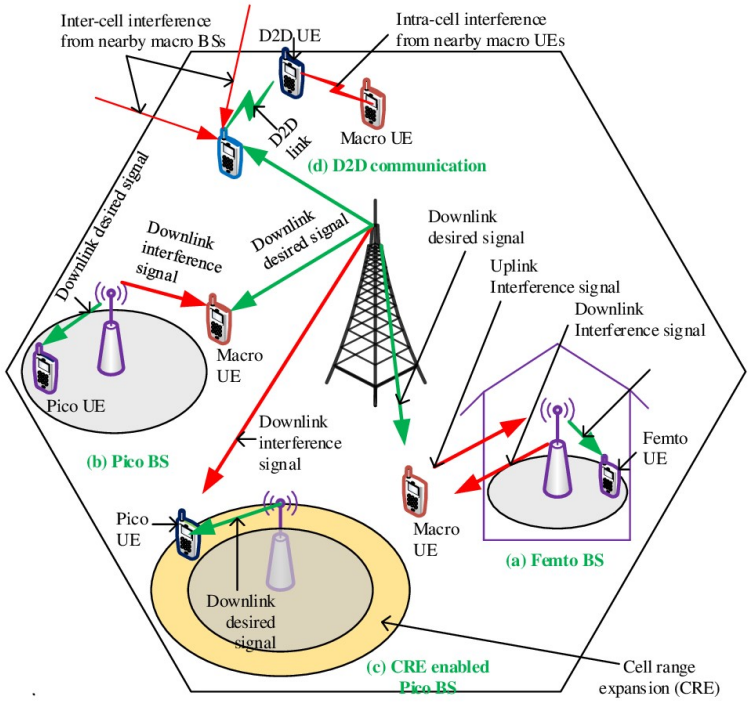


**Figure 1.2:** Interference scenario in HetNets

Massive deployment of small cells in the coverage of macrocell creates a boundary overlap in the network, which ultimately decreases the downlink Received Signal Strength (RSS). Also, utilization of access control severely impacts the signal strength of macrocell, especially in the case of femtocell deployed in closed subscriber group mode (CSG), which grants access to some user while restricting others. Although, allocation of orthogonal frequencies to small cells is a promising way to address the problem of interference in 5G UDN, however, this approach comes at the expense of degraded system capacity and high overhead on the limited system bandwidth [12]. As stated earlier, cells can adopt frequency reuse method

as a means of coordination, where the same frequency can be reused among different cells for proper cooperation. Hence, cooperation techniques among small cell will definitely play an important role in interference coordination and to achieve high network capacity in 5G UDN.

Interference problem in LTE can be addressed in three major ways, namely: user-centric, network-centric and combination of both [18]. In user-centric approach, UE receivers are equipped with advanced interference mitigation functionality capable of exploiting interference suppression schemes such as interference rejection combining (IRC). However, this technique has operational limitation when considering the number of antennas that can be used by a UE for different interference suppression purposes. On the other hand, interference mitigation on the network side which involves ICIC and CoMP is more robust due to the capability of resource partition in the power, time, space and frequency domains. In 3GPP releases 10 to 12, one or combination of these is referred to as intercell interference coordination (ICIC) and enhanced ICIC (eICIC) techniques (time domain) [19]. Interference mitigation is performed in the frequency domain through orthogonal frequency channels either by dynamic or static allocation of resources. At the same time, LTE release 10 standardized Almost Blank Sub-Frame (ABSF) as the interference coordination technique in the time domain, while improvement in MIMO technology are exploited for use in the spatial domain [20].

However, in 5G UDN, the network-centric approach can be extended for better network performance. Towards this end, two methods that involve a proactive time domain ICIC and reactive carrier domain ICIC are proposed. To succinctly differentiate the areas of

application and adaptability of the two techniques to changing network conditions such as traffic and density, the time domain algorithms are proposed for outdoor deployment while the carrier domain algorithms are employed for indoor small cells. Consequently, due to the challenging interference coordination and the signaling overhead involved in ultra dense deployment of small cells, distributed algorithms are used to mitigate interference in 5G UDN.

Motivated by the above, this thesis addresses interference problem as a way to guarantee low latency and energy efficiency, provide higher throughput and improve end-to-end performance in the envisioned 5G UDNs. The motivation behind this thesis is to propose robust and intelligent power control algorithms, capable of mitigating interference in the envisioned 5G UDNs.

## 1.3 Problem Statement

Interference is one of the multiple significant obstacles that Ultra Dense Networks (UDN), which is expected to be the best ways to meet user experience and support future wireless network deployment will face. This thesis deals with designing low-cost robust algorithms with less complexity, to mitigate interference for enhanced system performance in 5G UDN. Specifically, the research addresses interference and capacity problems from the point of cell association for offloading purpose, power and spectrum allocation, as well as multiple access power sharing framework, to support heavy traffic and massive connectivity.

One major challenge faced by 5G UDN is the integration of the existing ICIC techniques with new ones, in order to achieve the expected higher performance requirements. More

importantly, the peculiar nature of UDN demands not only a scalable and distributed ICIC schemes, but also a solution that provides seamless coordination between the large numbers of involved nodes for optimum performance. Some of the requirements are enhanced spectrum utilization, peak transmission rate and better energy efficiency. Hence, to achieve these goals, combination of 5G UDN and variety of other techniques such as multiple input multiple output (MIMO), cooperative multipoint (CoMP) and carrier aggregation (CA), will be of great benefit.

Different schemes based on resource and power allocation techniques were first designed for macrocell-only network where cell edge users are mostly affected by severe interference from neighbouring cells. One of such is the Fractional Frequency Reuse (FRR) scheme which involves partitioning of resources in time and frequency domains. This scheme achieves interference reduction by dynamically applying frequency reuse factor higher than one to cell center users, and factor of one to cell edge users. However, this orthogonalization is done at the expense of improved throughput due to reduction in the total available bandwidth at the centre and edge of the cells. In addition, utilization of advance antennas with frequency domain signal orthogonalization, time domain coordinated scheduling and spatial cell coordination has proven to efficiently mitigate inter-cell interference when adequately coordinated.

Also, most ICIC mitigation schemes mentioned above are based on static pattern which renders them unsuitable for dynamic load conditions such as UDN. Besides, it is observed that static designs lead to variation of the scheduled sub-band fraction with the network configuration, which degrade the network capacity. Therefore, more sophisticated techniques

are required to solve the challenging problem of interference management, mobility and cost in densified networks. Indeed, deployment of various types of small cells in high density provides users with high connection rate. Hence, the use of traditional inter-cell coordination schemes for interference mitigation results in high signaling overhead, which makes distributed control a preferred choice for interference mitigation in 5G UDN.

Moreover, advancement in backhaul technology has given rise to large amount of information to be exchanged promptly among BSs. Consequently, introduction of advanced interference mitigation schemes such as cooperative MIMO transmission becomes possible due to tighter and faster coordination among cells and UEs, using adequate channel state information (CSI) feedback from UEs to the intended receiver [21]. Also, the joint combination of cell association and power control (CAPC) scheme for multi-tier interference mitigation can be extended to the resource aware CAPC, thereby satisfying multi-objective role of energy efficiency, better network throughput and load balancing.

Another aspect that will impact the interference dynamics and overall system performance of 5G UDN is spectrum allocation. Spectrum sharing arises as a result of considerable scarcity, coupled with inefficient use of the available spectrum. The spectrum sharing methods currently being used in traditional wireless systems is capable of providing efficient spectrum utilization. Nevertheless, there are new spectrum sharing challenges imposed by the emergence of 5G UDN on interference characteristics, due to increased traffic demand and building layouts, especially as applied to vehicular communication. Furthermore, integration of multiple advanced techniques such as mmWave, D2D, relays, massive MIMO and CA can potentially improve the network capacity of 5G UDN about 10-100 fold [22].

However, improper coordination attempt among these advanced techniques introduces more complexity to the consideration given to interference mitigation, cost and resource efficiency. Thus, the ever-increasing data-driven demand in 5G calls for the design of new waveform that satisfies both throughput and capacity demands. One of the techniques proposed to achieve this objective is the non-orthogonal multiple access (NOMA), which uses the principle of signal superposition for multiplexing in power domain. The success of NOMA scheme in terms of throughput relies on the accuracy of power allocation directly to each user [23]. Hence, in an attempt to find an optimal resource allocation scheme, the solution space may become excessively complex.

Therefore, the goal of this thesis is to design advanced interference mitigation techniques for 5G UDN, compatible with legacy technologies, based on the challenges identified above. The challenges mentioned constitute the main drivers for the contributions of this research, including the developed algorithms, simulations and performance gains presented in the following chapters.

## 1.4 Thesis Aim and Objectives

The aim of this research is to investigate various interference mitigation methods capable of providing solution to interference encountered in UDN. The aims of the research are therefore addressed through the following objectives:

1. Our first objective is to carry out a detailed survey on legacy techniques, the existing state-of-the-art research on user association/cell selection and traffic load balance

towards interference coordination, emerging enabling technologies and proposed solutions. Several technologies that can be harnessed to develop an enhanced and efficient ICIC algorithms capable of providing scalable and distributed functionalities, seamless coordination among nodes and reduced power consumption are identified.

2. The second objective is to design a cell/user association with a focus on eICIC techniques for traffic load balance. This is achieved by proposing a dynamic range expansion technique using pathloss measurement reports from macro BS and various SINR-based bias values to increase coverage and capacity. The proposed method is formulated as a mixed integer programming problem (MIP), attempting to determine users' association based on minimizing resource block allocation. The aim is to identify degree of coordination among cells towards an improved system capacity in UDN.

3. The third objective is to develop a model to evaluate and address the interference problem in vehicular communications. The proposed formulation utilizes a deterministic signal propagation model to characterize transition of vehicle's status from the transmitter from line of sight (LOS) to non-line of sight (NLOS) in high mobility vehicular environment. Various expressions are derived to maximize the ergodic capacity and outage probability of the CUE/VUE links. The expressions are transformed into Power Allocation and Spectrum Sharing (PASS) optimization, while an intelligent algorithm is developed to reduce the computational complexity of the formulated optimization and arrive at optimal solution. The aim is to maximize the ergodic capacity of cellular users (CUEs) by taking into consideration the

Quality of Service (QoS) requirements of both vehicle-to-vehicle (V2V) and vehicle-to-infrastructure (V2I) links.

4. The fourth objective investigates non-orthogonal multiple access (NOMA) technique, integrated with state-of-the-art massive multiple input multiple output (MIMO) and carrier aggregation (CA) technologies, as promising solution to improve spectral efficiency, enhance capacity and reduce interference in 5G UDN. The proposed NOMA-MIMO solution, simulated under perfect and imperfect channel state information (CSI) employs transmit antenna selection technique to reduce complexity involved in simultaneous use of multiple antennas. Also, low complexity zero forcing (ZF) beamforming is applied to remove the ICI introduced through superposition coding in NOMA. In the proposed CA-NOMA solution, we formulate the problem as joint bandwidth and power allocation optimization, with weighted-sum assignment for energy efficiency (EE) analysis. The non-convex optimization problem is transformed into convex equivalence to reduce complexity, while a low complex iterative algorithm is developed to achieve optimal solution.

## 1.5 Research Design and Methodology

The first part of this thesis attempts to find answers to questions about cell selection and user association techniques capable of reducing interference in UDN. A comprehensive overview of approaches used in the last decades to enhance performance in this area is first carried out to determine basic compatibility requirements for the potential interference mitigation

techniques for the envisioned 5G UDN. Based on this, current and emerging technologies, with their key limitations, that can be used to leverage these techniques are identified and noted. This is meant to provide answers to several questions such as cooperation among BSs, coverage issues and effect of different pathloss models on the gains actualized from user association techniques.

Interference in future generation networks as in the case of UDN with stringent demands transcends the use of only one method to mitigate. At the same time, utilizing effective techniques devoid of unnecessary signaling overheads are also important. Power control is one of the most important techniques that can be used to mitigate interference and improve energy efficiency. In this thesis, advanced mathematical tool with intelligent algorithms that can adapt to traffic demands, limit signaling exchange and balance transmit power among users in each investigated scenarios are used. The performance of each proposed design is evaluated and compared with existing techniques in the literature. Extensive MATLAB simulation tool is used to evaluate the performance of the proposed algorithms. The choice of MATLAB is motivated by its ability to capture adequately the analysis of UDN, to meet the requirements of generality and reproducibilty for modeling not just part of, but the entire system.

## 1.6 Thesis outline

This thesis addresses interference challenges encountered in Heterogeneous Cellular Networks (HCNs) and the envisioned 5G UDN. The presented work is organized into seven chapters. The first chapter introduces the research background, motivation and problem statement.

Investigation into various interference mitigation techniques that can offer solutions to interference experienced in UDN forms the aim of the thesis, also contained in the chapter. Each chapter begins with the introduction which details the main contribution and overview. A brief related work on the research topic discussed in the chapter is also included. Analysis, which include a system model for evaluation, of the technical solution provided to the problems addressed are presented.

Fig. 1.3 shows thesis organisation with detailed key implementation structure contained in Chapters 4 to 6.

**Chapter 2:** Provides a comprehensive overview of different categories of user association/cell selection and power control techniques. The benefits of load balancing and power control on interference coordination, in addition to coverage and capacity improvement are highlighted. Some key limitations of the existing interference management schemes are identified through a thorough review of recent ongoing research. Efforts made to address these challenges in this thesis are given. The chapter concludes with a summary of the contribution made to address the identified challenges.

**Chapter 3:** This chapter begins with a brief introduction of the contents therein, followed by a review of related work in the topics discussed. Key elements of LTE architecture such as frame structure, protocol and network architecture are discussed to demonstrate dependence of integrating small cell and legacy architecture on successful network densification. Due to the importance of having adequate knowledge of channel and systems models on interference mitigation, basic concepts of these models are described. Overview of state-of-the-art access technologies, especially Non Orthogonal Multiple Access (NOMA), presented in Chapter 6,

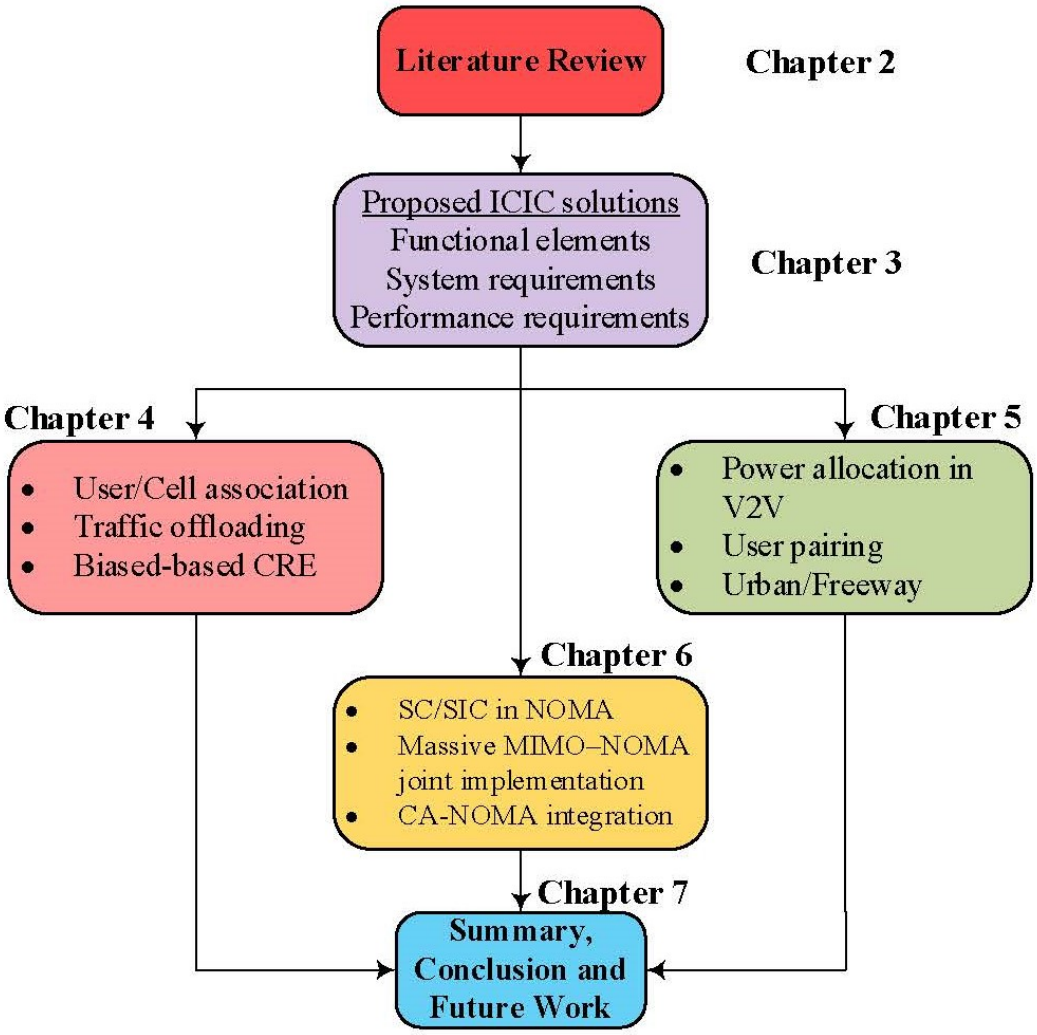


**Figure 1.3:** Thesis outline detailing key implementation structure

are introduced to justify its superiority over Orthogonal Multiple Access (OMA), which are presented in Chapters 4 and 5. The chapter is concluded with discussion and summary of the key topics discussed therein.

**Chapter 4:** Presents an interference coordination solution based on traffic offloading and cell association, using cell range expansion (CRE) combined with LTE Rel. 11 standardized further enhanced ICIC (feICIC) technique. The potential benefits of adaptively setting the CRE bias value to consider multiple parameters for better performance are first studied.

The feasibility of using the feICIC is theoretically examined by exploiting the tractability of stochastic geometry, modeled on Poisson Point Process (PPP). As detailed previously in Chapter 3, key system parameters such as the coverage/outage probability, spectral efficiency (SE), network capacity and users fairness are optimized to show the advantage of reduced power feICIC over the widely studied Almost Blank Subframe (ABSF) scheme in UDN. Simulation results of the approach showing great improvement on network throughput, power consumption and fairness among users are presented.

**Chapter 5:** Studies interference challenges in vehicular networks, including factors affecting vehicular network capacity. Similar to Chapter 4, PPP is used to model CUE and BS locations, in addition to employing stochastic geometry to differentiate Line of Sight (LoS) from Non Line of Sight (NLoS) links. This model helps to analyze the network performance in terms of coverage probability, sum and minimum ergordic capacities. The first part derives the capacity expectation of any given cellular user (CUE), called the ergodic capacity, in urban scenario. Thereafter, power allocation and spectrum sharing (PASS) optimization problem is formulated, subject to different requirements of high capacity for CUEs and ultra reliability for vehicle-to-vehicle users, VUEs. The complex optimization is decomposed into power allocation and spectrum sharing sub-problems, while a robust algorithm with low complexity is developed to solve the problem. Finally, simulation results are presented to show improvement in overall coverage, as well as sum and minimum ergodic capacities of CUEs.

**Chapter 6:** This chapter investigates non-orthogonal multiple access (NOMA) scheme as the next generation radio access technology for the envisioned 5G networks. First, the

chapter introduces and surveys research work relevant to this area. Next, fundamentals of downlink NOMA technique are discussed, with main focus on power-domain NOMA. An optimization of NOMA networks, in conjunction with massive multiple input multiple output (MIMO) technology is performed to investigate the performance gains over conventional multiple access techniques in terms of spectral efficiency (SE), energy efficiency (EE) and network capacity, while considering users' fairness. Thereafter, a novel approach of integrating NOMA-based network with carrier aggregation (CA) to increase users' data rate and further enhance network performance is examined. To realise the goal of maintaining green communication in 5G network, an optimization to maximize the EE of the network through weighted-sum assignment is formulated. The non-convex optimization is transformed into its equivalent convex problem and then develop an iterative algorithm to solve it. Since research involving NOMA schemes is still at its infancy, the CA type suitable for NOMA solutions remains an open challenge. Hence, as at the time of submitting this thesis, a paper investigating these solutions has been submitted for publication.

**Chapter 7:** Summaries, discussions, conclusions and limitations of the solutions proposed, with possible areas of future research, are presented.

# Chapter 2

# Background and Literature Review

## 2.1 Introduction

In Chapter one, this research was introduced by identifying the need to design a robust algorithm for interference coordination in 5G UDN with the aim of achieving the expected improvement in overall system performance. Some key techniques used in the management of interference for legacy technologies were highlighted, with a statement on possible schemes that can perform considerably well for the envisioned future generation wireless networks such as UDN.

This chapter discusses extensively evolution towards interference management in heterogeneous networks with a great focus on various types of interference, modern interference management techniques and how these schemes are expected to be incorporated in the 5G UDN. In this context, general overview of different types of interference and user association techniques and their impact on communication link quality are revisited. Some limitations

of these techniques and solutions are identified. Finally, key enabling technologies and techniques for interference management in 5G UDN, which form the basis for this research, are highlighted.

The rest of the chapter is organised as follows. Section 2.2 presents a background of different types of user association and power control schemes, outlining the effect of load balance and power management on interference reduction, enhanced coverage and capacity improvement of the network. Technical challenges of these techniques and enabling technologies for interference management in 5G UDN are presented in Section 2.3. Section 2.4 reviews related literature on user association and power control techniques currently in use to mitigate interference. Section 2.5 summarises the chapter with a short description of contributions made in this thesis to address the identified challenges.

## 2.2 Background

This section explores different types of existing techniques in user association and power control schemes. Accordingly, various interference management techniques in heterogeneous network, which can either be deployed independently or jointly for robustness are described. The section also covers technical challenges of interference in 5G network, overview of work done in addressing these challenges and the summary of all topics covered in the section.

### 2.2.1 Cell/User Association and Power Control Schemes

This subsection describes different levels of user and base station association characteristics with a view to capture the importance of traffic load balance and transmission power reduction in heterogeneous networks. The first part describes cell association and biasing, while the second part outlines distributed power control schemes for interference management as shown in Figure 2.1.

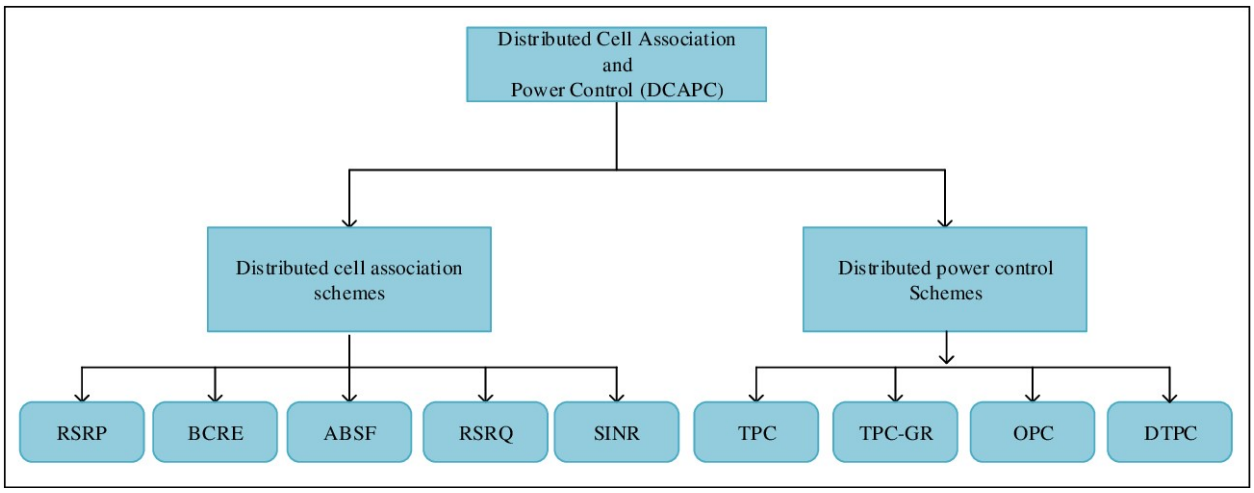


**Figure 2.1:** Distributed cell association and power control schemes

#### 2.2.1.1 Distributed Cell/User Association Schemes

Most work in the literature use cell association and user association interchangeably for multi-tier cellular networks [12]. In generally, cell selection allows a user to camp on to a cell that provides the highest downlink signal, while user association is a process that assigns mobile users to base stations for better signal reception. Thus, the two terms attempt to achieve the same goal. For the purpose of clarity and without any loss of generality, the use

of these two terms is maintained throughout this thesis. The following are different types of cell associations schemes and their limitations reported in the literature.

*Reference Signal Received Power (RSRP) Scheme*: In LTE, cell selection based on RSRP associates a user with the BS whose signal is received with the highest average strength [12]. This approach works well to maximize network throughput for homogeneous network with uniform traffic. However, varying transmit power of base stations in heterogeneous networks, and in the envisioned 5G UDN, can lead to traffic load imbalance and render small cells underutilised. In addition, RSRP is suboptimal since it captures only the received power from individual cell without reflecting the channel quality. RSRP is implemented by adding a bias value to the footprint of a low power node such as picocell, to compensate for the variation in channel quality between macro and pico BSs.

*Signal-to-Inteference-plus-Noise Ratio (SINR) Scheme*: Unlike RSRP, this scheme takes into account the quality of channel in cell selection process. Resources available for cell selection at every transmission time for macro and pico BSs are classified into protected and non-protected resources [24]. Users can therefore benefit from the offloading effect by selecting the cell index with additional bias value $\alpha_{SINR}$.

*Reference Signal Received Quality (RSRQ) Scheme*: This is another approach specified by LTE for cell selection operation. Both RSRQ and RSRP function in the same way, except that cell selection based on RSRQ is performed without offset value. Although, RSRQ can be defined in so many ways, but the most common definition is given as the ratio of RSRQ to the received signal strength indicator (RSSI).

*Cell Range Expansion (CRE) Scheme*: In order to derive maximum benefits from traffic offloading and compensate for the downlink/uplink asymmetry, range expansion technique is used to virtually increase the footprint of low power nodes to offload more users from macrocell. The CRE scheme adds an offset value to the RSRP to increase the coverage area of low power nodes [25]. However, users offloaded in this manner may experience severe interference from neighbouring cells, especially when the bias value is too high. This greatly limits the offloading gain of the approach. Moreover, the choice of an ideal offset value varies according to different geographical locations between BSs and users which, in turn, contributes to variations in interference levels. One approach proposed in LTE to improve the offloading gain is to perform orthogonal transmission of biased and unbiased BSs by combining ICIC with CRE. Detailed description of work on this is presented in Chapter 4.

*Almost Blank Subframe (ABS)*: This is a scheme (eICIC) introduced by 3GPP LTE-A to protect users offloaded through CRE biasing from severe interference from macrocell. The idea is to leave certain sub-frames of macrocell (unbiased BS) blank so that offloaded users within the biased low power nodes are scheduled, while the remaining normal sub-frames are allocated to cell edge users [26]. Therefore, more sub-frames are required to be blanked when a high offset value is used for offloading. However, this greatly improves the throughput of offloaded users at the expense of time sub-frame and throughput of the macrocell. Hence, the ratio of blank over total number of sub-frames, referred to as ABS ratio, is an important factor to consider when range expansion is applied for cell selection.

#### 2.2.1.2 Distributed Power Control Schemes

Power control is an important method to maintain connectivity, mitigate interference and improve energy efficiency in wireless cellular networks. The topic has been extensively studied over the years and the results have provided a pathway towards continuous evolution of cellular technology [27]. In the context of maintaining connectivity in the presence of time variation and channel uncertainties, the receiver is required to sustain a minimum level of signal received for channel estimation. Although, sustaining network connectivity by transmitting signal with smallest power by each node will extend battery life and maximize traffic-carrying capacity of the entire network. However, this is not always the case because of the presence of hidden nodes, especially in the case of network with high density. Apart from connectivity, power control helps guarantee efficient spectral reuse and quality of user experience in systems where maintenance of perfect orthogonality is difficult.

With the proliferation of wireless devices and limited battery power therein, conservation of energy is essential to sustain the lifetime of the terminals and entire network. Traditionally, homogeneous networks permit adjustment of transmission powers to all nodes such that they fall within range of the nearest neighbour. On the contrary, transmission powers in heterogeneous networks are adjusted according to the need of the network. Thus, different power control algorithms are usually combined to produce a hybrid technique in order to strike a balance between user and network demands. Such algorithms must be capable of adapting to the physical environment, density and mobility pattern of the network [28]. In addition, due to the exponential growth of wireless devices, the algorithm should be distributed so as to avoid computational complexity and huge overheads inherent in

centralized designs. The rest of this subsection presents an overview of different power control algorithms in the literature proposed for classical networks. These schemes have been modified and used in several ways to reduce interference with the evolution of wireless technology.

*Target-SINR Power Control*: This approach allows BSs to track and achieve their fixed target signal strengths at minimum transmit power with the assumption of feasible SINRs. However, when the SINRs are infeasible, BSs that are not able to attain their fixed target transmit at high power levels creates unacceptable interference to other users. TPC enables transmitted power of each base station to be controlled using local measurements, so that minimum signal-to-interference ratio requirement can be met [29]. The distributed algorithm converges when there exists a power setting that corresponds to the minimum SIR attained by all BSs. For interference management and efficient channel utilization through frequency reuse, it is critical to prevent excessive power transmission above the level required to meet the minimum SINRs. The algorithm achieves this aim by iteratively updating transmit power of each base station up to a level where optimum performance is reached. This update is performed with the knowledge that other base stations' power levels are fixed. Interestingly, other base stations are aware of this action and are correspondingly updating their power levels in response. The algorithm then converges exponentially to the desired performance by this local exchange of information. Mathematically, to minimize the total power $p$ by varying transmit power to satisfy fixed SINR constraints $\gamma$, given a desired threshold $\rho_i$ for BS $i$

$$\begin{aligned} &\text{minimize} \sum_i p_i \\ &\text{s.t.} \quad \gamma_i \geq \rho_i, \quad \forall i \end{aligned} \tag{2.1}$$

The following iterative power update algorithm proposed by Foschini and Miljanic is then used to compute the optimal solution of (2.1);

$$p_i[t+1] = \frac{\rho_i}{\gamma_i[t]} p_i[t], \quad \forall i \tag{2.2}$$

where $\gamma_i$[t] and $p_i$[t] represent the target SINR and transmission power of BS $i$. Each BS can monitor its individual received SINR and independently update with the distributed algorithm (2.2) asynchronously. Thus, each BS $i$ increases its power when its target SINR constraint $\gamma_i$ is less than $\rho_i$ and decreases it otherwise. However, the iterative power update in (2.2) diverges to the infinite power without convergence if the SINR constraints (2.1) are not feasible.

*Opportunistic Power Control (OPC)*: This approach minimizes interference and achieves high capacity through multiuser diversity. The idea is to increase power level of the transmitter when the channel condition is good and without interference, and allocate low power to the transmitter when the channel is experiencing low path gain and high interference [30]. This partially eliminates excessive interference and enhances the total system throughput. However, the algorithm sacrifices fairness among users for improved system performance due to non proportional variations in path gains and throughput between two users. The major advantage of OPC algorithm is the ability to cope with network density, unlike target SIR

which experiences performance degradation when network is congested. Moreover, OPC exploits fairly high delay tolerance in data and fluctuation in wireless channels to maximize overall system throughput. Given $p_i^{(t+1)}$ as the transmit power, node $i$ updates its power at time $t+1$ according to

$$p_i^{(t+1)} = I_i\Big(R_i^{(t)}, p_i^{(t)}\Big) \tag{2.3}$$

where $R_i^{(t)}$ is the effective interference of node $i$ at time $t$, and $I$ is the iterative power update function of node $i$, which is also a function of $R$ and $p$. By setting the derivative of utility function given by

$$U_i^{OPC} = \sqrt{\gamma_i} - \lambda_i p_i \tag{2.4}$$

to zero with respect to $p_i$, and

$$p_i = \frac{1/(2\lambda_i)^2}{R_i} \tag{2.5}$$

Thus, the iterative power update function of the OPC algorithm can be explicitly written as [30]

$$p_i(t+1) = \frac{\xi_i}{R_i[t]} \tag{2.6}$$

where $\xi_i = 1/(2\lambda_i)^2$ is a non-negative constant. Indeed, the transmit power in (2.6) is inversely proportional to $R$, and establishes the opportunistic behaviour of the algorithm to transmit with low power when the channel is bad and vice versa. It is also noted that, at

convergence, the algorithm satisfies the following equation for all $i$

$$p_i^{(t)} R_i^{(t)} = \xi_i, \quad \forall i \tag{2.7}$$

The term $\xi_i$, called the target signal-interference product (SIP) is directly proportional to the transmit power of node $i$ and determines its willingness to transmit. Hence, the higher the value of $\xi_i$, the higher the amount of power transmitted by node $i$. In general, the payoff function can be designed in the form $U_i = U_i(p) - C_i(p)$ to incorporate utility $U_i(p)$ and cost $C_i(p)$ functions such that the cost function accounts for the price imposed to discourage users from transmitting at high power. This approach helps to manage resources efficiently and improve overall network utility. Application and improvement of this technique for joint energy efficiency maximization and interference coordination in next generation 5G UDNs are presented in Chapter 5.

*TPC with Gradual Removal (TPC-GR)*: Unlike TPC where non-surpported BSs create unfavourable channel conditions under infeasible SINRs, TPC-GR algorithms were proposed to enforce transmit power reduction or gradual removal of non-surpported BSs with infeasible SINRs [31], [32]. All users in the network perform feasibility check in a distributed manner by temporarily removing any user whose required target-SIR exceeds its maximum power, and then resumes transmission when its required transmit power is below a desired threshold. In this manner, the algorithm minimizes outage probability and help users reach their target-SINR with minimum consumption of gross transmit power. Indeed, TPC-GR works in a similar manner as OPC, however, it addresses excessive power transmission in the infeasibilty

region for unconstrained cases in OPC. As opposed to non convergence of TPC due to maximum transmit power, which causes undesirable interference to others, TPC-GR reduces the transmit power or gradually removes some users.

The TPC-GR algorithm operates in two modes to combine the functions of the OPC algorithm. In the first mode, transmit power of the user is updated using TPC when the channel is good, and in the second phase, OPC is applied when the effective interference is above a threshold. During this period, some non-supported users are identified by TPC-GR for gradual removal. The function of OPC in this manner is to remove interference when the channel is poor, and consequently admit more supported user into the system. It is noteworthy, however, that this function of OPC is not the same as the original application in both poor and good condition as earlier discussed. To this end, the TPC-CG algorithm is true for a given continuous power update function $f_i(\mathbf{p})$, for all $i$, which is an increasing function of the effective interference function of $R_i$ for values below a threshold, or a decreasing function of $R_i$ for values above the same threshold. The power update function then follows the expression [32]

$$p_i(t+1) = f_i(\mathbf{p}(t)) \triangleq \begin{cases} \gamma_i R_i(\mathbf{p}(t)), & \text{if } R_i(\mathbf{p}(\mathrm{t})) \leq R_i^{th} \\ \frac{\eta_i}{R_i(\mathbf{p}(t))}, & \text{if } R_i(\mathbf{p}(\mathrm{t})) \geq R_i^{th} \end{cases} \tag{2.8}$$

where $\gamma_i$ denotes the target-SINR for BS $i$, $R_i^{\mathrm{th}}$ represents the effective interference threshold and $\eta_i$ is a constant. Intuitively, an increase in $R_i$ for a given BS in the TPC mode will result in a corresponding increase in the transmit power, until at a point when further increases in $R_i$ results to decrease in transmit power of the BS. These three parameters are adjusted so

that (2.14) is continuous and true for

$$\eta_i = \gamma_i (R_i^{\text{th}})^2 \tag{2.9}$$

Clearly, the performance of TPC-GR algorithm depends on the threshold value of $R_i$ chosen by the BSs. Therefore, the algorithm converges to a unique fixed point in both feasible and infeasible cases when the BSs carefully adjust their effective interference thresholds to reduce power consumption and outage ratio.

*Dynamic SIR tracking Power Control (DTPC)*: It was shown earlier that TPC algorithm can be used to achieve better throughputs when BSs are able to reach their fixed target SINRs. Moreover, the algorithm performs very well in voice services where attaining a higher value of SINR than the given threshold has little effect on the QoS. However, this is not true for data services where a higher SINR significantly improves network throughput. As a result, the DTPC algorithm was proposed to maximize system throughput subject to a given feasible lower bound for the BSs' SINR in wireless cellular networks [33]. This approach is implemented by using TPC and OPC in a selective manner. In DTPC, a node can dynamically set its target SINR to a higher value than the minimum target SINR in a distributed manner when the effective interference is less than a given threshold, or maintain a fixed target SINR at minimum desirable level. The target SINR value is a decreasing function of the effective interference. Again, this improves the system throughput at the expense of increased power consumption. It is important to note that improving system's throughput depends highly on how interference is effectively managed. From the user's point

of view, the objective of power control is to support a user with its minimum acceptable throughput, whereas aggregate throughput maximization is the case from a system's point of view. These two objectives are contradicting in the sense that the former case requires that the near-far effect is compensated for by allocating high power levels to users with poor channels, compared with UEs experiencing good channel. In the latter case, few users with good channels are allocated high power levels while very low, or even zero power levels are allocated to others. Therefore, this forms the basis for using important metrics such as the outage ratio, aggregate throughput and transmit power to compare the performance of different power control schemes. Using system information approach to define throughput for each BS as

$$T_i(p) = W \log_2(1 + \gamma_i(\mathbf{p})) \tag{2.10}$$

where $W$ is the channel bandwidth and the aggregate throughput is given as

$$T(\mathbf{p}) = \sum_i T_i(\mathbf{p}). \tag{2.11}$$

Therefore, the problem of throughput maximization subject to a given feasible lower band of SINR for all users in DTPC is formulated as [33]

$$\begin{aligned} &\max_{\mathbf{p}\geq 0} \sum_i T_i(\mathbf{p}) \\ &\text{s.t.} \quad \gamma_i \geq \rho_i, \quad \forall i \end{aligned} \tag{2.12}$$

At the extreme cases of the generalized equation for TPC and OPC in (2.14) where $R_i \to 0$ or $R_i \to \infty$, the proposed power update function eventually becomes either TPC or OPC, respectively. Hence, the DTPC algorithm follows by re-writing (2.14) as

$$f_i^{DPTC}(\mathbf{p}(t)) = \gamma_i(\mathbf{p}(t))R_i(\mathbf{p}(t)) \tag{2.13}$$

in which the target SINR $\gamma_i(\mathbf{p}(t))$ is dynamically set as

$$\gamma_i(\mathbf{p}(t)) = \begin{cases} \frac{\eta_i}{R_i^2(\mathbf{p}(t))}, & \text{if } R_i(\mathbf{p}(\mathrm{t})) < R_i^{th} \\ \hat{\Gamma}_i, & \text{if } R_i(\mathbf{p}(\mathrm{t})) \geq R_i^{th} \end{cases} \tag{2.14}$$

where $\hat{\Gamma}_i$ is the minimum acceptable target SINR for BS $i$. For DTPC to be continuous, parameters $\hat{\Gamma}_i$ and $\eta_i$ are adjusted appropriately and the value of $R_i^{th}$ set as

$$R_i^{th} = \sqrt{\frac{\eta_i}{\hat{\Gamma}_i}} \tag{2.15}$$

Also, the minimum acceptable target SINR in (2.13) is set to the same value as (2.2). The convergence of DTPC algorithm is examined using the two-sided scalable generalized framework for standard power updating functions. At convergence, the iterative function has a unique fixed point. The generalized scalability proof is presented in Chapter Five.

The state-of-the-art cell selection and power control schemes discussed above for wireless networks are inadequate in addressing the interference dynamics in the envisioned 5G UDNs. Specifically, the standard cell association schemes require proper setting of parameters such

as bias values, resource partitioning and transmit power for optimized performance. In the same vein, the power control schemes are unable to address outage and interference problems between low priority users (LPUEs) and high priority users (HPUEs). However, to achieve optimum performance in 5G networks, any of the cell selection schemes can be jointly used with one or more power control schemes. Detailed description on how this can be achieved is presented at the end of this chapter.

### 2.2.2 Interference Management Techniques in Heterogeneous Networks/UDN:

In the envisioned 5G networks, some key demands to be addressed are high data rate, improved capacity, decreased latency and better QoS. To achieve this goal, it is very important to fully understand the dynamics of inteference associated with small cell densification and proffer appropriate solutions. This section summarizes the major challenges and solutions of interference management.

Due to the multi-tier multi-cell deployment of macrocells and dense deployment of small cells, comprising picocells, femtocells, D2D and RRHs, UDN architecture further results to a two-tier, i.e., macro-tier and small-tier networks. Macro evolved NodeBs (MeNBs) provide coverage for macrocells intended to offer service and coverage for high mobility users. On the contrary, small cells, which cover smaller area and transmit with low power, are served by small evolved NodeBs and provide services to small number of users with low mobility [34]. Two kinds of deployments are considered for dense networks:

- co-channel deployments, where the same frequency band is used by MeNBs and SeNBs, and
- non-co-channel deployments, where different bands are used by MeNBs and SeNBs.

These two deployments are depicted in Figure 2.2.

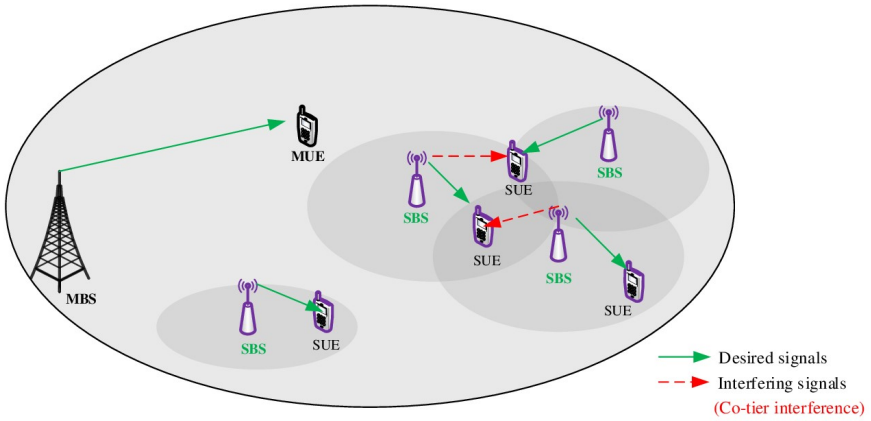


**(a)**

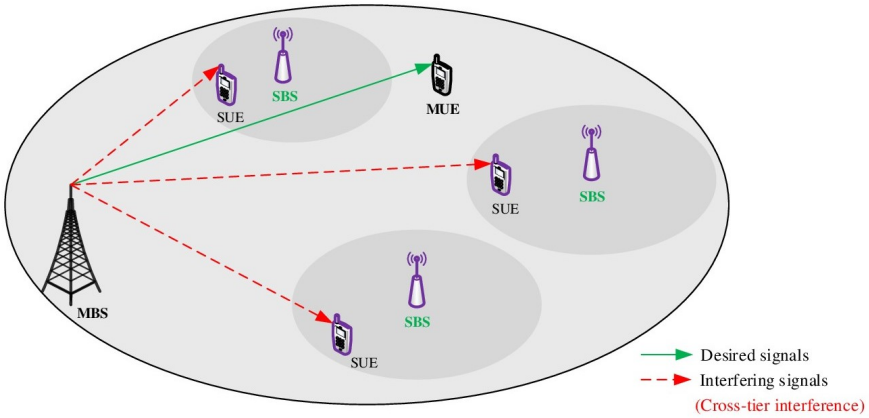


**(b)**

**Figure 2.2:** Illustration of deployment types in UDN (a) Non co-channel deployment with dense small cells, resulting in co-tier interference. (b) Co-channel deployment with uniformly placed small cells, leading to cross-tier interference.

The major impairment in co-channel deployments is cross-tier interference, which can be seen as interference encountered between macro-tier and small-tier. This is the interference

experienced by UEs served the SeNB from MeNBs or interference towards UEs served by the MeNBs from SeNBs. In general, UEs served by MeNBs are referred to as MUEs, while UEs under the coverage of SeNBs are called SUEs. As stated in chapter one, varying transmit power between interfering signal from HPNs and useful signal from LPNs creates more challenging interference from MeNBs towards SUEs. However, this is not the case in non-co-channel deployments as a result of different bands used among tiers. Although, this leads to reduced spectral efficiency of the entire system. From the operator's perspective, traffic can be offloaded to small cells in the coverage of MeNBs as long as the latter remains in active mode [35], [36]. This forms the basis of the work presented in Chapter Four.

Based on the deployment scenarios described above, two types of interference are encountered in multi-tier cellular system.

***Intra-cell interference:*** This occurs when a BS transmits to or receives signal simultaneously from multiple UEs on the same time/frequency resources.

***Inter-cell interference:*** This is the interference created among different BSs and users served by different BSs as a result of simultaneous transmission and reception on the same time and frequency resources.

Furthermore, inter-cell interference can exist in two forms in UDN as cross-tier and co-tier interference. In wireless networks where Orthogonal frequency division multiple access (OFDMA) is the access technique used in the downlink, intra-cell interference is non existence due to orthogonality between users. In addition, downlink-to-uplink (DL-to-UL) interference can arise when a BS transmits in the downlink towards a neighbouring BS receiving in the UL. Also, uplink-to-downlink (UL-to-DL) interference results from UE receiving in the DL

being interfered by another UE transmitting in UL. Depending on the mode of operation in the DL or UL, BSs and UEs can function either as transmitters (TXs) or receivers (RXs). Different domains for interference mitigation are highlighted in Table 2.1.

**Table 2.1:** Domains for interference mitigation

| Domain | Application |
|---|---|
| Time | Time allocation |
| Frequency | Frequency allocation |
| Code | Code assignment (CDMA) |
| Space | Beamforming, MIMO |
| Power | Transmit power control |
| Transmit path | Downlink/Uplink |
| User | Scheduling of users |

Major categories of interference management techniques are shown in Figure 2.3 [37], [38].

For the purpose of this thesis, the solutions presented in Chapters 4 - 6 cover major categories under the three interference management techniques, due to their relevance to this research. However, other categories are mentioned at one point or the other in the thesis.

#### 2.2.2.1 Inter-cell Interference Coordination (ICIC)

This involves advanced techniques such as power control, spectrum splitting and decoding of the desired information signal, used in conjunction with channel estimations from the received signal to reduce interference. Two techniques that are widely used in wireless communication systems for this purpose are successive interference cancellation (SIC) and parallel interference cancellation (PIC) [39]. The basic idea of SIC scheme is the ability of a base station to decode its intended signal from several interfering signals transmitted

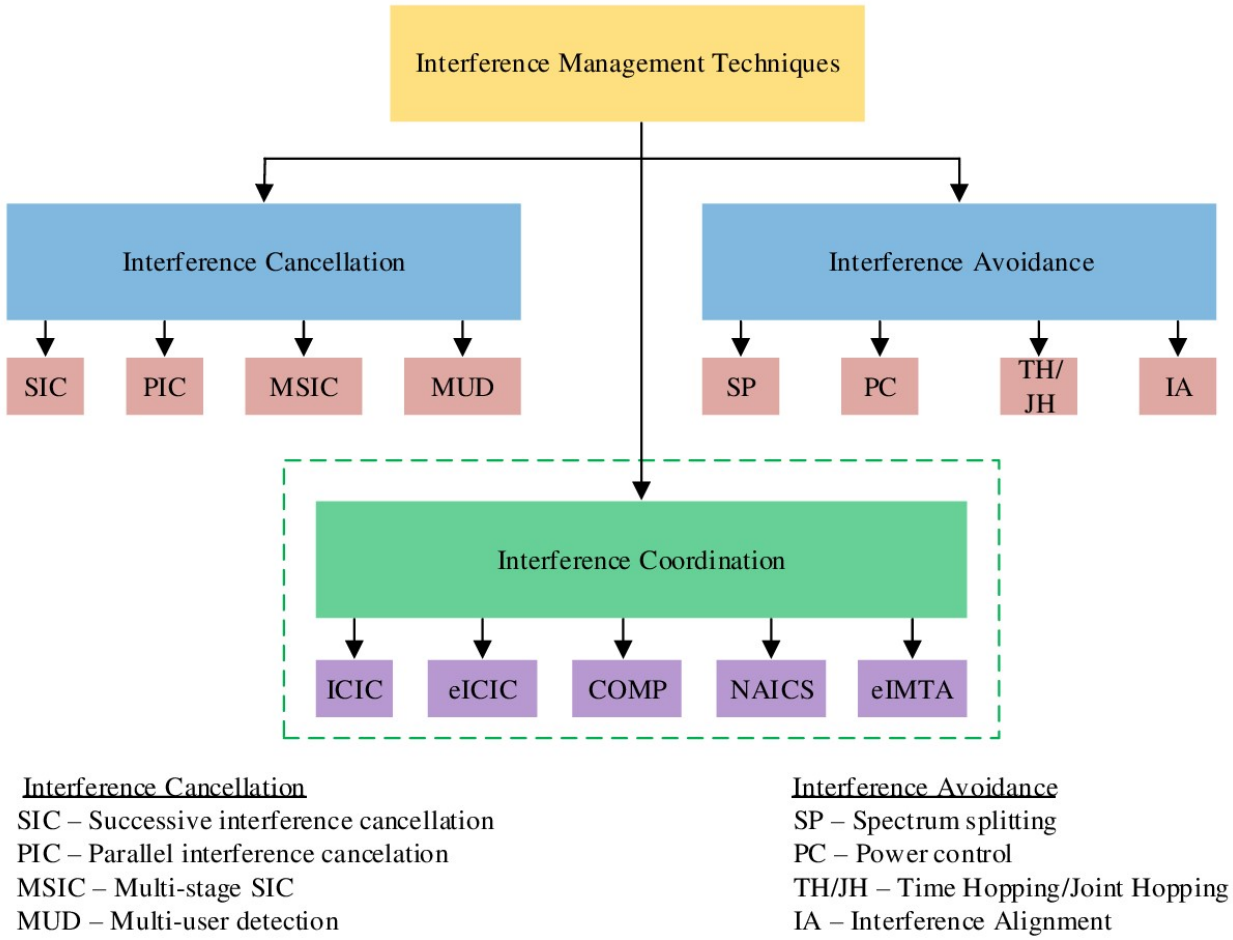


**Figure 2.3:** Interference Management Techniques

simultaneously. In some cases where the intended signal is not the dominant signal, the base station first detect and decode the strongest interfering signal, and thereafter subtract or cancel it from the combined received signal. Subsequent strongest interfering signals can then be detected and decoded from the obtained cleaner combined signal, and so on. This process continues until it reaches an optimal level when all stronger interference signals are cancelled, leaving only the desired intended signal to be decoded. However, the propagation error inccured by this approach is corrected by using union bound to decode a high enough SINR with high probability [38]. However, PIC scheme estimates data from all signals using

matched filters to eliminate interference and achieve better bit error rate (BER), with less computational complexity than SIC. The transmit power of the base station can therefore be optimized in either time or frequency domains to enhance performance of cell-edge users. Two major categories of static ICIC algorithm extensively used are soft frequency reuse (SFR) and fractional frequency reuse (FFR) methods. The main difference between the two is that SFR permits full frequency reuse, while FFR only allows a fraction of the frequency band to be used [40].

#### 2.2.2.2 Enhanced Inter-cell Interference Coordination (eICIC)

The ICIC technique discussed above was specifically designed for macro-only networks. The more robust eICIC technique in time domain was included in release 10 of LTE-A [41]. It embraces cochannel deployment of small cells in the coverage of macrocell, in addition to capability for time and phase sychronization in heterogeneous networks. Main features of eICIC used for improvement in spectral efficiency in the DL transmission are ABS and biased user association, also known as CRE. These two techniques have been discussed in Section 2.2.1. Additional improvement considered by 3GPP on eICIC is named further eICIC (FeICIC). FeICIC mitigates interference at the control plane level, rather than at the data plane level only. Hence, interference coordination is effectively achieved by the combined features of power reduction and sub-frame muting at BSs, and interference cancellation abilities from users [42], [43]. However, muting of some MeNB's sub-frames in ABS-based eICIC/FeICIC can lead to outage and spectral efficiency degradation, which invalidates the benefit obtained in performance improvement.

#### 2.2.2.3 Coordinated Multipoint (CoMP)

In LTE-A network, CoMP is developed as part of the move to reduce interference, improve data rate coverage, increase cell-edge thorughput and throughput of the entire system in both co-channel and non-cochannel deployments [44]. The basic idea of CoMP is to advance the traditional single-tier multi-user system structure to a multi-tier multi-user architecture. This is to eliminate the concept of cell edge users since a user close to the edge of the cell can, at the same time, be enclosed and served by several active nearby BSs. Hence, users with low signal qualities can enjoy better service from nearby BSs if they can work in cooperation or coordination, in such a way that simultaneous transmission of signal to/from other points do not cause severe interference, or better still, transform the interference problem into an opportunity for service improvement[45]. The X2 backhaul is a logical interface that enables exchange of communication between MeNBs for the realization of interference coordination requests. In the envisioned 5G networks, certain factors such as delays and bandwidth limitations, arising from conflict in sharing the same physical infrastructure with non-X2 platforms are bound to be challenging [46]. Therefore, CoMP techniques are designed to support much more dynamic coordination and lower latency requirements, in contrast to semi-static coordination design for ICIC techniques. Thus, the type of CoMP techniques that can be applied at any particular time depends on the latency and capacity characteristics of the backhaul and the associated performance expectations. In 3GPP, the three categories of CoMP techniques identified for DL transmission based on backhaul constraints between scheduling complexity and coordinated points are; coordinated

scheduling/coordinated beamforming (CS/CB), joint processing/joint transmission (JP/JT) and dynamic/transmission point selection (DPS/TPS).

#### 2.2.2.4 Network Assisted Interference Cancellation and Suppression (NAICS)

Study of NAICS came to fruition with the advancement in receiver implementation which allows more feasible non-orthogonal transmission and makes interference cancellation more manageable. NAICS provides a more robust and effective interference suppression at the receiver side with network coordination. Individual user in the network is provided with information related to the number of interferers and interfering modulation order to assist with interference cancellation task [47]. Usually, real and interfering signals are received simultaneously, while the UE's receiver decodes and subtracts the interfering data stream so as to provide necessary information about resource allocation and Modulation and Coding Scheme (MCS). To achieve this, users are provided with the Radio Network Temporary Identifier (RNTI) containing the interfering users for the purpose of decoding the data and downlink control information (DCIs) for successive interference cancellation [48]. Major classifications are:

- *Interference cancellation receivers*, example of these are symbol level interference cancellation, parallel interference cancellation (PIC) and linear-code level SIC.
- *Interference suppression receivers*, examples are linear minimum mean square error - interference rejection combining (LMMSE-IRC), with variants widely LMMSE-IRC and enhanced LMMSE-IRC, and
- *Maximum likelihood receivers* (ML), comprising reduced complexity ML.

#### 2.2.2.5 enhanced DL-UL Interference Management and Traffic Adaptation (eIMTA)

This technique is developed for allocation of both DL and UL sub-frames dynamically in LTE time division duplex (TDD) system to address the problem of asymmetrically changing traffic condition [44]. Moreover, eIMTA provides higher efficiency for better communication using the same bandwidth for UL and DL. Since the same frequency is used for both transmissions, the system does not require a duplexer, thereby leading to energy conservation. Novel techniques are currently being used to analyse the impact of eIMTA and TDD on efficient resource allocation in small cell technology to reduce interference. More importantly, power control and carrier aggregation techniques have been developed recently to address the impact of traffic patterns on the dynamic ratio selection [49–52]. These approaches have resulted into the following categories of interference management techniques studied for eIMTA:

- **Interference mitigation based on eICIC/FeICIC:** The strategy and interference mitigation schemes from eICIC and FeICIC are adapted for reuse in TDD DL/UL arrangement to support dynamic traffic situation.

- **Interference suppressing interference mitigation (ISIM):** This scheme is examined for macrocells and small cells transmission in the UL to allow suppression of multiple dominant DL to UL interfering signals using LMMSE-IRC.

- **Scheduling dependent interference mitigation (SDIM):** Scheduling policy such as transmit power and resource allocation are adjusted by each BS taking into

consideration the traffic load, DL-to-UL and UL-to-DL interference, and channel quality.

- **Cell clustering interference mitigation (CCIM):** Participating BSs form a group of cluster with all BSs within a cluster transmitting in the same pattern so that interference from DL-to-UL and UL-to-DL within each cluster are avoided.

#### 2.2.2.6 Carrier Aggregation (CA)

The introduction of CA by 3GPP LTE-A Release 10 was to provide better coverage, high data rate and low latency requirements through wider transmission bandwidth. With CA technology, multiple component carriers (CC) can be aggregated up to 100 MHz for a single user in a continuous or non-continuous manner. Continuous CA is when multiple available CCs are placed adjacent to each other, while in non-continuous, the CCs are separated over the frequency band. Thus, CA supports aggregation of up to five CCs with same or different bandwidth to achieve high data rate transmission, while preserving backward compatibility to legacy technologies. Three different CA scenarios are available, namely: interband continuous CA, intraband non-continuous CA and interband non-continuous CA. The type of CA used and fraction of the total CCs assigned to a user depend on the network requirement, traffic load and user's capability. Specifically, the non-continuous CA enables utilisation of idle frequency bands, and also exploits the broad frequency range to achieve transmission of data across multiple carriers. Although this introduces serious variations in the transmission performance and channel characteristics such as Doppler shift and pathloss. To address this problem, an effective resource allocation and management algorithms that

can adaptively adjust transmission power and MCS for different CCs should be developed. Details on solution based on inter-band non-continuous CA integrated with non-orthogonal multiple access (NOMA) scheme is presented in Chapter 6.

## 2.3 Technical Challenges of Interference in 5G UDN

In all the interference management techniques discussed in Section 2.2.2, adequate cooperation and coordination among the BSs, whether acting as TXs or RXs, are required to fully exploit the deployment benefits. In addition, they help to improve cell-edge throughput and the overall system spectral efficiency. However, the cooperation and coordination process involved impose a lot of signaling overhead, which demands a robust backhaul requirements especially in terms of capacity, coverage, latency and accurate synchronization among the BSs. These requirements are stringent, especially in multi-tier ultra-dense scenario where cells operate under resource reuse pattern. Moreover, self organizing nature, mobility patterns, network topology and handover process complicate the interference problem in dense deployment environment. Self organizing requires continuous monitoring and sensing of the radio environment in order to dynamically and adaptively mitigate interference. Three types of self organizing approach are:

- *Self-configuration* involves newly deployed nodes or a group of nodes to be automatically configured when switched on, or after a major change or failure.

- *Self-healing* enables cells to perform automatic failure recovery after service outage through temporary reconfiguration of the surrounding nodes for minimum QoS guarantee, and

- *Self-optimization* allows cell to monitor and optimize their settings, either per cluster, cell or single site, to reduce interference and improve coverage.

Therefore, challenges encountered in the implementation of interference mitigation techniques for 5G UDN can broadly be categorized as represented in Figure 2.4.

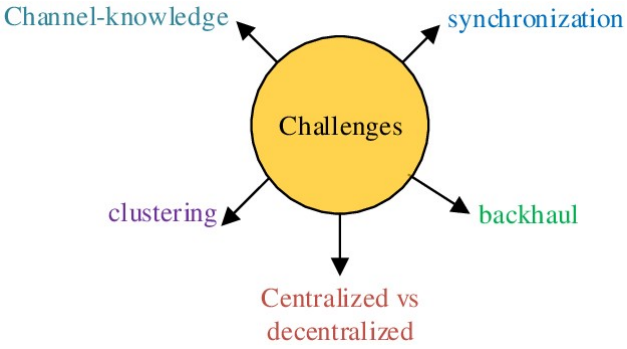


**Figure 2.4:** Implementation challenges in interference management

### 2.3.1 Synchronization

Since the emergence of wireless communication, frequency synchronization allocation has been applied. Thus, high accuracy demands for time and phase synchronization has become very important with the development of 3G and 4G mobile communication systems. Legacy schemes such as Code Division Multiple Access (CDMA) 2000, Time Division Synchronous Code Division Multiple Access (TD-SCDMA) and the recent Time Division LTE (TD-LTE) require micro-second accuracy between neighbouring BSs [53]. One way to achieve this is to

install a Global Positioning Systems (GPS) receiver at every point, which results in limited indoor deployment, high cost and maintenance difficulty. Alternatively, time synchronization networks can be built using a synchronization protocol that delivers timing information through transport networks. In a multi-tier ultra-dense network, perfect synchronization in time and frequency domains is required between coordinated UEs served by cooperative and coordinated BSs. Strict synchronization requirements are particularly crucial to compensate for signal timing offsets (STOs) and carrier frequency offsets (CFOs) in operations that demand low latency like vehicular communications [54]. Specifically, time synchronization is required at the symbol level for cooperation, while time synchronization is demanded at the frame level in coordination. Although, classical time synchronization techniques may be employed with the aid of estimated STOs to pre-compensate or post-compensate potential desynchronizations at the respective transmitters and receivers, to achieve time synchronization in point-to-multipoint and multipoint-to-point communication. However, these schemes do not readily apply to coordinated multipoint-to-multiuser (MtM) systems where simultaneous transmission is accomplished in the same resource. As a result, end-to-end time accuracy, high reliability and maintenance/management convenience can be achieved through the evolution of the time transport, reference source and synchronization network architecture.

### 2.3.2 Backhauling

In network densification regime, connection between BSs, mobile devices and the core network need to be support with a low latency, high capacity backhaul for enhanced data

throughput and user experience. Two main approaches in which backhaul technologies advancement aims to support 5G UDN are [55]:

- *Cloud Radio Access Network (Cloud-RAN) Architecture*: High bandwidth and low-latency requirements in dense urban centres motivated the need for Cloud-RAN with CoMP techniques. In such systems, centralized processing of transmit-receive signal for a large number of BSs is implemented by a single processor. Thus, UE can experience high QoS as a result of transformation of dense interference-limited wireless system into almost interference-free system. This technique is known as Multipoint Equalization (MPE), and achieves remarkable performance gains on the condition that accurate CSI is exchanged between the Cloud-RAN and each user. In addition, the Cloud-RAN needs to cover a large number of cell sites. Cloud-RAN can be deployed in a specialized settings such as stadiums where high traffic demand requires highly intergrated infrastructure and large signaling overhead. Recently, the IEEE 1914.1 commenced study on the Next Generation Fronthaul Interface (NGFI) which supports introduction of a fronthaul transport network with the capabilities of data statistical multiplexing, to replace fibres for the Common Public radio Interface (CPRI) transport system [53].

- *Wireless Backhaul Technologies*: Spartial densification of small cells in positions such as street poles, building walls and lamp posts can be capital intensive, especially when wired backhaul is utilized. Wireless backhaul technology could help solve this problem by connecting the gateway nodes through a fiber backhaul to the core network, and then to both the small cells and feeder links. In practice, due to channel propagation

properties, line-of-sight (LoS) gateway nodes are usually connected via microwave and millimeter wave spectrum, while LoS/non-line-of-sight (NLoS) feeder links are connected through the sub-6 GHz spectrum.

Potential techniques for capacity improvement in wireless backhaul technologies include:

- Encouraging dynamic spectrum sharing between feeder and access links.
- Optimizing end node locations for MIMO by employing single-user spatial multiplexing on each NLoS feeder link.
- Employing spatial multiplexing techniques, such as distributed multi-user MIMO among LoS links radiating from each gateway node to multiple feeder links.
- Exploiting high modulation order quadrature amplitude modulation (QAM)for high signal to noise ratio (SNR) and channel coherence time for reduction in channel feedback rate and pilot overhead.

Wireless backhaul, supported by millimeter wave communication offers an example where high spatial multiplexing order is utilized. Also, massive MIMO can be operated in the low frequency bands to enable multiple vertical and horizontal beamforming potentials for macrocells when equipped with two-dimensional antenna arrays [56].

### 2.3.3 Channel Knowledge

In wireless system, to derive interference management techniques requires the acquisition of channel knowledge partaining to the MIMO systems channel matrices for both the desired

and interfering channels at the BSs. Channel knowledge exploitation can help achieve reduction in total power consumption and guarantee QoS in UDN with massive MIMO. Usually, channel estimation is performed at the users side in FDD systems, and then fed back to the BSs. An extension of this approach is to conduct channel estimation and feedback detected at the UEs from multiple BSs for coordination and cooperation among BSs. This approach is known as spatial soft-cell with joint non-coherent multi-flow beamforming [57]. However, channel matrices estimation in a dense network is practically intractable due to inaccuracy in estimating possible weak links and the difficult feedback and pilot planning realization. Therefore, a solution involving TDD reciprocity where coherent time DL and UL propagation channels are exploited so that channel knowledge can be acquired by BSs from UL pilot-based transmission is proposed. This eliminates the imperfect feedback effect and the overhead involved in estimated channel feedback. Therefore, perfect calibration of the hardware in the DL and UL radio frequency (RF) pattern at BSs and UEs is essential for perfect propagation channel reciprocity. As for the BSs, stable hardware performances and relatively slow variability in the surrounding scenario can help to achieve perfect calibration. On the other hand, calibration at UEs may experience imperfection due to variations in the environment caused by power, temperature and time [34].

The following highlights some of the challenges of channel knowledge at TXs in UDNs:

- network planning requirement for pilot signals,
- in FDD systems, imperfect feedback links leading to performance degradation,
- in TDD systems, imperfect calibration of the RF chains leading to performance loss,

- high computational complexity due to multiple channels estimation,
- low SNR and imperfect estimation of interfering channel matrices causing low performance, and
- excessive overhead involved in feed back process for the estimated channels in the case of FDD systems.

Performance degradation due to imperfect channel knowledge, arising from imperfect calibration in TDD and imperfect feedback and estimation in FDD, can be avoided with a robust algorithms that consider statistical error characterization and channel knowledge [58], [59].

### 2.3.4 Clustering

Managing the backhaul and overhead challenges, especially in CoMP-JT networks, requires limited number of BSs to cooperate at any given instant of time. Hence, to reduce complexity, the question of which set of BSs should form cooperative clusters in order to maximize coordination/cooperation gains readily arises. In general, clustering can either be static or dynamic depending on whether BS deployed (BS-centric) or UE deployed (UE-centric) [60], [61]. In the static configuration, geographical criteria such as BSs' positions and framework of the surroundings form the design parameters and are usually kept constant over time. On the contrary, dynamic clustering allows continuous adaptation of the clustering strategy by varying parameters such as UE locations and RF conditions. Although, a practically infeasible ideal clustering configuration exists in which a set of cells with strongest links

serve each potential UE location. Finding corresponding set of optimal cells that can jointly serve UEs in this manner would result to significant signalling overhead among BSs. Rather, this approach is used as a benchmark for performance evaluation of any substantial clustering scheme found in practice. Static clustering can further be extended to non-overlapping and overlapping clusters [62]. In the case of non- overlapping clusters, also known as disjunct with respect to the cells involved, two different optimization guidelines are possible. One is to maximize the average SINR achieved by a certain position under a particular fixed clustering. Another possibility is to maximize a certain outage measure corresponding to achieving a particular minimum SINR at some positions. However, overlapping cluster schemes are designed to address the problem of low SINR experienced by UEs at cluster borders in the clustering schemes discussed earlier. Hence, spatially overlapping clusters which is a special form of fractional frequency reuse scheme, but with careful selection of reuse factor 1, is used with different system resources to achieve optimal choice of overlapping and assignment of resources to clusters [63, 64].

### 2.3.5 Centralized and Decentralized Approach

Interference management can be achieved either in a centralized, decentralized or hybrid manner, depending on the architecture used.

**Centralized Approach:** This approach involves management of resource and power allocation by a central control entity according to information received from different cells. Optimal resource allocation is achieved through this approach at the cost of high signaling overhead due to constant exchange of signaling messages between the cells and the controller.

**Decentralized Approach:** This approach does not involve the central controller. Each cell makes resource and power allocation decisions independently regardless of the actions of the other cells . Although, decentralized schemes are cheap to implement, they do not guarantee optimal resource and power allocation results.

**Hybrid Approach:** Hybrid ICIC schemes are proposed as a trade-off between the centralized and decentralized schemes. In this approach, resource and power allocation decisions between the different cells are performed by a central controller, while UE scheduling is performed by the BSs in a decentralized manner.

### 2.3.6 Key Enabling Technologies for Interference Management

In Sections 2.2 and 2.3, important research issues for multi-tier and the envisioned 5G ultra-dense networks in the areas of mobility management and load balancing via dynamic BS association, coordination and cooperation were identified. Solutions towards various interference challenges identified were also provided. The following section provides a review of the most recent state-of-the-art interference mitigation techniques found in the literature, with summary of main contributions and limitations in the reviewed articles. At every stage, a brief summary of the contributions made in this thesis to address these issues is presented.

## 2.4 Related Literature

The expected rollout of 5G networks and its use cases in 2020 demands an urgent need to develop a combination of solutions to mitigate interference created by the coexistence

of these devices. Distributed solutions using self-optimization network (SON) are currently in use to effectively manage inter-tier interference and achieve load balancing in 5G dense networks [65]. Major benefits of this approach are the ability to provide reliable and low delay backhauls for densely deployed small cells. Moreover, ultra-fast backhauls are also crucial in the exchange of very large volumes of data between small cells and the core network. Although, indoor femtocells can use low-cost backhauls relying on the existing digital subscriber line (DSL), this approach would lead to degradation in the overall network performance and QoS of users. As pointed out in subsection 2.3.2, backhauls remain one of the major challenges mitigating the widespread deployment of small cells. Indeed, different types of nodes and communications are currently being adopted to support dense small cell architecture. One of such is device-to-device (D2D) communications which establish seamless and high-speed connections among wireless devices by exploiting the available spectrum. Some benefits of D2D communications include improved communication delay, traffic reduction in the core network, efficient spectrum and energy utilization. In addition, D2D offers support for various emerging technologies such as proximity-based social networks [66], public safety [67, 68] and vehicle-to-vehicle (V2V) communications [69, 70]. The introduction of D2D creates a two-tier network architecture which comprises of the conventional macrocell layer which involves communication between the BS and UE, and the unplanned D2D layer comprising randomly distributed D2D UE (DUE) and cellular UE (CUE). Hence, interference management becomes a critical issue in D2D communications when the same radio resources are shared between DUEs and CUEs.

In this thesis, interference management techniques and solutions in the envisioned 5G UDN are studied under cell/user association/load balancing, power control and user pairing approaches.

### 2.4.1 Interference mitigation via traffic offloading

The exponential growth in the number of wireless devices imposes a lot of demands for network capacity and effective interference management solutions. In recent years, various mathematical theories have been employed to decide the optimization objective, complexity, performance and study the best network selection techniques for wireless networks. However, current cell association techniques in use for interference management in legacy networks may not provide the required enhanced performance expected in ultra dense deployment of small cells. Therefore, finding effective methods to tackle the cell association problems towards interference mitigation in this new paradigm shift is a hot research topic. Cell association in OFDMA co-channel networks is referred to with different terms in the literature as cell selection, cell assignment, user association, BS assignment, and cell-site selection. User association and cell selection are used interchangeably throughout this thesis. For the purpose of clarity, Figure 2.5 shows various research directions where user association schemes are implemented [71].

The work in [25] demonstrates the offloading benefits of biased user association between macrocell and small cells in terms of the attainable fairness and capacity improvement. Cumulative distribution functions (CDFs) of the difference in DL SINR between the

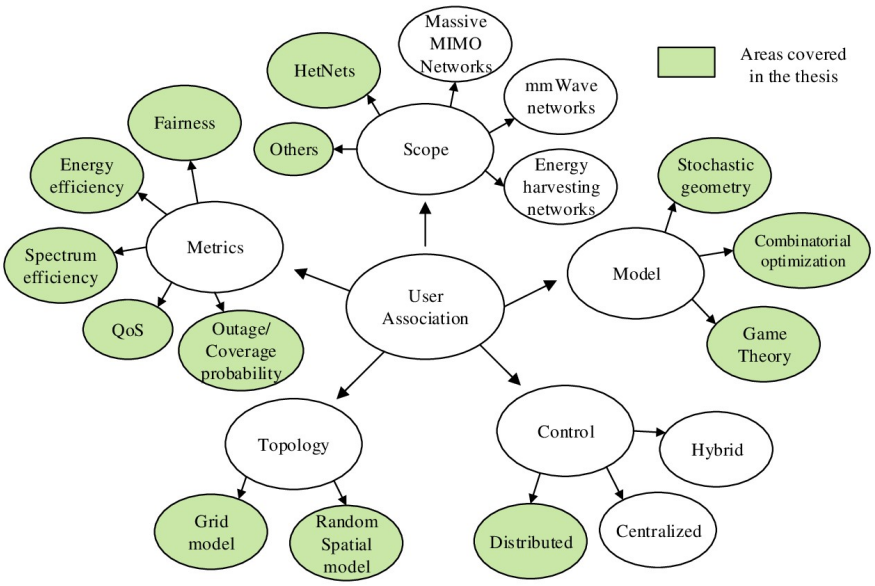


**Figure 2.5:** User association algorithm framework for interference mitigation in 5G UDN [71].

macrocell and small cells are captured as a continuous function of the CRE bias. This semi-analytic approach is used with ICIC to investigate the offloading benefits and improvement in network performance. The number of macrocell users (MUEs) that are offloaded to small cells, e.g., picocells, for a given range expansion bias (REB) are captured with the CDF. Based on this information, the 5th percentile user capacity and the total system capacity was evaluated as a function of the REB. However, the group of offloaded users to small cells as a result of additional bias value experience strong interference from the neighbouring macrocells, especially when these users are located at the cell edge. Thus, the offloading benefits might be compromised by the strong interference. Hence, the bias value has to be properly selected to achieve a balance between load balance and overall throughput of the network. A more tractable cell association framework for SINR analysis in the DL of heterogeneous network using Q-learning was developed in [72]. The idea is to find the

optimal bias value that minimizes the number of users in outage based on learning from individual user's past experience, and depending on the available radio resources between the MeNBs and small cells. Several other interference mitigation schemes to optimize both the bias value and the eICIC resource partitioning in HetNets have been proposed in the literature [73–75].

- **Outage/Coverage Probability Solutions:** This is the main performance metric employed to evaluate user's performance in wireless network. Outage/coverage probability is often combined with stochastic geometry in user association to achieve optimal spectrum allocation and maximized network throughput subject to different load conditions [76, 77]. In this context, numerical evaluation techniques were employed on multi-tier DL HetNets to determine the optimal bias value based on the highest SINR and coveage rate. The authors in [74] proposed a framework that analyses joint resource partitioning and offloading in a two-tier network topology, with the capability of extension to multi-tier setting. Each tier of BSs and UE locations were modeled as an independent Poisson point process (PPP), with each tier differing in deployment density, transmit power and pathloss exponent. These assumptions provided an insight to formulation of rate complementary CDF (CCDF) as a function of the resource partitioning parameters and CRE, for the determination of the most appropriate spectrum partitioning ratio. The authors however concluded with the following observations: (1) increasing small cell density decreases optimal bias association with resource partitioning, (2) rate coverage from optimal bias association has no effect on small cell density when resource partitioning is not applied, (3) fraction of offloaded

users in both cases above increases with increasing small cell density, and (4) optimal bias association decreases with decrease in backhaul capacity. Further extension on the above work were carried out in a multi-tier network for improvement on the spectrum partitioning and user association in terms of the achievable coverage probability [75] and also the coverage with a certain throughput guarantee [78]. Contrary to the aforementioned works, joint user association and resource allocation problem was studied for both UL and DL interference-limited scenarios in [79]. The spectrum partitioning ratios and optimal user association bias factor were obtained through coverage rates to maximize the theoretical mean proportional fair utility. The result revealed that optimal result can be achieved in a distant-based user association under some network parameters such as the power control and path loss. In addition, the result showed that the DL and UL asymmetry does not have effect on the user association outcomes, provided that all tiers are able to attain their target SIR. Therefore, the proportion of users associated to a tier should match the optimal proportion of spectrum allocated to the affected users. Simulations showed better performance of the resource partitioning in the DL in terms of utility, while performing better in the UL with power control.

### 2.4.2 Interference mitigation via Power control

Resource allocation has become an essential research topic since the adoption of OFDMA as the radio access technology for the current and future generation wireless networks. Research focus has been on resource allocation under rate and fairness constraints before the

emergence of small cell densification. However, research in the recent literature has proposed resource allocation algorithms for co-channel deployments in a multi-tier environment. In majority of these cases, the formulated resource allocation optimization problems are mixed integer utility function problems which are generally NP-hard due to restrictions on some constraints. Hence, to reduce the complexity and find the sub-optimal but efficient solutions that satisfy fairness and QoS requirements, the best way is to decompose the resource allocation optimization into resource and power allocation sub-problems. Thus, the essential requirements for multiple access design and optimization in wireless networks are to [80]:

- maximize fairness among the nodes,
- maximize network throughput,
- minimize delay, and
- improve energy efficiency through power management.

In general, the optimization problem aims to solve resource and power allocation problems subject to power, spectrum and QoS constraints. Although, intra-cell interference is mitigated in the DL transmission through the use of OFDMA, users still suffer from severe inter-cell interference when they are allocated the same time and frequency resources. The cell-edge users are the most affected because of their proximity to nearby cells. Traditional power control schemes employed in two-tier networks are not sufficient and robust enough to mitigate interference in dense small cell deployment. For instance, the approach employed by users based on channel inversion causes remarkable degradation of small cell SINR due to

power variation between cell-edge users and the surrounding small cells. Instead, dynamic power control proves more effective than allocating a fixed power to the BSs.

The work in [81] studied power control using a decentralized dynamic ICIC method to dynamically allocate bands to cell-edge users through message signaling over X2 interface. The idea behind this approach is the complicated and variable shape of cell area in communication environment which changes user distribution patterns. Cell-edge bands selection therefore becomes difficult and requires optimization based on the time-varying environments. Hence, the approach accounted for control delays in the surrounding to achieve increased throughput by autonomously optimizing FFR parameters in the system. In [82], a meta-heuristic-based DL power allocation algorithm was proposed to guarantee the required QoS and minimize the average inter-cell interference level by power control tuning in each cell. Since the complexity of the evolutionary algorithm grows with the number of cells, the authors further proposed a solution based on stochastic search to perform an efficient exploration of the search space. In contrast to majority of the previous literature, this work makes no assumption on both the propagation conditions and network topology, which makes it flexible to be employed in any realistic deployment. In addition, several performance metrics such as power consumption, cell-edge and average per-cell capacity were simultaneously optimized in the methodology. Simulation results showed an achievement in effective network-centric optimization of the proposed framework in terms of reduced energy consumption. In wirelss communications, green communication and energy efficiency are important and promising research topics for the realization of 5G goals. Green communication concerns routing adaptation, information sharing, energy/spectrum

awareness, and data caching to save energy and maintain balance in the resource utilization of both mobile and wireless networks [83]. To this end, power control algorithms provide a good means to improve both spectral and energy efficiency. A game theoretic power control framework was investigated in [84] to improve energy efficiency and reduce power comsuption, thereby maintaining the interference level below a given threshold. The formulated game is distributed and incorporated location-aware weighted bargaining with a denoted balancing factor. In this work, location-aware weighted bargaining in conjunction with utility function were demonstrated to be an important performance metrics for the future 5G UDN. The convergence of the algorithm established an effective trade-off between efficiency and fairness, in addition to satisfying each user's QoS requirement.

Several power control algorithms exist in the literature to achieve different QoS objectives and enhance the performance of DL OFDMA system[85–90]. These algorithms are implemented either as joint power control and scheduling or as joint power and UE association for ICIC in the DL OFDMA or UL SC-FDMA. Recently, non-orthogonal multiple access (NOMA) was proposed as a strong candidate technology for the 5G cellular networks. The primary reason for adopting NOMA in 5G owes to its ability of simultaneously allocating the same frequency and time resources to multiple users in the same cell. NOMA techniques exist both in power and code domains. Power domain NOMA achieves interference cancellation at the recievers through SIC technology with throughput gains of around 20% reported in the literature, whereas multiplexing is attained in code domain NOMA [91]. However, a major drawback to the application of NOMA is how to allocate transmit power and determine whether a frequency resource block should be allocated to multiple users in

their respective cells. To address this problem, the authors in [92] proposed a low complexity user pairing and power allocation (UPPA) algorithms to improve the one earlier proposed in [93] where the complexity is proportional to the number of users. The algorithm adopts a fixed power allocation to pair two users based on their channel conditions and proportional fairness priority coefficient. Simulation results showed the algorithm to reduce interference and achieve high throughput gains in the network with lower achievable complexity that is not affected by the number of users. Although, in-depth research about NOMA is still at its infancy, some of its recent applications towards interference mitigation in 5G are found in mm-Wave [94], WiFI technologies [95] and virtualized wireless networks (VWNs) [96].

### 2.4.3 Interference mitigation via User Pairing approach

In view of the cross-tier interference introduced in HetNets due to the frequency reuse among cells, user diversity gain of user pairing (UP) approach has been exploited to alleviate interference in wireless networks. User pairing is usually used in conjunction with power control algorithms in order to achieve the desired network performance in terms of deployment environment, sum rate gains, and high throughput with minimum implementation complexity. However, achieving an optimal solution for joint optimization under single-input single-output (SISO) and multiple-input multiple-output (MIMO) systems is challenging. Generally, the easiest UP algorithm is random pairing where users are randomly selected by the BS to form clusters [97]. Although, this algorithm offers low computational complexity at the cost of optimal sum rate performance as a result of not taking into account the users'

channel gains. Several applications of UP abound in Full Duplex (FD) networks [98–100], two-tier HetNets [101], D2D [102], and V2V communications [103, 104].

Considering the advantage of FD network in servicing both DL and UL users by same resources efficiently, a resource allocation optimization problem can be implemented to minimize transmission completion time in FD. Two issues addressed with this approach are self-interference and user-to-user interference [98]. A low complexity user scheduling algorithm with power control was proposed to find the optimal power by relaxing interger problem to real number problem. The result showed a remarkable reduction in interference coupled with achievement in spectral efficiency. In [101], non-cooperative game theory was employed to solve the problem of cross-tier interference. The algorithm was designed to alternately schedule high channel gain macro-tier users and low channel gain femto-tier users to be active in one time slot and inactive in the next time slot. Numerical results demonstrated overall improvement in the average macrocell capacity and an increase in the percentage of femtocells that were able to surpass their SINR threshold.

Cellular communication network underlaid with D2D has currently emerged as a promising solution towards increased capacity and to extend network coverage area. However, introducing D2D in cellular communication networks exposes terminals to more severe interference due to resource sharing between D2D UE (DUE) and cellullar UE (CUE). Analysis and mitigation of such interference problem exploring UP approach formed the basis of the work presented in [102]. Two power control methods (PC-1 and PC-2) were proposed to determine whether to reduce or increase the transmit power level of BS or transmitter of D2D pair based on the estimated current SINR. Results of these two power control methods

in terms of Cumulative Distribution Function (CDF) of SINR showed improved performance over various numbers of CUEs and D2D pairs with and without power control. Unfortunately, this work did not consider Bit Error Rate (BER) and throughput performance in order to capture the effect of modulation and detection levels due to frequency reuse in the system.

In a similar manner to D2D, V2V underlay cellular communication possesses the ability to increase special efficiency (SE) by reusing network spectrum. This also leads to serious interference between cellular and V2V communications if not properly designed. To address this issue, many studies focused on designing instantaneous resource allocation to mitigate the interference. In realistic setting, what the CUEs are interested in for capacity maximization is the amount of data transmitted at every access to the BS. Maximizing the network capacity can be done in two ways during one access period: dynamic allocation and position ergodic maximization schemes [103]. In dynamic allocation, resource allocation is performed once at every sampling time after which all the maximized capacities are averaged to obtain the average capacity. On the other hand, position ergodic capacity performs resource allocation at one time only after deriving an expression for CUEs' capacity expectation, considering all possible positions. Both schemes can be applied to freeway and urban environments, although, channel variations and implementation complexity are factors to consider when making a choice. Wang *et al* considered the freeway scenario in studying the resource allocation that maximizes the position ergodic capacity of CUEs. Following the derivation of expression for the poisition ergodic capacity maximization of CUEs, a resource allocation optimization problem was formulated to maximize the capacity of all CUEs and vehicular UEs (VUEs), subject to different QoS constraints. The optimization problem

was thereafter decomposed to power allocation and user-pairing subproblems and a robust algorithm designed to solve it. Finally, simulation results showed that the algorithm was capable of reducing computational cost while maintaining better performance.

Recently, the introduction of massive MIMO as one of the key technologies for 5G cellular networks has led to increase in SE, when the same cellular spectrum is used by both CUEs and VUEs. Therefore, V2V underlay massive MIMO networks is a promising way to provide low latency and more reliable vehicular communications. However, the inter-cell interference introduced when several CUEs and VUEs share the same spectrum may become severe if not properly managed. Managing this interference from the perspective of geometric programming technique formed the basis of the work in [104]. The authors formulated a large-scale fading based power control and user-pairing mechanism for different SE constraints for both V2V pairs and CUEs, by considering both perfect and imperfect CSI and SEs for MRC and ZF. While the simulation results showed a significant improvement in reliability and SE of V2V transmission, there is a slight degradation in the achievable sum SE, compared to the fixed maximum power scheme. In addition, it was shown that ZF outperformed MRC because of its interference supression capabilities.

### 2.4.4 Discussion

The literature discussed above have attempted to address the problem of interference in wireless communication system. Due to the coexistence of different systems and services in wireless networks, coupled with the high cost of frequency bandwidth, spectrum reuse becomes inevitable in order to maximize the spectrum utilization. Common types of

interference arising from spectrum sharing in wireless system are self interference, multiple access interference, adjacent interference and co-channel interference, among others. Based on the interference types described above, sources of interference could be from other BS operating in the same frequency band and/or mobile terminal within the same cell. Different techniques have been proposed to address these interference problems in cellular networks, with many performing more effectively in some application areas while others show strong performance in other areas of operation. Despite the above, interference challenges still persist in communication networks. Added to the challenge is how to implement some state-of-the-art interference mitigation techniques such as FFR, SIC and CoMP in the 5G technology with expected huge capacity and network size. Also, there is a common consensus in the research circle that no single technique is capable of mitigating interference because of the interference dynamics in cellular networks. Hence, combination of these schemes is desirable in the management of interference in the envisioned 5G UDN. This formed the basis of the solution proposed in this research towards an effective interference management with low complexity implementation.

## 2.5 Chapter Summary

The problem of interference in dense small cell regime arises due to different cell boundaries and massive sharing of the frequency spectrum within the cells. This chapter outlined several interference management techniques, including main contributions and milestone proposals towards significant solutions for combating ICI which are expected to be employed in the 5G communication technology. The chapter also provided considerable insights into different

approaches that have led to categorizing interference into either practical, theoretical, interference cancellation, coordination or avoidance schemes. In this context, definitions of different user association and power control schemes as well as interference management techniques in HetNets proposed by 3GPP are succinctly presented. In particular, the coordination and avoidance techniques which require the application of certain restrictions on the resource allocation in a coordinated manner between the cells for the purpose of interference mitigation. The restrictions are usually applied in time, frequency and power domains. The impact of these schemes on the communication link quality was also revisited. Most of the literature reviewed proposed joint and cooperative use of frequency domain signal orthogonalization, time domain coordinated scheduling, and spatial domain cell coordination with advanced antenna diversity to mitigate interference dense small cell regime [34, 42, 56, 71]. Specifically, Section 2.3 highlighted some major technical challenges and key enabling technologies for interference management in 5G UDN. Finally, major contributions of traffic offloading, power control and user pairing techniques for interference mitigation in the past years were investigated in Section 2.4, with in-depth highlight of the missing parts and suggestions for improvement in future studies. Basically, these three areas form the core topics of investigation in Chapters 4, 5 and 6 of this thesis. A summary of the existing subchannel allocation techniques with different components used to mitigate interference is presented in Figure (2.6).

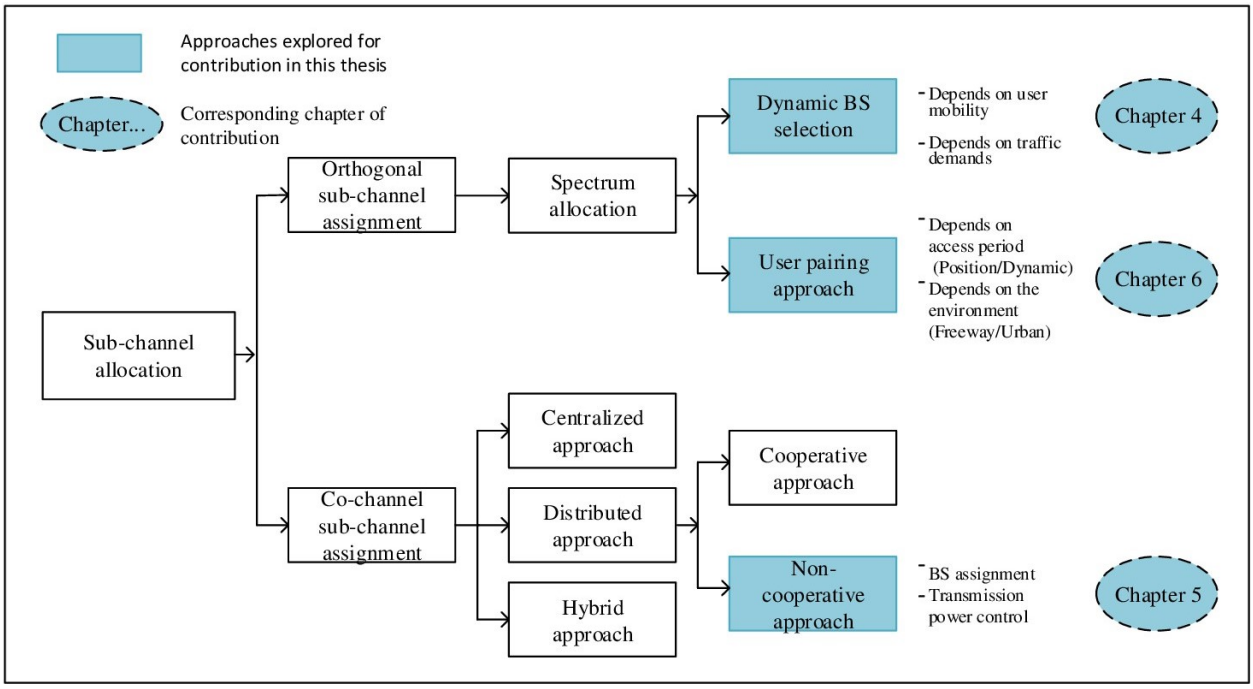


**Figure 2.6:** Chart illustrating the existing resource allocation towards interference management and the contribution of this thesis

# Chapter 3

# Fundamental Concepts in Interference Modelling and Analysis

## 3.1 Introduction

Mitigating interference at all levels in wireless system requires adequate knowledge of the channel and system models. In addition, basic performance evaluation metrics are important to access the performance of any approach employed for interference management. This chapter introduces the fundamental concept of LTE cellular architecture focusing on frame structure, protocol architecture, network architecture, communication channel and OFDMA technology. Also, channel models, system models and performance metrics commonly used for performance evaluation in wireless networks with concepts of several candidate technologies and architectures for enabling 5G networks are presented.

## 3.2 Literature Review

The success of network densification largely relies on the effective integration of small cell with the existing mobile access architecture for provision of seamless device-to-core connectivity. Thus, new network structures capable of providing requirements such as scalability, security, transparent integration and limited backhaul capacity are needed to meet the expected 5G demands [105]. These requirements have been extensively discussed in Chapter 2 of this thesis. Also, considering the huge variation in the implementation details of small cell architecture, having a consistent design approach to support compatibility becomes imperative. To address this challenge, the Femto Forum network architecture incorporated a reference model for small cells that contains all the network elements and interfaces [106]. In small cell networks, communication between UEs in different tiers results in various levels of interference. The most severe being cross tier interference due to significant variation in the transmit power level. The severity of the interference also depends on the radio frequency allocation option - whether orthogonal frequency allocation, partially shared spectrum allocation [107] or co-channel frequency allocation [108]. However, current demand for improved spectral efficiency, ultra low latency and massive device connectivity has birthed non-orthogonal multiple access (NOMA) as a new access technique in 5G UDN. The concept of NOMA is to allow some degree of multiple access interference at the receiver for capacity enhancement [109]. Due to the complexity of cellular networks driven by increasing connectivity, defining and understanding appropriate metrics for performance analysis has become complex. Metrics play important role in the analysis, design, management and operation of wireless networks [110]. To this end, the following

sections present comprehensive overview of 3GPP LTE architecture, state-of-the-art access techniques and performance metrics examined in this thesis.

## 3.3 LTE Cellular Architecture

LTE represents a collective name given to standard of next generation evolution of wireless technology deployed to provide high-speed wireless data communication, low latency in Radio Access Network (RAN), improve bandwidth and spectral efficiency. It consists of four domains viz: user equipment (UE), Evolved Packet Core (EPC), Evolved UTRAN (E-UTRAN) and Service domain [111]. The UE, EPC and E-UTRAN form the Internet

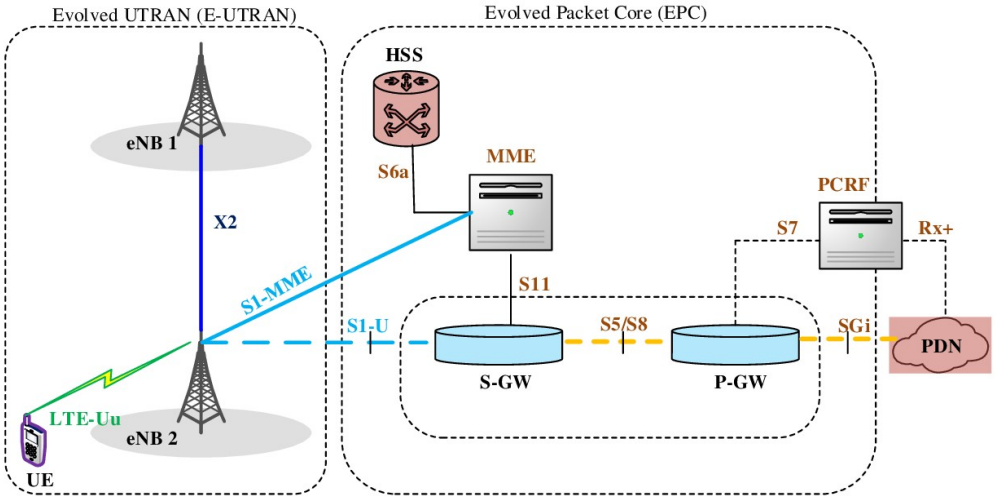


**Figure 3.1:** 3GPP LTE Evolved Packet System Elements [111].

Protocol (IP) based connectivity layer which are also referred to as the Evolved Packet System (EPS) as shown in Figure 3.1. The E-UTRAN consists of several evolved NodeBs (eNBs) BSs distributed throughout the coverage area of the network to manage and control all EPS functions. The eNBs provide a layer two connectivity between the EPC and the

UE, and are interconnected by the X2 interface which is used for handover and dynamic interference management. In addition, the eNB initiates the Radio Resource Connection (RRC) and performs prioritized QoS radio resource allocation to UEs in both DL and UL, termed scheduling. It also routes user plane data towards the Serving Gateway (S-GW). This scheduling function of eNB is to simplify network structure and reduce latency. On the other hand, the LTE-Uu and S1 interfaces connect the eNB to the UE and EPC, respectively. Other functional elements of the LTE architecture are Mobility Management Entity (MME), Serving Gateway (S-GW), Packet Data Network Gateway (P-GW), Policy and Charging Rules Function (PCRF) and Home Subscriber Server (HSS).

### 3.3.1 LTE Protocol Architecture

The 3GPP radio protocols were designed to set up, reconfigure and release the radio bearers facilities needed to maintain end-to-end connection and communication between UE and the network. The protocol architecture can be divided into control and user plane protocol stacks as shown in Figure 3.2. It consists of the physical layer, data link layer and the network layer located in Layer 1, 2 and 3, respectively [112]. In the control plane, Layer 2 contains the Packet Data Convergence Protocol (PDCP), Radio Link Control (RLC) and Media Access Control (MAC). However, Layer 3 of the control plane only consists of the Radio Resource Control (RRC). The functional elements of the control plane are Packet Data Convergence Protocol (PDCP), Radio Link Control (RLC), Radio Resource Control (RRC), Medium Access Control (MAC) and Physical Layer (PHY).

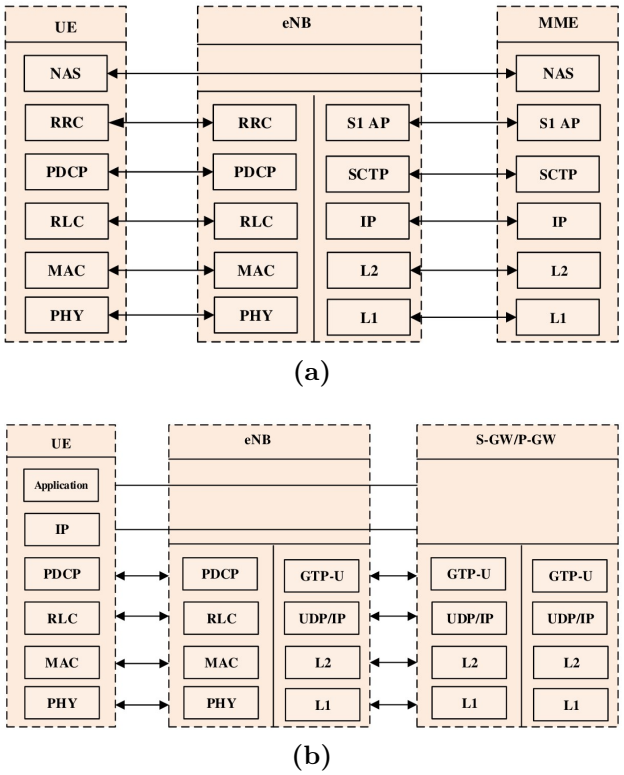


**Figure 3.2:** LTE Protocol Stack for [112] (a) Control-plane (b) User-plane

### 3.3.2 LTE Frame Structure

The LTE frame structure operates in two topologies as either Type 1, applicable to FDD or Type 2 application for TDD as illustrated in Figure 3.3. The total frame duration is 10 milliseconds with a total of 10 subframes in a frame and each frame containing 2 time slots. In addition, one subframe duration is 1ms, while two consecutive time slots in a frame will form one subframe with 10 of such subframes forming one radio frame. The Type 1 FDD topology comprises each of 0.5ms slots, making up of total 20 slots. On the other hand, Type 2 TDD contains two half frames, with total frame duration of 10ms and 5ms duration each, resulting in10 ms total frame duration. Subframes #0 and #5 are respectively used by the DL transmission for both Type 1 and Type 2. Comparatively, Type 2 has flexible

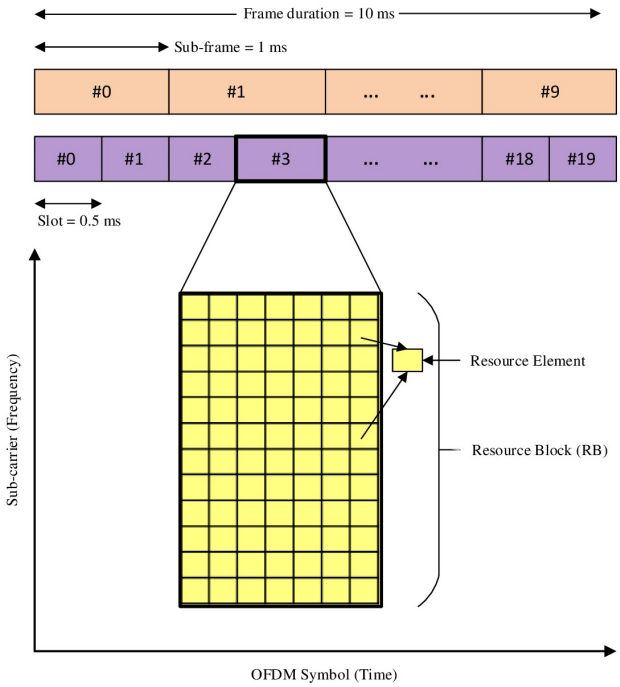


**Figure 3.3:** LTE Frame Structure [113].

configuration for some special subframe and UL-DL ratio. The frame structure described above requires a special global timer for network control and synchronisation [114]. In LTE, the resource block (RB) is the minimum scheduling unit for the DL and UL transmission One RB consists of one sub-frame in the time domain at interval of 1-ms, called Transmit Time Interval (TTI) and 12 sub-carriers in the frequency domain each with bandwidth of 15-KHz. Therefore, 100 RBs make up one TTI in the frequency domain while the time domain contains 14 OFDM symbols. Demodulation of data channel and control in the DL and mobility measurements are carried out by the common reference signal (CRS).

### 3.3.3 The X2 Interface for connectivity among eNodeBs

Communication and information sharing is possible through interconnection of various nodes in the LTE network via X2 interface. Two eNodeBs such as macrocell and picocell can

share information necessary for the implementation of interference coordination algorithms for network enhancement. The medium of connection in practical implementation scenario are either microwave, Ethernet or fibre. The performance of implementation algorithm for latency and throughput requirements depends on the type of medium employed for connection in the network [115]. For example, a high latency medium may not perform reasonably well in a case where fast interference information is exchanged between the eNodeBs such as the dynamic interference coordination algorithm. Two types of information that can be exchanged over the X2 interface are:

- **Interference and Load information:** Load balancing aims to ease congestion by uniformly distributing UE traffic load among eNodeBs. Bandwidth usage pattern in real-time and non-real-time between the eNodeBs can also be exchanged for information related to load condition. This information is useful for the eNodeBs both in the DL and UL to report real-time interference experienced by eNodeBs, perform joint load balancing through cell re-selection optimization and handover for existing associated and prospective UEs.

- **Handover information:** The X2 interface is also responsible for the UE handover between two eNodeBs. However, the core network can manage handover between eNodeBs in the absence of the X2 interface.

## 3.4 Orthogonal Frequency Division Multiple Access (OFDMA)

The limitation on capacity and throughput in legacy networks motivated the development of OFDMA as the access technology for 3GPP LTE network. The wireless network is a multi-user system that is constrained by limited bandwidth and number of channels. Thus, the available radio resources must be shared among multiple users in the network. In OFDMA technique, the implementation of multi-user communication in Orthogonal Frequency Division Multiplexing (OFDM) is extended to allocate subcarriers to different UEs simultaneously so that multiple UEs can receive data at the same time [115]. In other words, the sub-carriers are arranged in overlapping manner to mitigate the inter-symbol interference (ISI) caused by neighbouring channel to each sub-carrier Besides, reference symbol and control channel are spread in such a way to aid in the determination of channel response propagation and also convey network information.Some of the advantages of OFDMA are provision for multi-user diversity, efficient spectrum utilisation, receiver simplicity and better Bit Error Rate (BER) performance in fading environment. However, despite the advantages, OFDMA needs to overcome the problem of timing synchronization between users to prevent errors in the system. In addition, OFDMA needs to deal with the problem of co-channel interference and Peak-to-Average-Power-Ratio (PAPR) that occurs in the frequency domain. Among the methods used to reduce PAPR are stochastic selective mapping (SLM) and partial transmit sequences (PTS) [116].

## 3.5 Non-orthogonal Multiple Access (NOMA)

The existing cellular networks apply orthogonal multiple access schemes either in frequency, time or code domains. However, these access techniques may not meet the increasing demand expected from the future radio access technologies. This has led to the development of NOMA as a candidate access technique to meet the requirements of 5G systems [117]. NOMA is different from other access techniques in that it allows each UE to be distinguished by their power levels when they operate at the same time and in the same band as can be seen in Figure 3.4a. The SIC receiver then partitions the UE in the DL and UL channels through the use of superposition coding at the transmitter.

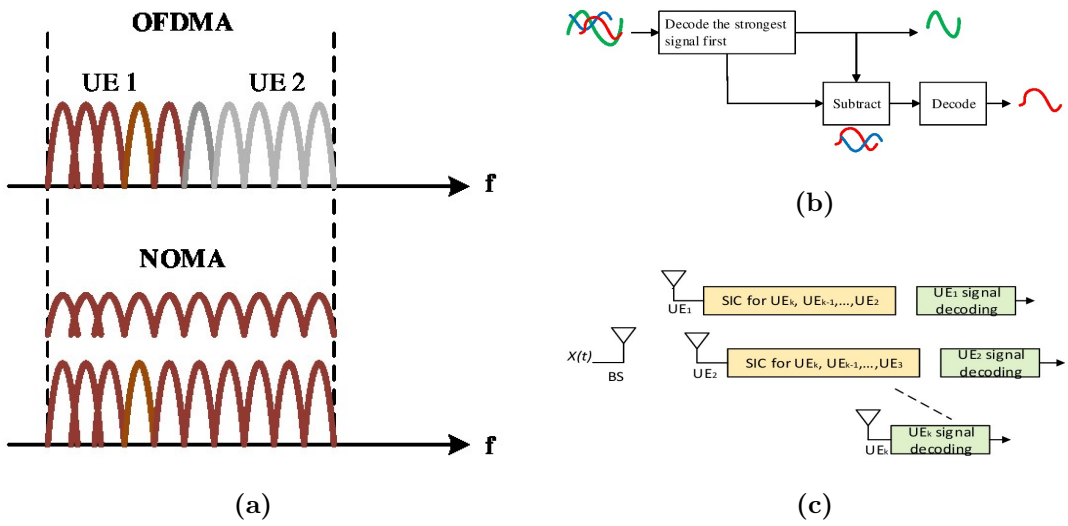


**Figure 3.4:** NOMA Implementation [117] (a) NOMA and OFDMA spectrum sharing for two users (b) Successive interference cancellation (c) DL NOMA approach for K-users

Implementation of NOMA is different for DL and UL transmissions. In the DL, each UE uses SIC to decode their signal after the information waveform has been superimposed by the BS for its intended UE as shown in Figures 3.4b and 3.4c. Moreover, UE located far

away from the BS receives high power while less power is allocated to the UE located near the BS. This allows close UE to cancel out the signal of the UE located far from the BS.

However, in the UL NOMA, the BS uses SIC to differentiate individual user's signal. The BS first decodes the signal emanating from the nearest UE and lastly decodes signal for the UE located far off. NOMA technique is not without imperfections, some of which are error propagation, decoding complexity, quantization error, residual timing offset and power allocation complexity [118]. Details on NOMA and its implementation towards enhanced performance in 5G networks form the basis of the proposed solution presented in Chapter 6.

## 3.6 System Model

The first step towards analysing and conducting performance evaluation on the network is through system modeling. A quality system model provides the best platform by simplifying the experimental processes in order to estimate and characterise network for theoretical analysis. Thus, the outcome from such analysis can serve as a guide for network engineers to effectively translate network planning into a realistic setting and at the same time improve the existing system.

### 3.6.1 Channel Model

The propagation channel in wireless system can be classified in different ways to encompass multpath fading, distance-dependent path-loss and log-normal shadowing The channel gain

between a UE $j$ and its serving BS $k$ in an outdoor link or between an access point (AP) $k$ and its served UE $j$ in an indoor link is expressed by [113]

$$g_{j,k} = K_{j,k} d_{j,k}^{-\alpha} \Upsilon_{j,k} h_{j,k} \tag{3.1}$$

where $d_{j,k}$ denotes the distance between UE $j$ and BS $k$, $h_{j,k}$ is the power gain of the multipath fading channel, the log-normal shadowing from UE $j$ to BS $k$ is $\Upsilon_{j,k}$, and $\alpha$ denotes the path-loss exponent which depends on the type of propagation environment, whether indoor, indoor-outdoor or cellular. The channel gain in an outdoor-to-indoor link between a macro BS and its UE requires that the effect of penetration loss $P_L$ be accounted for, so that the channel gain can be given by

$$g_{j,k} = K_{j,k} d_{j,k}^{-\alpha} \Upsilon_{j,k} h_{j,k} P_L^{MBS} \tag{3.2}$$

Similarly, the link gain in an indoor-to-indoor environment between an AP and its UE in another AP is given by

$$g_{j,k} = K_{j,k} d_{j,k}^{-\alpha} \Upsilon_{j,k} h_{j,k} P_L^{AP} \tag{3.3}$$

The aforementioned represent fading wireless radio channel where the transmitted power threshold is above the received power of the desired signal. However, the signal strength of the communication channel can also take the form of Additive White Gaussian Noise (AWGN) where the transmitted power and the received power of the desired signal almost have the same magnitude [113].

### 3.6.2 Multipath Fading Effect

Multipath fading is a phenomenon that describes the effect of rapid fluctuations and variations in amplitude and phase of power received in wireless system. Such fluctuations and variations occur due to addition of several multipath signal components either constructively or destructively [119]. Generally, multipath is small scale fading owing to its occurrence in a short period of time and distance compared to shadowing and path-loss impairments. Some factors influencing multipath fading are UE speed, atmospheric ducting, transmitted signal bandwidth, spatial channel and surrounding objects speed. This results in signal phase shifting as well as constructive and destructive interference, resulting in Rayleigh fading modeled as standard statistical Rayleigh distribution.

## 3.7 Modeling Technique in UDN

### 3.7.1 Stochastic Geometry

The stochastic modeling has shown in recent times as a tractable performance mechanism for small cell dense network. The deployment of small cells in an unplanned manner results in their random placement and provides an insight into modeling their positions as a point process (PP) in 2 or 3-dimensional Euclidean space [20]. Moreover, interference characterization design and modeling in dense networks can be achieved with stochastic geometry models. This is as a result of stringent and tractable interference model required for the design and analysis of interference management and avoidance techniques in the dense cellular network. In addition, capacity variation in both network and link channels

in environments such as parks, downtowns, rural, sub-urban and residential areas prevents the BSs from maintaining a grid-based model. Hence, the adoption of stochastic geometry provides an efficient way to model, analyse and design networks with random topologies. In particular, stochastic geometry has been used in the past to model and analyse shared access systems such as ALOHA, carrier sensing multiple access (CSMA), single and multi-tier networks, and cognitive networks [120]. The power law representing the distance dependent signal power decay between the transmitter and receiver in a wireless system is given by

$$P_d(z) = P_t(y) K h_{yz} ||y - z||^{-\alpha} \tag{3.4}$$

where $y \in \mathbb{R}$ and $z \in \mathbb{R}$ denote the spatial locations of the transmitter and receiver, respectively, $P_t(y)$ represents the transmission power as a function of the transmitter location, $h_{yz}$ denotes a random variable representing random power gain between two locations $y$ and $z$, while $\alpha, ||.||$, and $K$ are path-loss exponent, Euclidean norm and propagation constant, respectively. The expression in (3.4) is simple and possesses singularity at the origin, hence regarded as the unbounded path-loss model and only used to calculate power received at the far field [20]. However, a more complicated but practical alternative bounded path-loss model is often used for analysis purpose. It is expressed as

$$P_d(z) = \frac{P_t(y) K h_{yz}}{\delta + ||y - z||^{\alpha}} \tag{3.5}$$

where the singularity at the origin is avoided by setting $\delta > 0$. This makes sense as the performance of the wireless network highly depends on the network geometry, which in

turn, is dependent on nature of the wireless medium and signal power decay. In other words, the SINR experienced by a receiver is highly affected by the network geometry, as the interference perceived by a test receiver is influenced by the test receiver's position in relation to positions of other network entities sharing the same channel simultaneously. Therefore, the SINR experienced by the receiver in the network is given by

$$\gamma(z) = \frac{P_t(y_o)Kh_{y_oz}||y_o - z||^{-\alpha}}{\sum_{y\in\mathcal{I}} P_t(y)Kh_{yz}||y - z||^{-\alpha} + N} \tag{3.6}$$

where $y_o$ and $z$ are locations of desired test transmitter and receiver respectively, $N$ is the noise power, $\mathcal{I} = \{y_1, y_2, ...\}$ denotes the set of interferers location and $\sum_{y\in\mathcal{I}}$ is the aggregate interference power seen at the receiver. The intensity and locations of $\mathcal{I}$ (interferers) solely depends on the medium access control (MAC), number of channels, network topology, user association and access systems such as CDMA, CSMA, TDMA and ALOHA [20]. However, to gain more confidence in modeling wireless network with stochastic geometry, the model needs to capture more system parameters. For example, most of the system models used in the literature only consider simple network characteristics such as single antenna and channel, and DL transmission with PPP distributed BS. Therefore, to derive the full potentials of stochastic geometry, it is essential to exploit advanced system models characterized by multiple channels, MIMO techniques, power control, CoMP and different resource allocation strategies. Other approaches to exploit are: (1) adoption of PP that provides more tractable modeling by accurately capturing cellular networks characteristics, and (2) to explore more options for the performance metrics and coverage probability beyond the Shannon's capacity

theorem [120]. Solutions based on stochastic geometry model in vehicular communication are presented in Chapter 5 of this thesis.

## 3.8 Performance Metrics in UDN

This subsection explains some commonly used performance metrics to model problems in UDN. These metrics are used throughout this thesis and are basically divided into two major related groups as SINR and rate groups. The SINR group comprises the coverage and outage probabilities while the rate group involves area spectral efficiency, average spectral efficiency (ASE) and the rate coverage.

### 3.8.1 SINR metric

The SINR is an important metric to measure the received signal power in comparison to the total interference power and the noise level. In addition, SINR can also be considered as a reflection of the transmission channel quality. For instance, in the DL transmission, assume a user to be located at the origin and a random distance $d$ from its serving BS, then the SINR can be given as [121]

$$\gamma = \frac{P_t h d^{-\alpha}}{\sum_{i \in \Phi/k} P_i g_i d_i^{-\alpha} + \sigma^2} \triangleq \frac{P_t h d^{-\alpha}}{I_r + \sigma^2} \tag{3.7}$$

where $P_t$ is the transmit power of the serving BS, $P_i$ is the transmit power of the interfering BSs, $I_r$ is the sum of interference from all other BSs except the serving BS $k$ of the UE at the origin, $\alpha$ is the path-loss exponent, $d^{-\alpha}$ denotes the large-scale fading, $h$ and $g$ are the

channel gains influenced by small-scale fading and shadowing effect, respectively, and $\sigma^2$ is the constant AGWN value. It can be inferred from (3.7) that the strength of signal received by a UE is strongly affected by interference from other BSs $I_r$, distance between UE and BS $d$ and the transmit power level $P_t$. In interference limited system, the noise power is ignored so that only the signal-to-interference (SIR) is calculated.

### 3.8.2 Coverage/outage probability

The probability of coverage, also termed as the success probability, is defined as the probability that grants a user the ability to achieve a SINR higher than certain SINR threshold $T$ (i.e., $P(SINR > T)$). In other words, it signifies that the link is good enough to maintain a successful connection that guarantees a considerable level of QoS in the network. The inverse of coverage probability is the outage probability or the SINR distribution which is the probability that the SINR of a user is below a given threshold value $T$ (i.e., $P(SINR < T)$). A user is considered to be in outage only if the SINR of the connection link to its serving BS is not strong enough to maintain successful connection. Therefore, the coverage/outage probability signifies the link quality between a UE and its serving BS and serves as an important metric for performance evaluation in wireless network.

### 3.8.3 Rate coverage/outage

The rate coverage provides a better performance metric in small cell networks. It describes the probability of the achievable rate of a user to be above a certain minimum value. On the other word, the probability that the achievable rate of a user falls below a certain

threshold is termed the rate outage. Although, there is a strong correlation between SINR and rate distribution in homogeneous networks, the case is different in HetNets or UDN [20]. As discussed in Chapter 2, the backhaul capabilities, influenced by the traffic and load condition of the cells, determine the achievable rate in small cell networks, in addition to the SINR distribution.

### 3.8.4 Average Spectral Efficiency (ASE)

The ASE in bits/s/Hz is the average transmitted data rate per unit bandwidth and represents the spectrum efficiency. Due to high data rate demands and scarcity of spectrum in 5G, the spectrum efficiency becomes a key performance metrics for 5G networks. Hence, the ASE is a measure of the quantity of users and services that can simultaneously be transmitted and supported by the limited radio spectrum. Theoretically, the Shannon theorem derives the ASE in terms of the SINR as [121]

$$R = \log_2(1 + \gamma) \tag{3.8}$$

where $\gamma$ is the SINR.

### 3.8.5 Area Spectral Efficiency

The reuse of spectrum per unit area arises due to the densification of small cells in cellular networks. The area spectral efficiency in bps/Hz/m$^2$ is the amount of bps transmitted by a given user per unit bandwidth over the cell coverage area supported by the BS in the cell.

Specifically, the authors in [122] defined area spectral efficiency as the metric to quantify spectral efficiency and spatial properties of point-to-point (PtP) and decode and forward (DF) communications with interference management. This definition clearly captures the tradeoffs between the link spectral efficiency of the users, the quality of communication link of the users and the spectral efficiency of the system.

### 3.8.6 Energy Efficiency (EE)

The EE measured in bps/Hz/J is another key performance indicator used for evaluation of dense networks in this thesis. It is defined as the achievable data rate within a given power consumption. In the DL context, it refers to the ratio of the spectral efficiency (SE) to the total power consumption of the BS. On the hand, in the UL, this ratio is between SE and the UEs within a given period. Let $P_c$ denote the power consumption by the BS in the DL or the UE in the UL, then the EE can be expressed as

$$EE = \frac{R}{P_c} \tag{3.9}$$

where $R$ is the ASE.

### 3.8.7 Network Throughput

Another metric to quantify the performance of UDN is the network throughput, generally defined as the successful rate of message delivery over a channel (in bps/Hz/m$^2$). The relationship between throughput, coverage probability and area spectral efficiency for a given

BS density in a given network is expressed as

$$T_r = D_s P_k (1 - P_{out}) R_o, \tag{3.10}$$

where $D_s$ and $P_k$ are the respective density and probability of active BSs, $P_{out}$ denotes the outage probability and $R_o \triangleq \log_2(1 + \gamma)$ is the network link capacity with $\gamma$ as the SINR threshold.

### 3.8.8 User satisfaction

The user satisfaction metric is used when the throughput of the user is to be compared with the maximum throughput of the entire network area. It is expressed as ratio of the sum of the throughputs for all users and the product of maximum throughput and the number of users

$$\theta = \frac{\sum_{n=1}^{N} T_n}{T_{max} * N}, \tag{3.11}$$

where $N$ is the number of users indexed by $n$, $T_r$ and $T_{max}$ are the throughputs and maximum throughputs of all users, respectively. The throughputs of all the users are almost equal if the value of $\theta$ is closer to 1, and vary considerably if $\theta$ is closer to 0.

## 3.9 Scheduling Schemes

Scheduling is an important factor to consider when radio resources are to be distributed among different categories of users in the network, when the channel condition and QoS

requirements are taken into account. Different scheduling schemes are designed to achieve distinct level of user and network enhancement. While some are designed to increase SE and maximize the network throughput, others are intended to maintain a balance between SE and fairness. Scheduling schemes can be divided into channel aware scheduling scheme (CASS) and channel unaware scheduling scheme (CUSS)[123]. The CASS schedules the user by taking into account the channel condition, which are primarily the channel fading effect. Example of CASS are Maximum Carrier-to-Interference Ratio (MCIR) and Proportional Fairness (PF). On the contrary, the CUSS do not consider the channel condition such as the effect of multipath and fading for scheduling. Round Robin (RR) is a major example of CUSS type. The PF are RR are the two commonly used schemes in both categories.

- PF scheduling is applied in dense networks where applications with low latency and different QoS requirements are desired for higher system performance. PF scheduling algorithm is used to balance between total capacity enhancement and fairness among all UEs. The algorithm attempts to provide all UEs with minimum level of service at the same maximizing total cell throughput. Moreover, it allocates more resources to users with good channel condition. In PF, if the average throughput experienced by UE $i$ on subcarrier $n$ in time slot $t$ is $T_{i,n}$, and the instantaneous data rate achieved by the UE on the subcarrier is $R_{i,n}$, then a given UE $j$ will be assigned subcarrier $n$ such that

$$j = \underset{i=1,2,\ldots,I}{\arg\max} \frac{R_{i,n}}{T_{i,n}} \tag{3.12}$$

- Round Robin is a type of scheduling that allocates resource blocks (RBs) one after another without considering the CQI. It presents a simple procedure for achieving the best fairness by allocating packet transmission time equally to each UE. In RR, fairness is achieved at the cost of decreased cell throughput as the scheduler does not depend on the instantaneous DL SINR values when making decisions on the number of bits to be transmitted [124].

## 3.10 Chapter Summary

This chapter presented fundamental concepts in interference modeling and analysis adopted to design, operate, manage and for network performance validity. First, an overview of available literature on LTE architecture and performance metrics to quantify fairness, throughput, energy/ power consumption and traffic load in the cellular network was carried out. Specifically, a summary of LTE architecture was provided to identify the importance of its elements to provide simpler functionalities, low redundancy, seamless connectivity/ handover and integration capabilities to other wireless access technologies. Also, with cellular network densification and limited resources, a comprehensive study of legacy and state-of-the-art access techniques as key drivers in moving from one cellular generation to another, was presented to analyse priorities of both users and network. In the same vein, a brief review of promising modeling techniques used in this thesis to model dense cellular network is presented. Generally, wireless network metrics are complicated since the network operates over unreliable propagation channel, is more dynamic and contains battery powered mobile

terminals. This complexity necessitates assumption of multiple performance metrics for cellular networks to fulfill the multi-objective optimization requirements.

# Chapter 4

# Dynamic Inter-Cell Interference Coordination in 5G Ultra Dense Networks (UDN)

## 4.1 Introduction

Wireless network densification promises to be a key driver towards improvement in user throughput and network traffic capacity. In Heterogeneous Networks (HetNets), low power nodes are deployed within the coverage of a macrocell to provide enhanced performance due to efficient resource and load sharing between the high power macrocell and low power base stations (BSs). The low power nodes, also referred to as small cells are composed of femtocells, picocells, Remote Radio Heads (RRHs), Relay Nodes (RNs) and Device-to-Device (D2D) devices. However, such densification comes at the expense of increased co-channel

interference (CCI), particularly for the cell edge users. Hence, since Rel-9/10, 3GPP has introduced enhanced Inter-Cell Interference Coordination (eICIC) techniques to improve the throughput of the network at the cell edge. The techniques involve two approaches. One of such is the cell range expansion (CRE) used to offload the macro BS (MBS) for possible association with small cells. The downside of this approach is that UEs at the edge of the cell experience severe interference from neighbouring macrocell. As a result, the second approach, called Almost Blank Subframe (ABS) was proposed to control MBS transmission with reduced power during certain subframes. During ABS, the MBS only transmits control channels and cell-specific reference signals, allowing small cells to schedule their serving UE, and hence maintain transmission continuity under its control. Thus, UEs at the expanded region of small cells can receive both control and user data downlink (DL) information. The ABS patterns are ranked by the MBS in ABS periods (APs) of 40 subframes in time domain and transmitted via the X2 interface to all the small cells.

Although eICIC improves the throughput of the cell-edge users by protecting them from MBS interference, this comes at the cost of performance degradation in MBS capacity, due to total blanking of certain subframes. To address this problem, the MBS can be conditioned to transmit at a reduced power level, thereby reducing interference caused to the nearby small cells. This is the basis for further enhanced ICIC (feICIC) techniques standardized in Long Term Evolution (LTE) Rel-11. Generally, optimal performance of expanded UEs in joint CRE and eICIC/FeICIC schemes depends on the value of CRE bias applied for offloading and ABS muting ratio, called duty cycle. Higher RE bias means more ABS ratio, forcing the MBS to mute more subframes. This will further cause degradation in the macro UE Quality

of Service (QoS), thereby requiring a robust resource allocation mechanism to balance the two requirements. Hence, transmission through feICIC has been proven to provide dual advantages of consuming less power and improving network capacity.

### 4.1.1 Motivation

The growth of mobile data volume is expected to necessitate addition of more capacity to the current cellular networks. This requirement can be achieved by cell densification which involves using a higher number of base stations with different transmission power and coverage. This leads to an increase in the spectral efficiency of the base station and improved cell-edge performance in urban areas. In addition, cell densification has the advantage of reusing the same spectrum within the network. While reusing same spectrum creates severe inter-cell interference in the network, presence of low power nodes such as pico BS in the coverage of macro BS for offloading strategy has been found to aggravate the interference dynamics. Hence, in order to fully maximize the offloading benefit, enhanced inter-cell interference coordination (eICIC) was proposed in 3GPP LTE Release-10. Generally, the proposed technique is approached in two ways. Firstly, cell selection bias or range expansion (RE) is used to offload the macro BS through association of UEs to low power nodes. Secondly, almost blank subframe (ABS) is configured to reduce interference to cell edge UEs in pico BS. In the first approach, users located at the edge of both macro and pico BSs are affected by severe interference due to poor channel conditions. Although the use of ABS will reduce interference experienced by pico BS from macro BS, the intermittent blanking of some subframes results in reduced capacity and inefficient utilization of the limited resources.

Hence, Further eICIC (FeICIC) was later introduced in Release-11 to serve users at reduced power levels. Even with FeICIC, there still exists a question of how to balance the bias value and ABS factor to achieve better result. These observations lead the way to propose a novel solution that seeks to maximize the performance gains of both schemes by joint optimization of the bias values and ABS patterns, for improved spectral efficiency and coverage.

This chapter consolidates on the existing FeICIC techniques, but takes it some steps further with the following specific major contributions:

- To realise the massive connectivity goal of 5G network, simulation of our proposed scheme will be carried out with different values of CRE and ABS ratio. Unlike the single ABS ratio approach used in the existing literature [125], common factors likely to affect 5G technology such as network density, users' mobility, deployment and coverage require dynamic resource allocation, rather than static approach.

- We derive a model based on Poisson Point Process (PPP), relying on stochastic geometry to obtain closed form expressions for the coverage/outage probability and total interference. This will provide a simple and tractable evaluation of the system performance.

- Based on the above, a comprehensive analysis of various optimization parameters such as Spectral Efficiency (SE), Proportional Fairness (PF), and coverage/outage probability, as clearly explained in Chapter 3 will be conducted. In the literature, usage of eICIC techniques have been considered with fairness and area capacity constraints to achieve better network throughput. Also, approach based on FeICIC modeled with

PPP for network performance evaluation has been studied. However, to the best of our knowledge, this is the first work that jointly considers FeICIC scheme, using stochastic geometry, by dynamically selecting bias values and ABS ratio to optimize SE, PF and coverage/outage probability. Simulation results will demonstrate our approach to consume less power, guarantee fairness among users and improve overall network throughput.

The rest of the chapter is organized as follows. Related literature will be discussed in the next section followed by the system model. Discussion of the simulated results is then presented while overview of the work done concludes the chapter.

## 4.2 Literature Review

Interference coordination in HetNets has benefited from different ICIC techniques widely studied in the literature. Since the conception of multi-tier HetNet where low power nodes are deployed massively in an unplanned manner to alleviate traffic congestion in macrocell network, inter-cell interference (ICI) and traffic imbalance have continued to pose challenge to the system. This has led to the inefficient utilization of the radio resources and the degradation in the network capacity. Among the significant solutions proposed to solve this problem is the work in [17] which incorporates time-domain, frequency-domain and power control techniques. The time-domain scenario requires the MBS to completely stop transmission at certain subframes to allow pico BS (PBS) schedule its UE at these blanked subframes, thereby serving as protection mechanism against MBS interference to PBS edge

users. Joint optimization of eICIC with CRE for interference cancellation and load balance then became a widely studied topic, with particular focus on user capacity and fairness [25, 26], and traffic offloading gain on user data rate [35, 36]. However, the approach degrades MUEs' capacity due to complete muting of MBS SFs. To solve this problem, the MBS can transmit at reduced power in some SFs to schedule its close UEs. Therefore, the technique was standardized by 3GPP and its improvement over eICIC in terms of average throughput and cell-edge performance has been studied in [125–128]. Due to the importance of CRE bias value and ABS muting ratio, these key parameters should be configured appropriately to guarantee optimal performance when the two schemes are jointly optimized. Hence, a novel solution proposed in this research employs FeICIC technique in combination with dynamic selection of bias value and ABS ratio to jointly maximize SE, PF and coverage/outage probability. The result will improve user's fairness and network aggregate throughput without any performance degradation.

## 4.3 System Model

Consider a two-tier Hetnet system shown in Figure 1 comprising of macro BSs (MBSs) and pico or small cell BSs (PBSs or SCBs), denoted as $\mathcal{K} = \{1, 2, ..., K\}$, where $K = 2$. The locations of MBS, PBS and UE are modeled as 2-dimensional homogeneous Poisson Point Process (PPP) distribution with densities $\lambda_m, \lambda_p$, and $\lambda_u$, respectively. Using PPP provides a tractable means for analysing some key performance indicators (KPIs) such as coverage probability, fairness and spectral efficiency. For analysis purpose and to realize ultra dense network, simulations are carried out over four picocell densities of $8\lambda$, $12\lambda$, $16\lambda$ and $20\lambda$.

Both the MBS and PBS have their transmission bandwidth $W$ set to 20 MHz. Moreover, the positions of both MBS and PBS are denoted by $\Phi_k$, while UE positions are represented by $\Phi_u$ which is independent of $\Phi_k$. The frame structure at the MBS is divided into two, such that reduced and full power mechanisms are employed. The frame structure during reduced power is termed reduced-power subframe (RSF), while during full power transmission is called normal subframe (NSF). During RSF, certain subframes (SFs) transmit at reduced power to protect Pico UEs (PUEs), especially those located at the cell edge or expanded region (ER), from severe MBS interference as shown in Fig. 4.1. In the conventional Almost Blank Subframe (ABS), MBSs completely suppress power levels in some SFs to prevent severe downlink interference to the PBS. This approach may lead to degraded system throughput

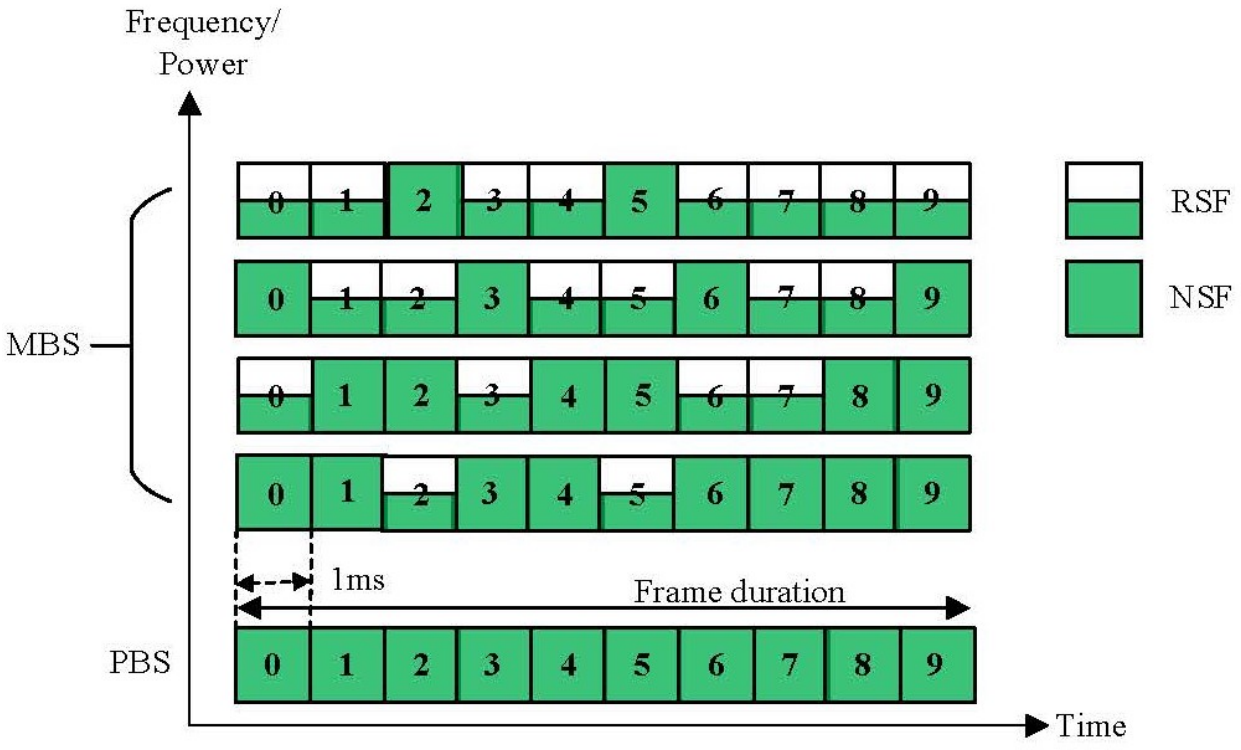


**Figure 4.1:** Frame structure of the proposed scheme with different values of duty cycle, $\beta$ = 0.2,0.4, 0.6, 0.8. The PBSs transmit at maximum power in all subframes.

when applied in ultra dense regime. On the other hand in the RSF, the MBS only limits its transmission power levels conditioned on $\alpha P_{tx}^{m}$, where $P_{tx}^{m}$ is the transmit power of the MBS and $0 \leq \alpha \leq 1$ is the power splitting factor. However, during NSF the MBS transmits both control and data signals at full power, $P_{tx}^{m}$, i.e., $\alpha = 1$. The PBSs transmit all scheduling resources such as data and control signals at full power $P_{tx}^{p}$ throughout the frame duration. The pathloss ratio $\tau_k$ of MBS and PBS is assumed to be 4. For simplicity, the HetNet scenario is also assumed to be interference limited where only inter-cell interference is dominant, hence background noise is neglected.

To initiate the RSF technique, take $\beta$ as the duty cycle of MBS NSFs, which is the ratio of number of NFSs to the total number of SFs in a MBS frame. Thus, duty cycle of the MBS when RSF is configured becomes $(1 - \beta)$.

### 4.3.1 Cell Association criteria with CRE

For cell selection process to be incorporated in the scheme in order to offload high traffic from the MBS, CRE technique is used. Different bias values of $B_m = 0$ and $B_p = B \geq 0$dB is initiated for MBS and PBS, respectively. The effective transmission power for MBS during NSFs and RSFs are $P_{NSF} = P_{tx}^{m} L^{m}$ and $\alpha P_{NSF}$, respectively. In addition, transmission power of PBS during NSF/RSF is $P_{NSF/RSF} = P_{tx}^{p} L^{p}$, where $L^{m}$ and $L^{p}$ denote losses due to external geometric parameters. When RSF is configured, the time resources of MUEs and PUEs at cell center and edge are $\rho_m = 1 - \beta$, $\rho_p = 1$ and $\rho_{cre} = \beta$, respectively. In the user association process, a UE will select the optimum serving BS in the $k$th tier with the strongest RSRP value as $J_{d,k} = P_k h_k B_k (d_k)^{-\tau}$. If the optimum serving BS is MBS

during NSF, then $J_{d,m} = P_{NSF} h_m B_m (d_m)^{-\tau}$, for MBS during RSF is $\alpha J_{d,m}$, and if PBS during NSF/RSF, $J_{d,p} = P_{NSF/RSF} h_p B_p (d_p)^{-\tau}$, where $h_m$ and $h_p$ are the channel gain with Rayleigh fading, i.e., $h_m \sim \exp(1)$ and $h_p \sim \exp(1)$, while $d_m$ and $d_p$ denote the distance between UE and its associated MBS and PBS, respectively.

Since BSs in HetNet possess varying transmit power levels in different tiers, modeling user association scheme based on the signal-to-interference-ratio (SIR) rather than the strongest RSRP yields a better result. Let $I_{NSF}$ be the aggregate interference experienced by a UE during NSFs from all MBSs and PBSs other than the respective closest serving BSs. Aggregate interference during RSFs can similarly be denoted by $I_{RSF}$. It is assumed that the interference experienced by the UE irrespective of the chosen mode of transmission , i.e., NSF or RSF, by the closest serving MBS is the same. Factoring in $I_{RSF}$ during RSF provides a good accountability for accuracy in our approach, unlike in ABS scheme where interference from other BSs is taken to be non existence when certain SFs are completely blanked. Hence, a typical UE will experience the following SIR values;

– SIR from closest serving MBS during NSF,

$$\gamma_{NSF}^{m} = \frac{J_{d,m}}{J_{d,p} + I} \tag{4.1}$$

– SIR from closest serving PBS during NSF,

$$\gamma_{NSF}^{p} = \frac{J_{d,p}}{J_{d,m} + I} \tag{4.2}$$

– SIR from closest serving MBS during RSF,

$$\gamma_{RSF}^{m} = \frac{\alpha J_{d,m}}{J_{d,p} + I} \tag{4.3}$$

– SIR from closest serving PBS during RSF,

$$\gamma_{RSF}^{p} = \frac{J_{d,p}}{\alpha J_{d,m} + I} \tag{4.4}$$

It is noteworthy that the cell association criteria with CRE is affected by the range expansion bias (REB) $B_k$, DL SIRs from serving MBS and PBS during NSF and RSF, respectively. Considering REB $B_k$ for the cell selection procedure, and scheduling threshold $\delta^m$ and $\delta^p$ for MBS and PBS, respectively, UEs are further categorized into the following four groups;

**Group 1:** MUE associated to MBS in NSF when $B_k\gamma_{NSF}^{p} \leq \gamma_{NSF}^{m}$ and $\gamma_{NSF}^{m} \leq \delta^m$ (4.5)

**Group 2:** MUE associated to MBS in RSF when $B_k\gamma_{NSF}^{p} \leq \gamma_{NSF}^{m}$ and $\gamma_{NSF}^{m} > \delta^m$ (4.6)

**Group 3:** PUE associated to PBS in NSF when $B_k\gamma_{NSF}^{p} \geq \gamma_{NSF}^{m}$ and $\gamma_{NSF/RSF}^{p} > \delta^p$ (4.7)

**Group 4:** PUE associated to PBS in NSF when $B_k\gamma_{NSF}^{p} \geq \gamma_{NSF}^{m}$ and $\gamma_{NSF/RSF}^{p} \leq \delta^p$ (4.8)

Based on the association rule, the probability that a UE is associated with any of the BS tiers during NSF and RSF is given by [129]

$$\mathcal{A}_k = \left(1 + \frac{\sum_{j=1, j\neq k}^{K} \lambda_j (P_j B_j)^{2/\tau_k}}{\lambda_k (P_k, B_k)^{2/\tau_k}}\right)^{-1} \tag{4.9}$$

The joint user association probability for NSF-MUE is given by

$$\mathcal{A}^m_{NSF} = 2\pi\lambda_m \int_0^\infty x \exp\Big( - \pi\lambda_m x^2 - \pi\lambda_p \Big(\frac{P^p B^p}{P^m}\Big)^{\frac{2}{\tau_p}} x^{\frac{2\tau_m}{\tau_p}}\Big) dx \tag{4.10}$$

*Proof:* Let the distance between a typical UE and its serving BS be $X_k$, with $(X_k > x_k, D_k > d_k)$. By applying the four categories of UE in (4.5) - (4.8) gives the association probabilities

$$\begin{aligned} \mathcal{A}^m_{NSF} &= \mathbb{P}\Big(B_k \gamma^p_{NSF} \leq \gamma^m_{NSF}, B_k P^p_{NSF} (d_p)^{-\tau_p}\Big) \\ &= \int_{x>0} \mathbb{P}\Big(\Big(\hat{P}^p \hat{B}^p\Big)^{\frac{1}{\tau_p}} x^{\frac{1}{\tau_p}} < x_p\Big) f_{X_k}(x) dx \end{aligned} \tag{4.11}$$

The joint probability of $D_k > d$ conditioned on association of a typical UE with the $k$th tier when $D_k > x$ and $X_k > x$ have the same distribution, and $n$ denotes the index of associating tier of a typical UE is

$$\mathbb{P}[D_k > x] = \mathbb{P}[X_k > x | n = k] = \exp(-\pi\lambda_k x^2) \tag{4.12}$$

The Probability Distribution Function (PDF) $f_{X_k}(x)$ can be written as

$$f_{X_k}(x) = \frac{d}{dx}\{1 - \mathbb{P}(D_k > x)\} = 2\pi\lambda_k x \exp(-\pi\lambda_k x^2), \quad \forall x \geq 0 \tag{4.13}$$

Combining (4.13), (4.12) and (4.11), we obtain (4.10). Similarly, user association probabilities for RSF-MUE, NSF-PUE and RSF-PUE are respectively given as;

$$\text{RSF-MUE:} \qquad \mathcal{A}^m_{RSF} = 2\pi\lambda_m \int_0^\infty x \exp\Big( - \pi\lambda_m x^2 - \pi\lambda_p \Big(\frac{P^p B^p}{\alpha P^m}\Big)^{\frac{2}{\tau_p}} x^{\frac{2\tau_m}{\tau_p}}\Big) dx \tag{4.14}$$

$$\text{NSF-PUE:} \qquad \mathcal{A}^p_{NSF} = 2\pi\lambda_p \int_0^\infty x \exp\Big( - \pi\lambda_p x^2 - \pi\lambda_p \Big(\frac{P^m}{P^p}\Big)^{\frac{2}{\tau_m}} x^{\frac{2\tau_m}{\tau_p}}\Big) dx \tag{4.15}$$

$$\begin{aligned}\text{RSF-PUE:} \qquad \mathcal{A}^p_{RSF} =& 2\pi\lambda_p \int_0^\infty x \exp\Big( - \pi\lambda_p x^2 - \pi\lambda_m \Big(\frac{\alpha P^m}{P^p B^p}\Big)^{\frac{2}{\tau_m}} x^{\frac{2\tau_p}{\tau_m}}\Big) \\ & \Big\{1 - \exp\Big( - \pi\lambda_m \Big(\frac{\alpha P^m}{P^p}\Big)^{\frac{2}{\tau_m}} x^{\frac{2\tau_p}{\tau_m}} \Big(1 - \Big(\frac{1}{B^p}\Big)^{\frac{2}{\tau_m}}\Big)\Big)\Big\} dx\end{aligned} \tag{4.16}$$

Setting $\tau_k = \tau$, (4.10), (4.14) - (4.16) yield;

NSF-MUE:

$$\mathcal{A}^m_{NSF} = \frac{\lambda^m \sqrt{P^m}}{\lambda^m \sqrt{P^m} + \lambda^p \sqrt{P^p B^p}} \tag{4.17}$$

NSF-PUE:

$$\mathcal{A}^p_{NSF} = \frac{\lambda^p \sqrt{P^p}}{\lambda^m \sqrt{P^m} + \lambda^p \sqrt{P^p}} \tag{4.18}$$

RSF-MUE:

$$\mathcal{A}^m_{RSF} = \frac{\lambda^m \sqrt{\alpha P^m}}{\lambda^m \sqrt{\alpha P^m} + \lambda^p \sqrt{P^p B^p}} \tag{4.19}$$

RSF-PUE:

$$\mathcal{A}^{p}_{RSF} = \frac{\lambda^{p}\sqrt{P^{p}B^{p}}}{\lambda^{m}\sqrt{\alpha P^{m} + \lambda^{p}\sqrt{P^{p}B^{p}}}} - \frac{\lambda^{p}\sqrt{P^{p}}}{\lambda^{m}\sqrt{\alpha P^{m} + \lambda^{p}\sqrt{P^{p}}}} \tag{4.20}$$

Ideally, in legacy networks, each UE will choose a nearby BS to associate with and maintain this connection as long as the QoS is better than a predefined threshold. However, due to severe interference, this technique may not yield an optimal result in UDN. More importantly, the number of UE associated with a BS should be estimated in ultra dense regime for load balancing. Thus, each UE benefits more by choosing a BS with better channel condition for maximized system throughput. This condition is optimized by key parameters such as BS density, bias value, and distance between BS and UE. Hence the UE's average number per tier is expressed as

$$\mathcal{N}_{k} = \frac{N^{u}_{k}}{N^{b}_{k}} = \frac{\mathcal{A}_{k}\lambda_{u}}{\lambda_{k}} \tag{4.21}$$

where $N^{u}_{k}$ and $N^{b}_{k}$ are the average number of UEs and BSs in the $k$th tier network, respectively. The corresponding average number of UEs during NSF and RPS are respectively given as

$$\begin{aligned} \mathcal{N}^{m}_{NSF} &= \frac{\mathcal{A}^{m}_{NSF}\lambda_{u}}{\lambda^{m}}, \qquad \mathcal{N}^{m}_{RSF} = \frac{\mathcal{A}^{m}_{RSF}\lambda_{u}}{\lambda^{m}} \\ \mathcal{N}^{p}_{NSF} &= \frac{\mathcal{A}^{p}_{NSF}\lambda_{u}}{\lambda^{p}}, \qquad \mathcal{N}^{p}_{RSF} = \frac{\mathcal{A}^{p}_{RSF}\lambda_{u}}{\lambda^{p}} \end{aligned} \tag{4.22}$$

### 4.3.2 Coverage Probability analysis

This section derives expression for the SIR coverage of a typical UE in the network. The coverage probability for a threshold $T$ of a UE associated to MBS and PBS during NSF and

RSF is given as

$$Z(T) = \mathbb{P}(SIR > T | u \in O_k) \tag{4.23}$$

where $\{O_k \in$ NSF-MUE, RSF-MUE, NSF-PUE, RSF-PUE$\}$. Hence,

$$Z(T) = \mathcal{A}^m_{NSF} Z^m_{NSF}(T) + \mathcal{A}^m_{RSF} Z^m_{RSF}(T) + \mathcal{A}^p_{NSF} Z^p_{NSF}(T) + \mathcal{A}^p_{RSF} Z^p_{RSF}(T) \tag{4.24}$$

Thus the conditional SIR coverage for a typical UE during access period are

$$Z^m_{NSF}(T) = \frac{2\pi\lambda_m}{\mathcal{A}_{NSF}} \int_0^\infty x \exp\Bigg( - \frac{T}{\gamma^m_{NSF}(x)} - \pi\lambda_m \mathcal{Q}(1, \theta_{NSF}, T, \tau_m) x^2 - \pi\lambda_p \Big(\frac{P^p}{P^m}\Big)^{\frac{2}{\tau_p}} \mathcal{Q}(B, \theta_B, T, \tau_p) x^{\frac{2\tau_m}{\tau_p}} \Bigg) dx \tag{4.25}$$

$$Z^m_{RSF}(T) = \frac{2\pi\lambda_m}{\mathcal{A}_{RSF}} \int_0^\infty x \exp\Bigg( - \frac{T}{\gamma^m_{RSF}(x)} - \pi\lambda_m \mathcal{Q}(1, \theta_{RSF}, T, \tau_m) x^2 - \pi\lambda_p \Big(\frac{P^p}{\alpha P^m}\Big)^{\frac{2}{\tau_p}} \mathcal{Q}(B, \theta_B, T, \tau_p) x^{\frac{2\tau_m}{\tau_p}} \Bigg) dx \tag{4.26}$$

$$Z^p_{NSF}(T) = \frac{2\pi\lambda_p}{\mathcal{A}^p_{NSF}} \int_0^\infty x \exp\Bigg( - \frac{T}{\gamma^p_{NSF}(x)} - \pi\lambda_p \mathcal{Q}(1, \theta_{NSF}, T, \tau_p) x^2 - \pi\lambda_m \Big(\frac{P^m}{P^p}\Big)^{\frac{2}{\tau_m}} \mathcal{Q}(1, \theta_{NSF}, T, \tau_m) x^{\frac{2\tau_p}{\tau_m}} \Bigg) dx \tag{4.27}$$

$$Z^{p}_{RSF}(T) = \frac{2\pi\lambda_p}{\mathcal{A}^{p}_{RSF}} \int_0^{\infty} x \exp\Bigg( - \frac{T}{\gamma^{p}_{RSF}(x)} - \pi\lambda_p \mathcal{Q}(1, \theta_{RSF}, T, \tau_p) x^2 - \pi\lambda_m \Big(\frac{\alpha P^m}{P^p B^p}\Big)^{\frac{2}{\tau_m}} \mathcal{Q}(\frac{1}{B}, \theta_{NSF}, BT, \tau_m) x^{\frac{2\tau_p}{\tau_m}} \Bigg) \Bigg\{ 1 - \exp\Bigg( - \pi\lambda_m \Big(\frac{\alpha P^m}{P^p}\Big)^{\frac{2}{\tau_m}} \Big(1 - \Big(\frac{1}{B}\Big)^{\frac{2}{\tau_m}}\Big) x^{\frac{2\tau_p}{\tau_m}} \Bigg) \Bigg\} dx \quad (4.28)$$

where $\mathcal{Q}(a, b, c, \tau_j) = a^{\frac{2}{\tau_j}} + bc^{\frac{2}{\tau_j}} \int_{(\frac{a}{c})^{\frac{2}{\tau_j}}}^{\infty} \frac{du}{1+u^{\frac{\tau_j}{2}}}$.

### 4.3.3 Spectral Efficiency analysis using CRE and RSF

The Shannon capacity is used to compute the sum and per-user SEs for the four categories of UEs as

$$C = \log_2(1 + \text{SIR}) \quad (4.29)$$

From [125], the sum SE is expressed as

$$\text{NSF-MUE}: \quad C^{m}_{NSF}(\lambda^m, \lambda^p, B, \alpha, \delta, \beta) = \beta \frac{G(\log_2(1 + \gamma^{m}_{NSF}), R_2)}{\mathcal{A}^{m}_{NSF}} \quad (4.30)$$

$$\text{NSF-PUE}: \quad C^{p}_{NSF}(\lambda^m, \lambda^p, B, \alpha, \delta, \beta) = \beta \frac{G(\log_2(1 + \gamma^{p}_{NSF}), R_4)}{\mathcal{A}^{p}_{NSF}} \quad (4.31)$$

$$\text{RSF-MUE}: \quad C^{m}_{RSF}(\lambda^m, \lambda^p, B, \alpha, \delta, \beta) = (1 - \beta) \frac{G(\log_2(1 + \alpha\gamma^{m}_{RSF}), R_1)}{\mathcal{A}^{m}_{RSF}} \quad (4.32)$$

$$\text{RSF-PUE}: \quad C^{p}_{RSF}(\lambda^m, \lambda^p, B, \alpha, \delta, \beta) = (1 - \beta) \frac{G(\log_2(1 + \gamma^{p}_{RSF}), R_3)}{\mathcal{A}^{p}_{RSF}} \quad (4.33)$$

where $G$ represents the gamma function used to derive the joint probability distribution function (JPDF) of $\gamma^m$ and $\gamma^p$ values in Section 4.3, while $R_1 - R_4$ are integration regions for the cell association criteria. Thus, the per user SEs are given as

$$\begin{aligned} C^m_{u,NSF} &= \frac{\lambda^m C^m_{NSF}}{\lambda_u \mathcal{A}^m_{NSF}}, \qquad C^m_{u,RSF} = \frac{\lambda^m C^m_{RSF}}{\lambda_u \mathcal{A}^m_{RSF}} \\ C^p_{u,NSF} &= \frac{\lambda^p C^p_{NSF}}{\lambda_u \mathcal{A}^p_{NSF}}, \qquad C^p_{u,RSF} = \frac{\lambda^p C^p_{RSF}}{\lambda_u \mathcal{A}^p_{RSF}} \end{aligned} \tag{4.34}$$

## 4.4 Results and Discussion

In this section, simulation is performed with different parameter values and results are analyzed to validate various assumptions made in the chapter. To emulate ultra dense scenario in 5G, MBS density $\lambda_m$ is set to 2.5 MBS/km$^2$ and four PBS densities $8\lambda_m$, $12\lambda_m$, $16\lambda_m$ and $20\lambda_m$ are considered. Both MBS and PBS transmit power are 46dBm and 30dBm, respectively. The system bandwidth is given as 20 MHz, while pathloss coefficient $\tau$ is set as 4 and assumed to be the same for both MBS and PBS. The power splitting factor is taken as $0 \leq \alpha \leq 1$. However, since the MBS transmits at reduced power rather than absolute muting of some subframes, the duty cycle is made to take values 0.2, 0.4, 0.6 and 0.8. This is particularly useful for fairness analysis among different users in multi-tier Hetnets.

### 4.4.1 Spectral Efficiency of cell edge users

Fig. 4.2 depicts the SE patterns of MUEs during NSF against different REB values, evaluated over various values of power reduction factors ($0 \leq \alpha \leq 1$). As can be seen, at $\alpha = 0$ (i.e. during coordination), the MBS transmits at full power which results in a marginally high

value of SE experienced by UEs in the expanded region. However, as the reduction factor increases, there is a slight drop in SE among UEs. The reason for this marginal difference in SE is due to the fact that reduction of power by the MBS has little or no effect on the cell center MUEs since the interference power from other MBSs is not strong enough to cause signal degradation. Moreover, as the expansion bias increases, there is gradual offloading of

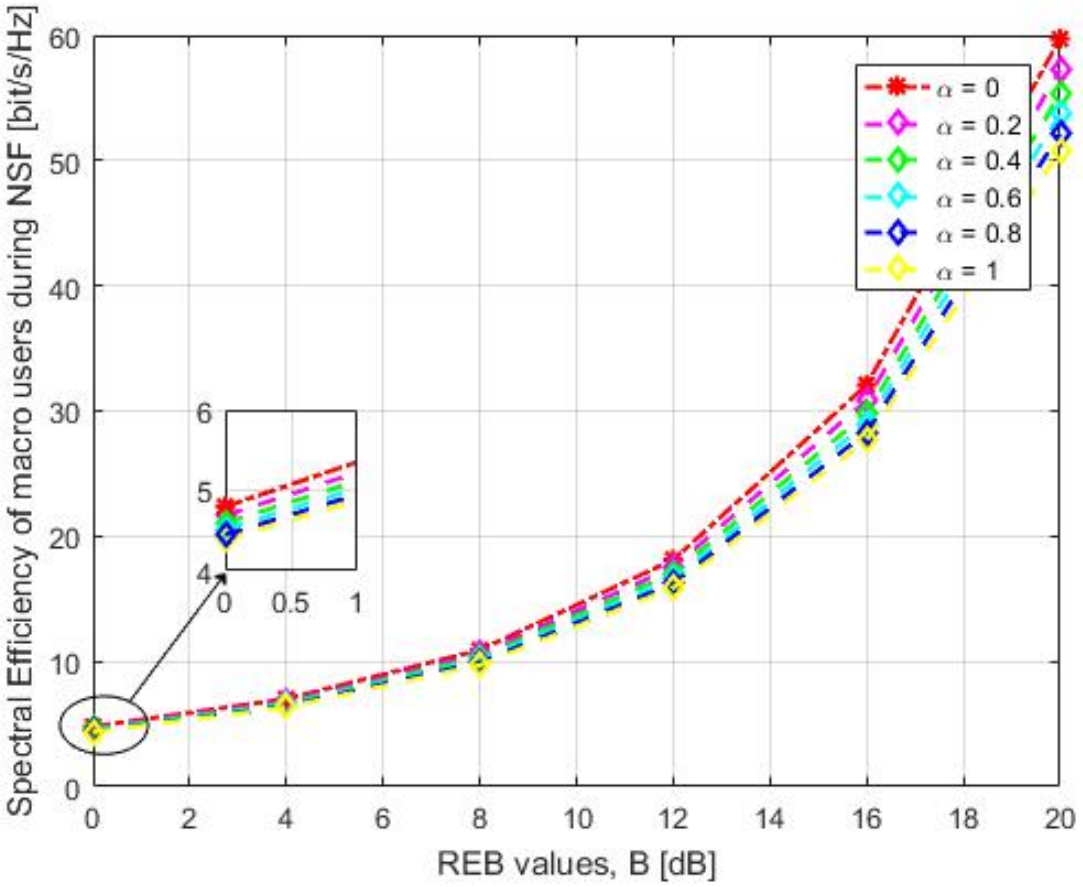


**Figure 4.2:** Spectral Efficiency of MUEs during NSF versus bias values at different power reduction factors.

MUE at the MBS cell edge to PBS, thereby reducing the number of MUE required to be coordinated. This results in increased SE for this group of UEs at the center of the cell. Further increase in bias value at 12 dB causes a sharp increase in SE due to more UEs being

offloaded to PBS. At this point upwards, SE is doubled at every increase in REB. On the downside, such an increase in the bias value may result in serious degradation in SE of PBS as more UEs are forced to compete for the available scarce resources. Therefore, a tradeoff is required for optimum values of REB that is capable of maintaining fairness among UEs.

Fig. 4.3 shows improvement on SE for MUEs during RSF versus the REB values against power reduction factors, compared to the scheme in [125]. It is interesting to note that the

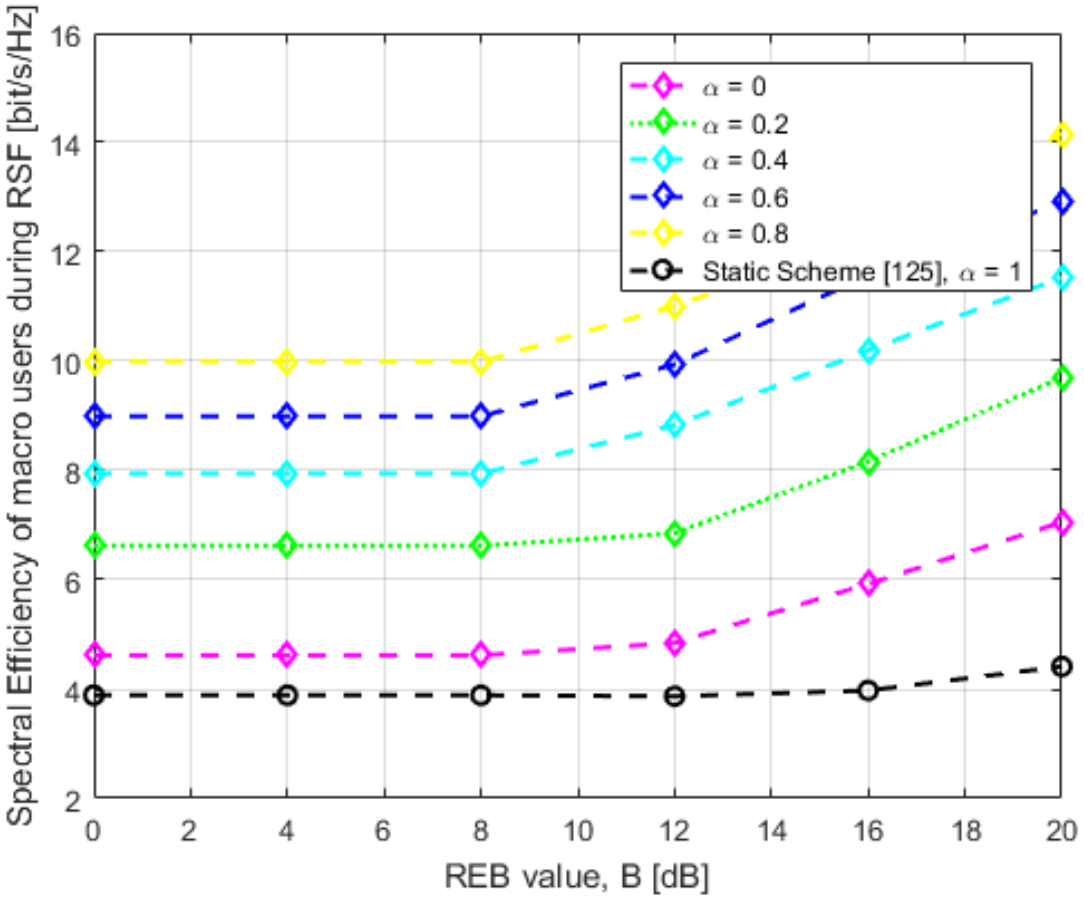


**Figure 4.3:** Spectral Efficiency of MUEs during RSF versus bias values at different power reduction factors.

SEs for all values of $\alpha$ remain constant up to REB value of 8dB before starting to increase considerably, with the exception of $\alpha = 0$ and $\alpha = 0.2$. During this period, whatever

value assumed by REB $B_k$ has no effect on the average number of RSF-MUEs provided $\sqrt{B_k} \leq \delta_k$ as shown in (4.5). Low power levels at $\alpha = 0$ and $\alpha = 0.2$, and $B_k = 8$ dB are not sufficiently high enough to offload RSF-MUEs to PBS, thereby resulting in constant SE values beyond $B_k = 8$ dB as compared to other $\alpha$ values. Consequently, the SEs of RSF-MUEs remain constant and valid up to point $B = 8$ dB. However beyond this point, and at higher $\alpha$ values, more RSF-MUEs at the boundary between MBS and PBS are offloaded to form new RSF-PUEs thereby reducing the number of RSF-MUEs, leading to an improved SEs in the network with $\sqrt{B_k} > \delta_k$. More importantly, the SE of the RSF-MUEs assumes sharp increase at $\alpha = 0.6$ and $B_k = 12$ dB, denoting an optimal values. It is also worth mentioning the high computational time required to execute the RSF approach. This is mainly attributed to the additional computation involved for the power reduction factor $\alpha$ optimization as against the eICIC approach. In addition, the increased network density to emulate massive connectivity requirement of 5G also contributed to increased computational cost. Nonetheless, the gains in terms of SE clearly outperforms the scheme in [125]. This is not surprising because, considering the adverse effect of increasing the bias value and duty cycle uncontrollably, our scheme optimized these values by formulating different expressions for UE association probability which is an advantage over the JCCDF derived in [125]. This validates the superiority of our approach over conventional schemes found in the literature. However, the SE of PUEs under NSF remains constant with increasing REB, for different values of power reduction factors, as shown in Fig. 4.4.

Fig. 4.5 depicts the SE patterns of UEs located in the expanded region of the PBS against different REB values during RSF. At this instance, the PBS density and duty cycle are set

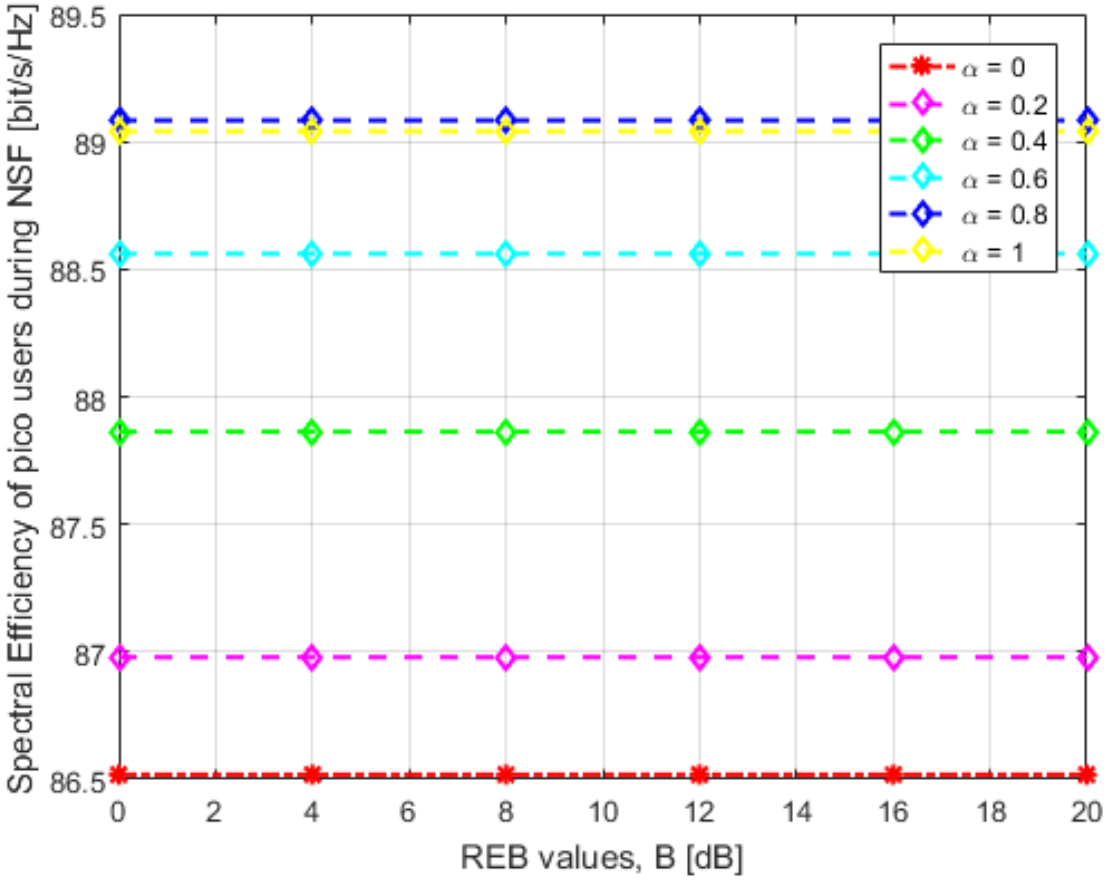


**Figure 4.4:** Spectral Efficiency of PUEs during NSF versus bias values at different power reduction factors.

to $8\lambda_m$ and 0.8, respectively. As the REB increases, some NSF MUEs located at the outer part of the MBS are offloaded to the expanded region of PBS and therefore become RSF PUEs, allowing more UEs to be scheduled during RSF. This will invariably result in low SE. Also, the rate of SE drop at $\alpha = 0$ remains steady as REB increases because this point corresponds to no coordination from the MBS, which maintains the interference power levels among PBSs as low as possible. On the contrary, the SEs at $\alpha = 0.2 - 1$ stay close as REB increases, with $\alpha = 1$ assuming closer value. The reason for this is that at $\alpha = 1$, the MBSs transmit at full power such that interference level to other neighbouring MBSs and PBSs

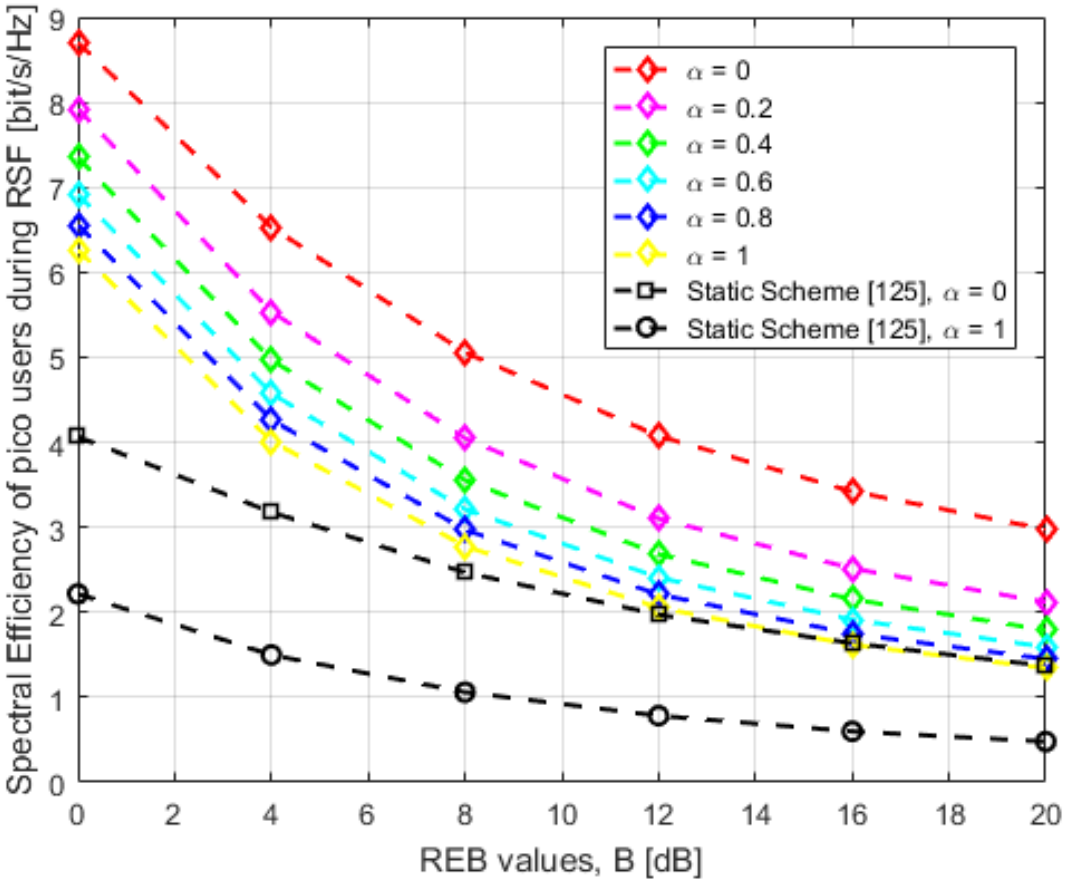


**Figure 4.5:** Spectral Efficiency of PUEs during RSF versus bias values at different power reduction factors.

is at the highest level. As the REB increases, more NSF-MUE are offloaded to form new RSF-PUE thereby leading to congestion in the PBS coverage area, hence the drop in SE. Finding an optimum value for both the REB and $\alpha$ would be an important consideration to guarantee tradeoff between the network throughput and fairness among UEs. On the contrary, in comparing with [125], we choose two important lower and upper limit points at $\alpha = 0$ and $\alpha = 1$ as basis for comparison. At these two points, it can be clearly seen that our scheme performs better, especially for the coordinated pico users. This is largely due to the fairness constraint incorporated in our scheme, which permits dynamic choice of network

parameter for optimization. It can be observed that with more users and higher REB values, the SE of [125] will likely shrink, thereby degrading the network performance remarkably. However, under this condition in our case, the worse scenario can still be managed with a low complex, robust optimized scheme.

### 4.4.2 Coverage Probability Analysis

This section presents the coverage probability analysis for the expression derived in Section 4.3.2. Fig. 4.6 depicts the effect of SIR range on the coverage probability of the network, simulated under different BS densities. As seen, the coverage probability increases with increase in the BS density. Logically, increase in BS density means less distance between the BSs, which invariably translates to more coverage. Consequently, the desired signal becomes stronger than the interference power, leading to improved SIR (see (4.1) - (4.4)) and coverage probability. Moreover, high BS density leads to small pathloss between UEs and BSs, thus resulting in better coverage. However, there may exist a point where further increase in the density will not contribute meaningfully to the network performance. Hence, exhaustive simulation is required to find an optimal threshold for the BS density. The statistic of UEs connecting to both MBS and PBS, in percentage, is shown in Fig. 4.7. For performance analysis, a total number of 50 mobile users are generated within, and distributed around the coverage area of the macrocell. Users are classified based on their mode of connection to picocells. The bias values chosen for the simulation range from 0 dB, denoting majority of users connecting to macrocell, to 18 dB when more users are shifted to picocells. The optimum bias value, which in this case occurs at 12 dB has high probability to minimize the

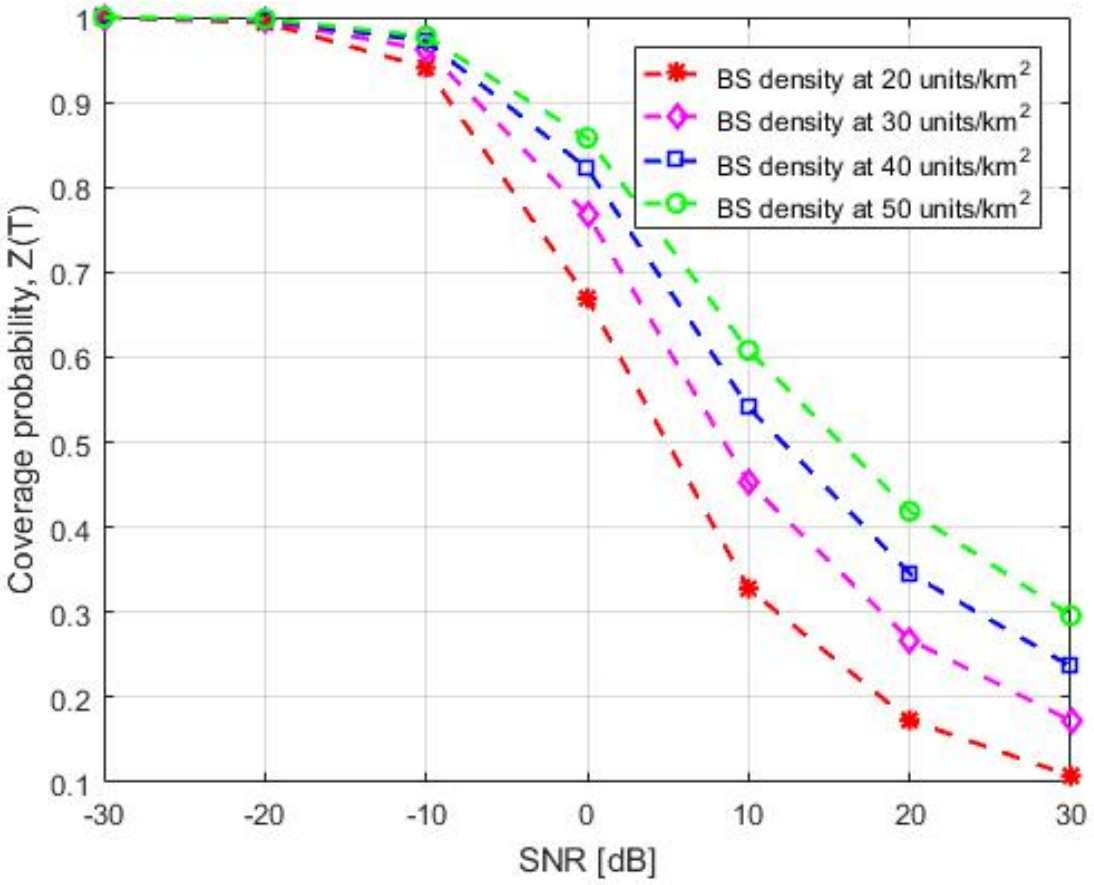


**Figure 4.6:** Coverage probability plot against SNR for different BS densities.

number of outage UEs, thus providing load balancing and a much better spatial reuse. It can also be seen that the higher the bias value, the larger the number of UEs that connect to PBS. This is because the number of UEs in the expanded region increases as the bias value increases. However, a very large bias value overloads the Pico BSs by making more users access the limited resources from the pico BSs. This clearly occurs, in our own case, when the bias value is 18 dB and beyond (see Fig. 4.5). The range expanded UE's throughput reduces at this point because UEs far away from the pico BSs are connected to the pico BSs while they receive high interference from macro BS. Thus, it is obvious that if the offset value is

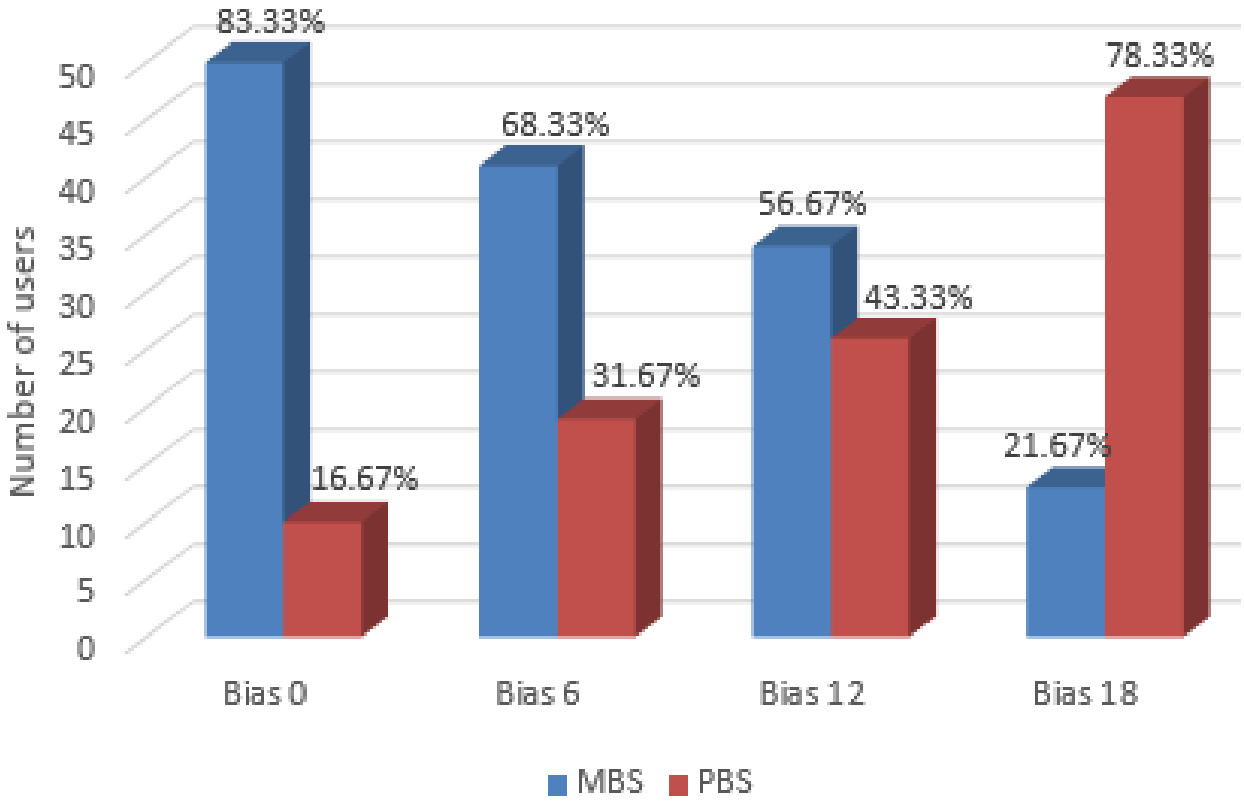


**Figure 4.7:** User association statistics.

not precisely selected, the increase of macro/pico UEs throughput sacrifices the throughput of pico/macro UEs. Furthermore, Fig. 4.7 demonstrates that the outage probability is an increasing function of bias value. The reason is that when the bias value increases, in the case of bias value 18 dB (21.67% / 78.33%), UEs far away from pico BSs are offloaded to picocells while they experience lower SINR value.

Therefore, with the optimal biasing factor (12 dB), the network nearly achieves the optimal cell selection technique. This demonstrates ability of biased-based cell association to significantly improve resource utilization, and considerably balance the traffic load, leading to increased gain and overall rate for most users. However, it is important to stress that

attaining optimal biasing factor for any particular system highly depends on the network density.

## 4.5 Conclusion and Future Work

In this chapter, we present a solution on joint implementation of power control based ICIC and CRE technique to jointly maximize SE, DL system throughput and coverage probability. Location of participating BSs and UEs are stochastically modeled as PPP for tractability. We incorporate cell selection technique for traffic offloading by assigning different bias values for the MBS. Unlike the static ABS ratio and fixed CRE value configuration adopted in most literature, our solution adopts selection of both ABS ratio and CRE values adaptively, taking into consideration traffic load and network requirement. Contrary to the widely used complete blanking of subframes by MBS, we distinguish the frame structure by reduced and full power, to efficiently control ICI and avoid degradation of MUE capacity. While similar approach has been used in [125], which we build upon, we however extend our solutions to emulate more challenging traffic condition and accommodate coverage probability analysis, which is a very important performance index in user association problem. Simulation results show better performance in terms of SE and coverage, while achieving about (35-40%) rate for UEs to select pico BS as serving cell.

Since next generation wireless systems will benefit greatly from joint implementation of various traditional schemes, with reduced complexity, future work to simultaneously optimize both downlink and uplink of our proposed solution for enhanced network performance will be considered. Hence, in furtherance to the model used in this chapter, the next chapter

presents a solution based on PPP, power and spectrum sharing for improved capacity and ICI reduction in vehicular communication, considered as one of the use cases for 5G UDN.

# Chapter 5

# Robust Power Allocation Towards Interference Coordination and Improved Capacity in 5G Ultra-Dense Vehicular Communication Networks

## 5.1 Introduction

Recent advancement in information and communication technology (ICT) has necessitated the envisioned 5G technology to accommodate an unprecedented heterogeneous and ultra-dense communication environment. The great potentials of vehicular communications to support intelligent transportation system (ITS), ensure reliability and provide various safety applications on our roads have continuously triggered hot research focus in recent years. The

concept of ITS, as shown in Fig. 5.1, involves communication among vehicles, called vehicle-to-vehicle (V2V) communication, and between vehicles and the infrastructure or road-side unit (RSU), termed vehicle-to-infrastructure (V2I or V2R) communication. However, despite the vast benefits, there are several challenges faced by vehicular communication such as traffic safety and congestion, which greatly affects the capacity requirements, especially in urban settings with high vehicle density. In addition, high urban vehicular density often leads to serious competition for the available network capacity by various applications and data-driven devices. Similarly, high vehicle mobility can restrict connectivity which can in turn

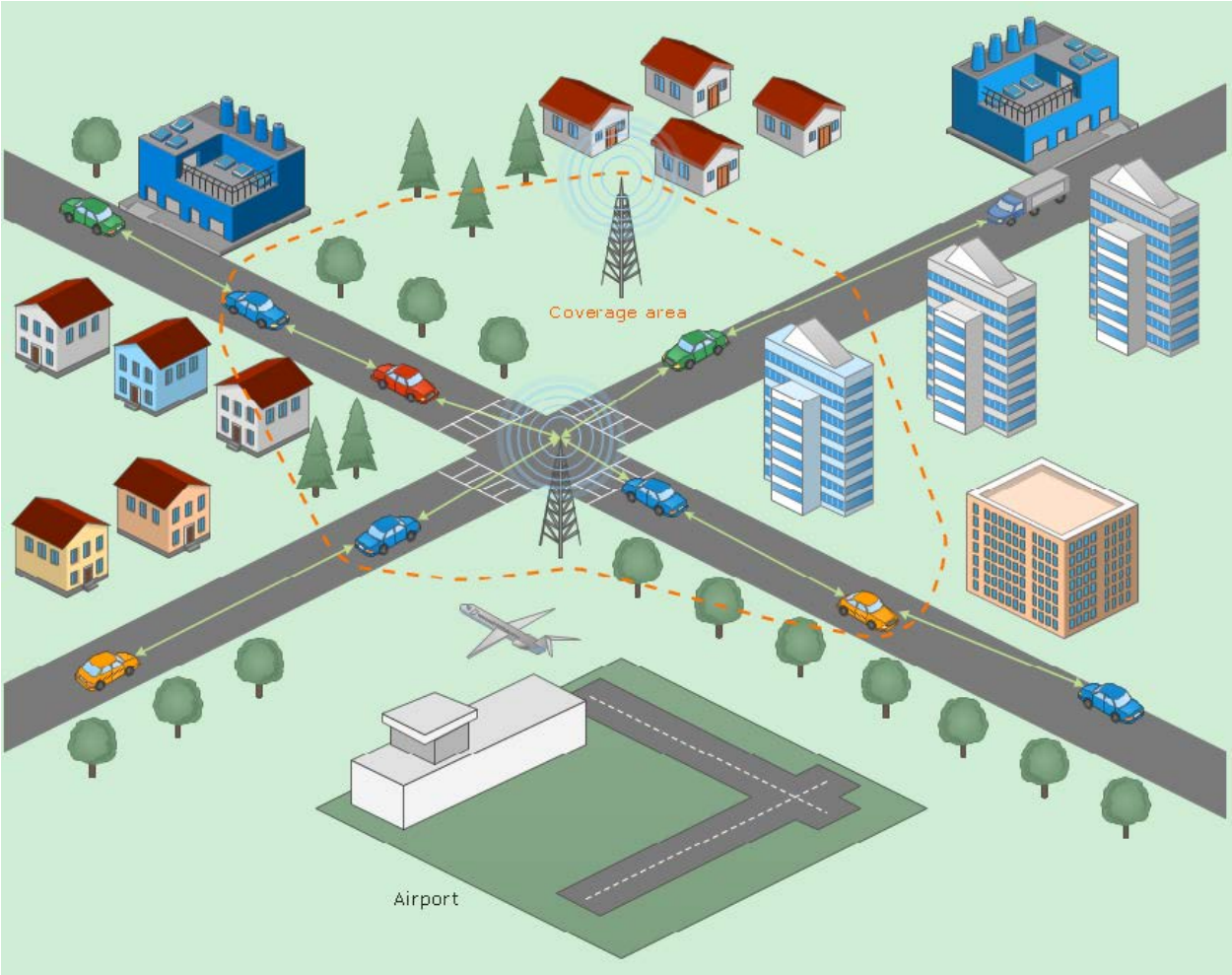


**Figure 5.1:** Vehicular communication in urban cellular networks [130].

delay important information delivery.

This chapter introduces 5G UDN use case which supports both V2V and cellular user communication sharing the same frequency band. In a V2V-enabled cellular communication, interference between the V2V users and cellular users can be particularly challenging. Hence, in order to derive maximum benefit from reusing the radio resources between the two communication links, there is need to design a dynamic interference mitigation scheme. The chapter also presents different results on SINR distributions for capacity improvement arising from both urban and freeway scenarios.

In Chapter 4, gains of deploying low power nodes in the coverage of macrocell for offloading purposes were presented. Thereafter, solutions based on reduced power subframes were proposed, where expressions for average capacity and throughput were derived, taking into consideration node density, transmit power and interference dynamics in UDN setting. Also, the multi-tier network is modeled such that BSs are randomly located with a specific transmit power, spatial density and path loss arrangement. The aim is to maximize sum capacity of the cells and maintain fairness among users.

Similarly, this chapter consolidates on this approach by exploiting traffic offloading benefit of V2V links from cellular networks, and then develop an interference aware power control algorithm to enhance network performance in terms of the ergodic capacity, in such a case when the V2V users share radio resources with downlink cellular users. For novelty purpose, we exploit the tractability of stochastic geometry on Poisson Point as a realistic representation of the urban environment to analyse the coverage of cellular users (CUEs) and vehicle-to-vehicle users (VUEs). Furthermore, the base station (BS) and CUE/VUE

locations are modeled as Poisson Point Process (PPP), similar to the model used in Chapter 4, to capture and address the line-of-sight (LOS) interference encountered in infrastructure co-located on the same street.

Since channel estimation errors and uncertainties are widely common due to high mobility of users (CUEs and VUEs), thereby invalidating different channel models and making the available network capacity difficult to estimate, imperfect channel state information (CSI) is considered to serve as metric for the reliability constraint in the resource allocation optimization of vehicular communications. Based on this knowledge, our optimization problem seeks to maximize sum ergodic capacities of all V2V/V2I links subject to different Quality of Service (QoS) constraints. The aim is to maintain the outage probability below certain SINR threshold and to guarantee link reliability for CUEs/VUEs pairs and V2V/V2I, while taking into consideration LoS/Non-LoS (NLoS) parameters.

### 5.1.1 Motivation

One of the promising features intended to enhance 5G UDN is ultra-reliable and low-latency communication (URLLC), provided by vehicular communication with potentials to support ITS and safety management. Vehicular communication underlaying cellular infrastructure has the advantage to provide shorter distance between devices, thereby reducing path loss and help improve transmission reliability. However, due to complicated communication environment and high mobility, providing efficient and reliable vehicular transmission to satisfy different requirements has become challenging. One of such challenges is interference caused by other networks to vehicle users, which invariably impacts the quality of service

of some vehicular applications. The interference is more severe when, unavoidably, V2V and cellular users reuse the same spectrum within the network. Hence, to realize the goal of achieving enhanced system performance, there is urgent need to design an efficient algorithm that jointly considers spectrum utilization and power control specifically for interference mitigation, while matching geographical information with data queue dynamics. Although, a lot of work has been done in the area of radio resource management for both cellular and vehicular communication. To date, none of the existing literature has been able to achieve interference reduction in vehicular networks through blended delay communication, dynamic links, CSI availability, as well as LoS/NLoS effect in the resource allocation optimization and performance analysis, respectively. Motivated by the aforementioned shortcomings, this chapter proposes a robust spectrum and power allocation scheme that opposes the general assumption that global CSI is unavailable at all network entities, and takes into account fast-varying and environmental conditions with less complexity. The main contribution of this chapter is highlighted below:

- Exploit the tractability of stochastic geometry on Poisson point as a realistic representation of urban streets to analyze the coverage of both cellular and vehicular UEs.

- Formulate an optimization with constraints that account for various requirements of V2I and V2V links, taking into consideration both slow and fast fading components of the CSI. Existing resource management algorithms, [103, 131] designed to satisfy differentiated requirements each for V2I and V2V links are extended to accommodate latency, capacity and reliability requirements jointly for both V2I and V2V connections.

To achieve this, strict constraints are set based on priority. For example, V2V applications require high latency and reliability requirements over high data rate demands for V2I links.

- Develop a model to capture and address the effect of LoS/NLoS interference resulting from co-located infrastructure in urban vehicular scenario.

- Derive closed-form expressions to maximize capacities of all V2V/V2I links.

- Derive an expression for the outage probability to evaluate the reliability requirements, based on the slow fading channel information available at the BS.

- Aggregate individual expressions to Power Allocation and Spectrum Sharing (PASS) formulation and designed low complexity algorithm to find its optimal solution.

The structure of the rest of this chapter is summarised as follows: Related literature are described in the next section followed by theoretical analyses of vehicular network model. Simulation results and discussion are presented next. Finally, the conclusion and future work areas are presented.

## 5.2 Literature Review

With vehicular network constituting a special family of Mobile Ad-hoc Networks (MANETs), a lot of efforts have been targeted at solving many contending issues so as to derive maximum benefit of V2V communications. Vehicles use different wireless access technologies to communicate among themselves and with the nearby infrastructure or RSU. Either

short range, such as Wi-Fi or long-range wireless access in vehicular environment (WAVE) technology may be used as the wireless technologies for cellular networks, although both technologies offer collective overall capacity if they co-exist. The authors in [132, 133] formulated resource allocation problem in multi-user OFDM system and incorporated it into security platform of physical layer. In [132], the authors investigated cooperation issue through spectrum sharing and joint power control as applied to physical layer security in cellular communication underlaid by D2D links. The aim is to achieve a better performance in terms of secrecy rate through formulated merge-and-split coalition formation algorithm for both CUE and D2D pairs. Also, [133] studied resource allocation policy and performance of packet routing protocols by proposing a vehicular mobility model that captures real-world vehicle movement. Effectiveness and performance gains of the proposed scheme were demonstrated via trace-generated simulations. Although, full CSI is assumed to be available at the BS in the existing resource allocation problems [134, 135]. However, this assumption may be invalid due to the difficulty in obtaining full CSI of the rapidly changing vehicular network topology. Thus, the resource allocation results take a non-negligible time to obtain, hence creating more challenges for channel modeling in vehicular networks [136]. The authors in [137] addressed this problem through power allocation formulation that jointly incorporates chance constraints and Non Orthogonal Multiple Access (NOMA) scheme. The objective of this approach is to improve spectrum efficiency and limit cross-tier interference. Recently, a lot of attention has been focused on mmWave band as a way to solve the problem of scarce spectrum utilization [135, 138, 139]. In pursuant of this, a typical urban street environment was modeled as a 3-dimensional Manhattan Poisson Line Processes (MPLP) in

[139] using stochastic geometry in combination with mmWave-specific channel model. The model considered variations in the propagation environment and LOS/NLOS interference effects. Using the same model, the work in [139] was extended further in [140] to maximize the ergodic capacity of CUEs by deriving a closed form expression that considers QoS requirements for both V2I and V2V links. However, the work in [135] proposed a blended swarm intelligence and matching theory to efficiently and dynamically pair vehicles for transmission and reception beamwidths optimization. In the paper, Queue State Information (QSI) and CSI were jointly considered when establishing V2V links. Finally, the authors in [141] formulated a resource allocation optimization in Device-to-Device (D2D)-overlaid vehicular communications. The paper accounted for fast variation in channel condition occasioned by high mobility nature of D2D overlaying vehicular networks. This is to ensure that the outage probability of the received signal is prevented from exceeding a certain threshold value. Also, the authors exploited the small variation in large-scale fading signal present in wireless channel of highway scenario to perform resource allocation and spectrum sharing, as against common formulations based on full knowledge of CSI at the BS.

## 5.3 System Model

Consider an urban area vehicular communication network consisting of $M$ CUEs and $K$ pairs VUEs as shown in Fig. 5.2. Denote the corresponding sets by $\mathcal{M} = \{1, 2, ..., M\}$ and $\mathcal{K} = \{1, 2, ..., K\}$, respectively and assume orthogonal RB allocation for the CUE to be performed by any reasonable scheduling scheme. In addition, two homogeneous Poisson Point Processes (PPP) are generated as $\Phi_x$ and $\Phi_y$. Also, multiple VUEs can be paired with

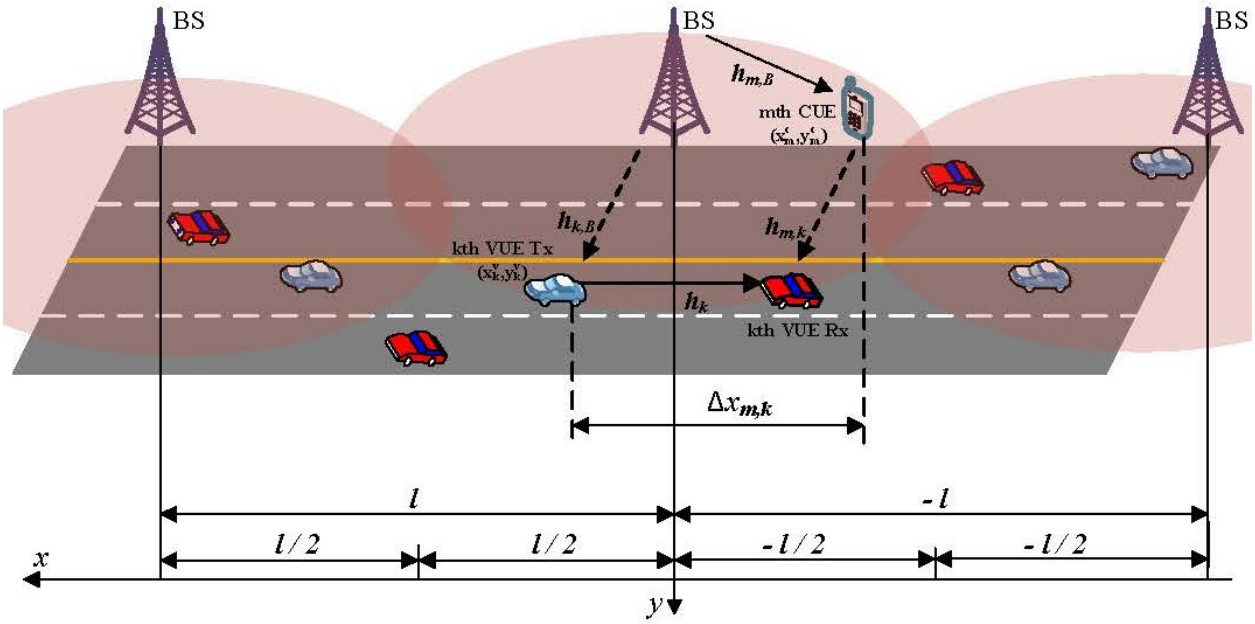


**Figure 5.2:** Interference scenario between V2V and V2I links in vehicular communication topology.

a particular CUE simultaneously for RB sharing [142], resulting in interference scenario depicted in Fig. 5.2. Assume a flat fading and narrow-band channel, the average power gain of the channel between the $m$th CUE and the BS can be expressed as

$$h_{m,B} = L_{m,B} D_{m,B}^{-\delta} S_{m,B} g_{m,B} \triangleq \alpha_{m,B} g_{m,B} \tag{5.1}$$

where $g_{m,B}$ denotes the small-scale fast fading component, $L_{m,B}$ represents the path loss coefficient, $D_{m,B}^{-\delta}$ is the distance between the $m$th CUE and the BS, $\delta$ is the path loss exponent. The path loss and shadowing effect of all links are incorporated in $\alpha_{m,B}$ to form the large scale fading components of the channel, while $S_{m,B}$ is the log-normal shadow fading

with distribution [103]

$$f_{S_{m,B}}(S) = \frac{\xi}{\sqrt{2\pi\sigma_s S}} \exp\left[\frac{(10\log_{10}s)^2}{2\sigma_s^2}\right] \tag{5.2}$$

where $\xi = 10/\ln 10$. The BS has knowledge of this information since it is dependent on users' locations and also vary on a slow scale. For $\alpha_{m,B}$ and $\alpha_{k,B}$, i.e., the links between CUEs/VUEs and the BS, the information will be estimated by the BS, while the BS receives periodically the parameter reports estimated at the VUE receiver based on CSI feedback interval $\Upsilon$ for $\alpha_k$ and $\alpha_{m,k}$, i.e., links between vehicles. The fast fading components of the channel variation over the period $\Upsilon$ with quantity $\varphi$ being the channel correlation between two consecutive time slots can be modeled using the Jakes' model for fading channel as [143]

$$\varphi = \varepsilon_0(2\pi f_d \Upsilon) \tag{5.3}$$

where $\varepsilon_0(\cdot)$ denotes the zeroth-order Bessel function and $f_d = vf_c/c$ represents the maximum Doppler frequency with $f_c$ being the carrier frequency, $v$ is the vehicle speed and $c = 3 \times 10^8$ m/s.

Pathloss model is used in cellular networks to determine LoS and NLoS links, since transition between LoS/NLoS links is common in urban setting due to high density of streets and skyscrapers. In this case, estimating pathloss through Euclidean distance calculation only works for randomly oriented buildings, but not V2I links where interference may result from co-located infrastructure on the same street [144]. Thus, PPP helps to characterize correlated shadowing effects in urban buildings. Therefore, to account for street geometry and capture

the effect of blockage and shadowing due to buildings in an urban setting, we consider the following:

- In urban scenario, there are different segments.
- Pathloss on different segments are added up
- Assume there are N segments in total, along the propagation paths, then there are (N-1) corners where signals change direction.

Let,

$\delta_j$ - represent pathloss exponent of segment $j$.

$\beta$ - represent loss at the corner of $j$ and $(j+1)$ segment, which is identical at different corners.

$\delta_L$ - denote pathloss exponent shared by LoS segments on different streets

$\delta_N$ - be the pathloss exponents for NLoS segments.

The pathloss added by extra beamforming gain in the antenna model at the BS is [139]

$$\Gamma_{dB} = 10\left(\delta_L \log_{10} l_1 + \delta_N \sum_{j=2}^{N} \log_{10} l_j\right) + (N-1) \tag{5.4}$$

Thus, following from (5.1), the corresponding channel gain between CUE $m$ and VUE $k$, VUE $k$ and the BS and VUE pairs are, respectively expressed as

$$h_{m,k} = L_{m,k} D_{m,k}^{-\delta} S_{m,k} g_{m,k} \triangleq \alpha_{m,k} g_{m,k} \tag{5.5}$$

$$h_{k,B} = L_{k,B} D_{k,B}^{-\delta} S_{k,B} g_{k,B} \triangleq \alpha_{k,B} g_{k,B} \tag{5.6}$$

$$h_k = L_k D_k^{-\delta} S_k g_k \triangleq \alpha_k g_k \tag{5.7}$$

Considering the base station association rule on the urban street topology as shown in Fig. 5.3, denote by $\lambda_{m,B}^2$ the set of LoS link with distance $x_{m,B}^2$ from the BS to $m$-th CUE,

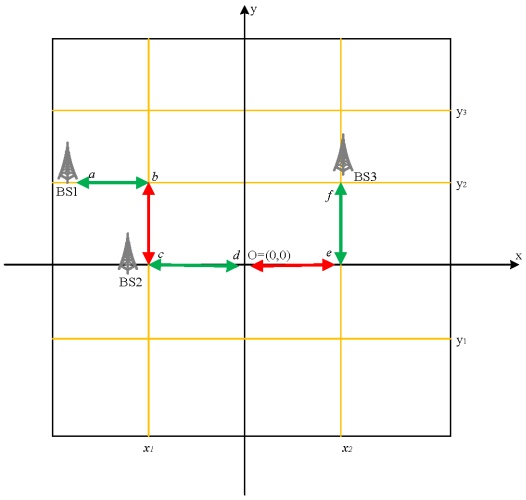


**Figure 5.3:** Cartesian coordinate system for typical urban street orientation

$\lambda_{m,B}^3$ the set of LoS/NLoS links with distances $x_{m,B}^3$ and $y_{m,B}^3$, and $\lambda_{m,B}^1$ the set of distances $x_{m,B}^1, y_{m,B}^1$ and $z_{m,B}^1$. Hence, LoS and NLoS segment path gains are, respectively, expressed as

$$u_L(x) = G(x)^{-\delta_L} \qquad \text{and} \qquad u_N(x) = c(x)^{-\delta_N} \tag{5.8}$$

where $G$ is the beamforming antenna gain of the BS added only to the LOS segment pathloss, being the closest and first path to the BS. Also, the term $c = 10^{-\Delta/10}$ represents the corner loss included in the NLOS propagation segment. The signal-to-interference-plus-noise ratio

(SINR) of the link from $m$-th CUE to the BS is given by

$$\gamma_m^c = \frac{P_m^c h_{m,B}}{\sigma^2 + I_T} \tag{5.9}$$

$$\begin{aligned}\text{where } I_T = & \sum_{\substack{k\in\mathcal{K} \\ x^2_{m,B}\in\lambda^2_{m,B}}} \rho_{m,k} P_m^v h_{k,B} u_L(x^2) \\ & + \sum_{\substack{k\in\mathcal{K} \\ (x^3_{m,B},y^3_{m,B})\in\lambda^3_{m,B}}} \rho_{m,k} P_m^v h_{k,B} u_N(x^3) u_L(y^3) \\ & + \sum_{\substack{k\in\mathcal{K} \\ (x^1_{m,B},y^1_{m,B},z^1_{m,B})\in\lambda^1_{m,B}}} \rho_{m,k} P_m^v h_{k,B} u_N(x^1) u_N(y^1) u_L(z^1)\end{aligned}$$

Note that $I_T$ is the sum LOS and NLOS of power received from the network, called total interference. Similarly, SINR at the BS for the link between $k$-th VUE pair is

$$\gamma_k^v = \frac{P_k^v h_k}{\sigma^2 + \sum\limits_{m\in\mathcal{M}} \rho_{m,k} P_m^c h_{m,k}} \tag{5.10}$$

where $P_m^c$ and $P_k^v$ represent transmit powers of the $m$-th CUE and $k$-th VUE, respectively, $\sigma^2$ is the channel's AWGN and $\rho_{m,k} \in \{0, 1\}$ denotes the spectrum allocation indicator, such that

$$\begin{cases} \rho_{m,k} = 1, \text{VUE pair } k \text{ reuses the spectrum of the } m\text{th CUE} \\ \rho_{m,k} = 0, \text{ otherwise} \end{cases} \tag{5.11}$$

It is noteworthy that interference only occurs between CUE and VUE pairs during spectrum reuse as indicated in (5.11). The importance of (5.9) and (5.10) in the analysis of network coverage in vehicular communications is shown later in Section 5.3.3. It is always impossible

in highway setting for the BS to estimate the information containing small scale fading values due to very high vehicular speeds. This compels the BS to assume average values for the small scale fading and full CSI of large scale fading. Thus, the capacity of $m$th CUE at a certain position can be expressed as

$$C_m^c = \mathbb{E}_g \left[ \log_2 \left( 1 + \gamma_m^c \right) \right] \tag{5.12}$$

Similarly, the capacity of $k$th VUE pair at a certain position is

$$C_k^v = \mathbb{E}_g \left[ \log_2 \left( 1 + \gamma_k^v \right) \right] \tag{5.13}$$

where the expectation $\mathbb{E}_g[.]$ is measured with respect to the fast fading distribution. In urban vehicular network settings, BSs are deployed at street level, where building blockages are considered as the main source differentiating LOS and NLOS links. In this manner, NLOS BSs constitute less benefit for association, hence ultra dense deployment of BSs does not enhance coverage. Thus, pathloss model with a LOS probability function based on Euclidean distance are often used to determine whether a link was LOS or NLOS. However, this works well for randomly oriented buildings, but does not properly model V2I networks where strong LOS interference may result from infrastructure co-located on the same street. Therefore, we assume a spatially consistent pathloss model as a function of both the street orientation and the absolute location of the BS and UE.

Maximising the average capacity of vehicular network during an access period can be achieved in two ways, namely: through dynamic allocation and position ergodic capacity

enhancement techniques [103]. The basic idea behind dynamic allocation concept is that resource allocation is performed instantaneously once at a time, i.e., during sampling period. Subsequently, the average capacity is computed by aggregating all the maximized capacities. On the other hand, position ergodic capacity scheme maximizes CUE/VUE link capacity via resource allocation optimization after initial derivation of expression for the position ergodic capacity of CUE. The ergodic capacity is defined as the capacity expectation, taking into consideration all positions. However, dynamic allocation of resources in highway setting is infeasible due to channel uncertainty, while resource allocation through ergodic capacity optimization is realizable with low complexity.

Hence, let a BS be positioned at the origin marked O and construct $X$ axis in the direction of the road with $Y$ axis along the horizontal plane, perpendicular to $X$, as depicted in Fig. 5.2. Denote the coordinates of $m$th CUE and transmitter of the $k$th VUE on the plane as $(x_m^c, y_m^c)$ and $(x_k^v, y_k^v)$, respectively. For simplicity, we consider a single lane such that each vehicle travels on the same direction, hence $(y_m^c)$ and $(y_k^v)$ remain unchanged. The midpoint between two nearest BSs constitutes the access period given as the path from $(\frac{-l}{2}, 0)$ to $(\frac{l}{2}, 0)$. The CUE maintains connection with the BS at this period after which it switches to another BS. At this instance, the spectrum of every CUE can either be reused by a VUE or not, according to (5.11), which results in two possibilities as discussed below.

### 5.3.1 Capacity when CUE spectrum is unpaired

Let $C_{m,0}^c(x)$ represent the capacity of $m$th unpaired CUE positioned at $(x, y)$, which only depends on $x$ since $y$ is assumed to be constant for vehicles driving on the same direction.

Furthermore, the SINR $\gamma_m^c$ of $m$th CUE can be obtained by replacing $D_{m,B} = \sqrt{x^2 + y^2}$ in $h_{m,B}$ and $h_{k,B}$ of (5.1) and (5.6), respectively, and setting $\rho_{m,k} = 0$ for $m$th unpaired CUE. Thus,

$$C_{m,0}^c(x) = \mathbb{E}_g \left[ \log_2 \left( 1 + a(x) g_{m,B} \right) \right] \tag{5.14}$$

Using exponential distribution with unit mean for the small scale fading component $g_{m,B}$, (5.14) can be computed as

$$\begin{aligned} C_{m,0}^c(x) &= \int_0^\infty \log_2 \left[ 1 + a(x) g \right] e^{-g} \, \mathrm{d}g && \text{(5.15a)} \\ &= \frac{1}{\ln 2} \int_0^\infty \frac{1}{a(x)} \, e^{\frac{-z}{a(x)}} \ln \left[ 1 + z \right] \mathrm{d}z && \text{(5.15b)} \\ &= \frac{1}{\ln 2} \int_0^\infty \frac{e^{\frac{-z}{a(x)}}}{1 + z} \, \mathrm{d}z && \text{(5.15c)} \\ &= \frac{1}{\ln 2} \, e^{\frac{1}{a(x)}} E_1 \left[ \frac{1}{a(x)} \right] && \text{(5.15d)} \end{aligned}$$

where (5.15c) is solved using integration by parts and (5.15d) follows from [145].

Hence, incorporating the position ergodic capacity defined as

$$\begin{aligned} \overline{C}_{m,0}^c &= \mathbb{E}_x \left\{ C_{m,0}^c(x) \right\} = \frac{1}{l} \int_{\frac{-1}{2}}^{\frac{1}{2}} C_{m,0}^c(x) \, \mathrm{d}x \\ &= \frac{2}{l} \int_0^{\frac{l}{2}} C_{m,0}^c(x) \, \mathrm{d}x \end{aligned} \tag{5.16}$$

and substituting (5.15a) into (5.16) yields the position ergodic capacity of the $m$th unpaired CUE given as

$$\overline{C}_{m,0}^c = \frac{2}{l \ln 2} \int_0^{\frac{1}{2}} e^{\frac{1}{a(x)}} \, E_1 \left[ \frac{1}{a(x)} \right] \mathrm{d}x \tag{5.17}$$

where $x \triangleq x_m^c$, $y \triangleq y_m^c$, $E_1(z) = \int_z^\infty \frac{e^{-t}}{t}\mathrm{d}t$ and $a(x) = P_m^c L_{m,B} S_{m,B}(x^2+y^2)^{\frac{-\delta}{2}}/\sigma^2$.

### 5.3.2 Capacity when CUE spectrum is paired

When the spectrum of $m$th CUE is reused by $k$th VUE, the capacity at a certain position $(x, y)$ is denoted by $C_{m,1}^c$. At this point, the second and last interference components in (5.9) tend to approximately 1, indicating that the interference is adequately small to be negligible. By substituting $D_{m,B} = \sqrt{x^2+y^2}$, $D_{k,B} = \sqrt{(x+\Delta x_{m,k})^2 + (y_k^v)^2}$ and (5.1), (5.6), (5.9), leaving out the negligible parts, into (5.12), we get

$$C_{m,1}^c(x) \triangleq \mathbb{E}_g\left[\log_2\left(1+\frac{a(x)X}{1+b(x)Y}\right)\right] \tag{5.18}$$

where

$$b(x) = \frac{P_k^v L_{k,B} S_{k,B}[(x-\Delta x_{m,k})^2 + (y_k^v)^2]^{\frac{-\delta}{2}}}{\sigma^2} \tag{5.19}$$

$\Delta x_{m,k} \triangleq x_m^c - x_k^v$, $X \triangleq g_{m,B}$, $Y \triangleq g_{k,B}$ and $a(x)$ had been defined earlier. Also, let $Z = \frac{a(x)X}{1+b(x)Y}$ such that $g_{m,B}$ and $g_{k,B}$ are assumed to be i.i.d exponential random variables with unit mean, therefore the cumulative distribution function (CDF) of $Z$ can be computed as

$$\begin{aligned} F_Z(z) &= \Pr\left\{\frac{a(x)X}{1+b(x)Y} \le z\right\} \\ &= \int_0^\infty \mathrm{d}y \int_0^{\frac{z[1+b(x)y]}{a(x)}} e^{-(x+y)}\mathrm{d}x \\ &= 1 - e^{-\frac{z}{a(x)}}\frac{a(x)}{a(x)+b(x)z} \end{aligned} \tag{5.20}$$

Thus, the ergodic capacity $C^c_{m,1}(x)$ of the $m$th CUE can be obtained as

$$C^c_{m,1}(x) = \frac{1}{\ln 2}\int_0^\infty \ln(1+z)\, fz(z)\, \mathrm{d}z \tag{5.21a}$$

$$= \frac{1}{\ln 2}\int_0^\infty \frac{1-F_Z(z)}{1+z}\mathrm{d}z \tag{5.21b}$$

$$= \frac{a(x)}{[a(x)-b(x)]\ln 2}\left[\int_0^\infty \frac{e^{-\frac{z}{a(x)}}}{z+1}\,\mathrm{d}z - \int_0^\infty \frac{e^{-\frac{z}{a(x)}}}{z+\frac{a(x)}{b(x)}}\,\mathrm{d}z\right] \tag{5.21c}$$

$$= \frac{a(x)}{[a(x)-b(x)]\ln 2}\left[e^{\frac{1}{a(x)}}\, E_1\left(\frac{1}{a(x)}\right) - e^{\frac{1}{b(x)}}\, E_1\left(\frac{1}{b(x)}\right)\right] \tag{5.21d}$$

where (5.21b) is obtained using integration by parts and (5.21d) follows from [145, Eq. (3.352.4)]. As obtained in (5.16), the position ergodic capacity $\overline{C}^c_{m,1}$, expressed as a function of the capacity of $m$th paired CUE is

$$\overline{C}^c_{m,1} = \frac{2}{l}\int_0^{\frac{l}{2}} C^c_{m,1}(x)\,\mathrm{d}x \tag{5.22}$$

Substituting (5.21a-5.21d) into (5.22) yields

$$\overline{C}^c_{m,1} = \frac{2}{l\ln 2}\cdot\int_0^{\frac{1}{2}} \frac{a(x)\left\{e^{\frac{1}{a(x)}}E_1\left[1/a(x)\right] - e^{\frac{1}{b(x)}}E_1\left[1/b(x)\right]\right\}}{a(x)-b(x)} \tag{5.23}$$

### 5.3.3 Coverage Analysis

In the previous sections, the capacities of both V2I and V2V links were analyzed under different QoS requirements. At every instance, the CUEs and VUEs exchange predefined sets of resources upon transmission requests during semi persistence scheduling period. Since latency and reliability are key requirements, scheduling is set at the same order of latency

requirement, thereby removing unwanted exchange of signal in each slot. Hence, the BS helps to reduce resource collision by performing holistic spectrum allocation, taking into consideration the position information supplied by each CUE/VUE, which are updated at the onset of scheduling process. Concurrently, human-to-human (H2H) traffic should be guaranteed while attempting to achieve continuous communication requirement in mobility-prone environment for message transmission efficiency. Equipped by this information, the vehicular network is challenged by co-channel interference due to dense topology, spectrum sharing among various users and time variant environment, caused by mobility. In this section, the impact of co-channel interference on network capacity is analyzed. Also, the effect of LoS and its complementary NLoS on network coverage will be presented.

The coverage probability can be derived under the condition that the received SINR is greater than a predefined threshold $\theta$, for a typical user located at the origin O. Using stochastic geometry as a tractable means of analysis, the coverage probability $p_c$, taking into account vehicular orientation and the system model derived in Section 5.3 can be expressed as

$$\begin{aligned} p_c &= \mathbf{P}[\gamma_m^c > \theta] \\ &= \mathbf{P}\left(\frac{P_m^c h_{m,B}}{\sigma^2 + I_T} > \theta\right) \end{aligned} \tag{5.24}$$

Obviously, the coverage probability defined in (5.24) can be viewed as an alternative interpretation of the complementary cumulative distribution function (CCDF) of the SINR, $\gamma_m^c$ and $\gamma_k^v$ derived in (5.9) and (5.10), respectively. Extracting the small scale components $g_{m,B}$ of the channel gain $h_{m,B}$ between $m$th CUE and BS, and putting $I_T = I_{\text{LOS}} + I_{\text{NLOS}}$

yields

$$p_c = \mathbb{E}_{I_{\text{LOS}},I_{\text{NLOS}}}\left[P_r\left(g_{m,B} > \frac{\theta(\sigma^2 + I_{\text{LOS}} + I_{\text{NLOS}})}{P_m^c h_{m,B}}\right)\right] \tag{5.25}$$

By applying the properties of small scale Rayleigh fading and assuming all links experience independent and identically distributed (i.i.d) fading where $g_{m,B} \overset{\text{i.i.d}}{\sim} \exp(1)$ with unit mean, we have

$$p_c = e^{(-q\sigma^2)}\mathbb{E}_{I_{\text{LOS}}+I_{\text{NLOS}}}\left[e^{(-q(I_{\text{LOS}}+I_{\text{NLOS}})}\right] \tag{5.26}$$

where $q = \frac{\theta}{P_m^c h_{m,B}}$. Thus, transforming (5.26) using the properties of Laplace transform yields

$$p_c = e^{(-q\sigma^2)} \prod_{j=1}^{N_{\text{LOS}}} \underbrace{\mathcal{L}_{I_{j,\text{LOS}}}(q)}_{\text{a}} \prod_{j=1}^{N_{\text{NLOS}}} \underbrace{\mathcal{L}_{I_{j,\text{NLOS}}}(q)}_{\text{b}} \tag{5.27}$$

Although, there exists two possibilities, namely: random and clustered distribution for modeling vehicles orientation, depending on the type of setting, i.e. urban or highway environment. However for simplicity, we assume random distribution for both urban and highway settings in this work. Under this assumption, the first part (a) of (5.27) can be extended as

$$\begin{aligned}
\mathcal{L}_{I_{j,\text{LOS}}}(q) &= \mathbb{E}_{I_{j,\text{LOS}}}\left[e^{(-q)I_{j,\text{LOS}}}\right] \\
&= \mathbb{E}_{I_{j,\text{LOS}}}\left[e^{\left(-q\sum\limits_{k\in\Phi} P_k^v h_{j,k} G(x)^{-\delta_L}\right)}\right] \\
&= \mathbb{E}_{I_{j,\text{LOS}}}\left[\prod_{k\in\Phi} \mathbb{E}_h e^{\left(-qP_k^v h_{j,k} G(x)^{-\delta_L}\right)}\right] \\
&= \mathbb{E}_{I_{j,\text{LOS}}}\left[\prod_{k\in\Phi} \frac{1}{1 + qP_k^v h_{j,k} G(x)^{-\delta_L}}\right]
\end{aligned} \tag{5.28}$$

Similarly, the NLOS interference in the second part (b) of (5.27) can be derived in the same manner by replacing pathloss for the NLOS segment with $cx^{-\alpha N}$, previously defined in (5.8).

### 5.3.4 Outage Probability Analysis

So far, previous sections focused on analysis of capacity as a vital requirement for V2I link. In this section, the latency and reliability requirements of V2V link are formulated as tight optimization constraints under outage probability analysis. However, the latency constraints of the V2V link require limited frequency bandwidth and number of resource blocks (RBs) assigned to each VUE in a duration of time. Hence, when a limited number of RBs $n_k$ is used for $k$th VUE transmission, at a certain number of bits $B_k$, the outage probability can then be expressed as [146]

$$p_k^o \triangleq \Pr\left\{\sum_{i=1}^{n_k} \tau \log_2\left(1+\gamma_{i,k}^v\right) < B_k\right\} \tag{5.29}$$

where $\tau$ represents number of complex symbols per RB and $\gamma_{i,k}^v$ is the SINR at the BS for the link between $k$-th VUE pair on the $i$-th RB. Thus, the reliability requirement in relation to the outage probability can be expressed as

$$p_k^o \leq p_o \tag{5.30}$$

where $p_o$ is the threshold for maximum tolerable outage probability. Unlike highway scenario with fast changing channel, the slow fading channel nature of urban environment enables the BS to perform resource allocation by setting appropriate reliability constraint. Firstly,

the upper bound of $p_k^o$ provides a better measure for a more strict reliability constraint to be imposed and is given by

$$p_k^o \leq \Pr\left\{\sum_{i=1}^{n_k} \tau \log_2\left(1+\bar{\gamma}_{i,k}^v \left|g_{i,k}\right|^2 \min\left\{\frac{1}{\left|g_{i,m,k}\right|^2},1\right\}\right) < B_k\right\} \tag{5.31}$$

where $g_{i,k}$ and $g_{i,m,k}$ are small scale fading components of the desired and interference signals of the V2V link, extracted from the corresponding average power gain of the channel, $h_{m,k}$ and $h_k$ as defined in (5.5) and (5.7), respectively. Hence, $\bar{\gamma}_{i,k}^v \triangleq \frac{P_{i,k}^v h_{i,k}}{\sigma^2+\sum\limits_{m\in\mathcal{M}} \rho_{m,k} P_{i,m}^c h_{i,m,k}}$ clearly incorporates the slow CSI. Then, it follows that

$$\gamma_{i,k}^v = \bar{\gamma}_{i,k}^v \left|g_{i,k}\right|^2 \frac{\sigma^2 + P_{i,m}^c}{\sigma^2 + P_{i,m}^c \left|g_{i,m,k}\right|^2} \tag{5.32}$$

Define $\omega(r) \triangleq \frac{(\sigma^2+r)}{\sigma^2+r\left|g_{i,m,k}\right|^2}$ such that $r \geq 0$, and the first derivative of $\omega(r)$ w.r.t $r$ will be

$$\frac{d\omega(r)}{dr} = \frac{\sigma^2(1-\left|g_{i,m,k}\right|^2)}{\left(\sigma^2 + r\left|g_{i,m,k}\right|^2\right)^2} > 0, \tag{5.33}$$

for $\left|g_{i,m,k}\right|^2 < 0$. Then,

$$\omega(r) \geq \min_{r\geq 0} \omega(r) = \min\left\{\frac{1}{\left|g_{i,m,k}\right|^2},1\right\} \tag{5.34}$$

Therefore, replacing the power $P_{i,m}^c$ received from the interfering CUEs in (5.32) by $r$ yields

$$\gamma_{i,k}^v = \bar{\gamma}_{i,k}^v \left|g_{i,k}\right|^2 \min\left\{\frac{1}{\left|g_{i,m,k}\right|^2},1\right\} \tag{5.35}$$

This implies that the expression in (5.30) is always satisfied if the strict reliability requirement defined by the upper bound probability in (5.31) is less than the maximum tolerable probability threshold $p_o$, expressed with additional stringent constraints as

$$\Pr\left\{\sum_{i=1}^{n_k}\tau\log_2\left(1+\left\{\bar{\gamma}_{i,k}^{v}\right\}^{\eta}\left|g_{i,k}\right|^2\min\left\{\frac{1}{\left|g_{i,m,k}\right|^2},1\right\}\right)<B_k\right\}\leq p_o \tag{5.36}$$

where $\bar{\gamma}_{i,k}^{v}\geq\left\{\bar{\gamma}_{i,k}^{v}\right\}^{\eta}$ for all $i=1,2,3,...,n_k$. In addition to satisfying the condition in (5.30), it would be necessary to ensure that $\left\{\bar{\gamma}_{i,k}^{v}\right\}^{\eta}$ is estimated from (5.36) for every $k$th VUE, and made to fall below $\bar{\gamma}_{i,k}^{v}$ on each RB used. Thus, let $\epsilon$ be the maximum tolerable latency per scheduling time for V2V communication, therefore the latency and reliability requirements can be given as [146]

$$\begin{aligned}\Gamma_k^v&=\left\lceil\frac{n_k}{\epsilon}\right\rceil\\ \bar{\gamma}_{i,k}^{v}&\geq\left\{\bar{\gamma}_{i,k}^{v}\right\}^{\eta},\quad\forall\, i=1,2,...,\Gamma_k^v\end{aligned} \tag{5.37}$$

where $\Gamma_k^v$ denotes the RB number allocated to the $k$th VUE during each scheduling time unit such that $\sum_{k=1}^{K}\Gamma_k^v\leq U$, where $U$ is the frequency bandwidth subbands. To satisfy the latency and reliability requirements of the VUEs, the solution of (5.37) must ensure allocation of at least $n_k$ RBs to the $k$th VUE within $\epsilon$ time. Moreover, an appreciable number of data packets should be sent within the latency region, in order to find optimal power and RB plan which maximizes the network position-average power requirements.

### 5.3.5 Proposed Power Allocation and Spectrum Sharing (PASS) Algorithm

In this section, the procedure for the proposed Power Allocation and Spectrum Sharing (PASS) Algorithm is described. Generally speaking, solutions to optimization problems involving joint power allocation and spectrum sharing are always hard. This is due to the complex, non-convex nature of the problem, involving tight coupling between power and interference, with combinatorial composition of both binary and continuous variables. Hence, the first step to solving the problem is to decompose the resource allocation into two sub-problems and then design an appropriate algorithm to solve it. In this case, we employ the Kuhn-Munkres assignment algorithm [147] to solve the problem which is of the form of generalized maximum cardinality bipartite matching. For brevity, let $r_0^c$ denote the achievable rate of the CUEs and $r_0^v \triangleq B_k/t_0^v$ represent the achievable rate of the VUEs, where $t_0^v$ corresponds to the latency requirement. Using the solution to the optimal power allocation sub-problem from [131] for ergodic capacity maximization of $m$th CUE and reliability requirement of the $k$th VUE given as

$$\begin{aligned} P_m^{c^*} &= \min(P_{max}^c, P_{v,max}^c) \\ P_k^{v^*} &= \min(P_{max}^v, P_{c,max}^v) \end{aligned} \tag{5.38}$$

where $0 \leq P_m^c \leq P_{max}^c$ and $0 \leq P_k^v \leq P_{max}^v$, $P_m^{c^*}$ and $P_k^{v^*}$ in (5.38) are the optimal transmitting power of the CUE and VUE, respectively, $P_{max}^c$ and $P_{max}^v$ are the respective maximum transmit power for each CUE and VUE, while $P_{v,max}^c = f(P_{max}^v)$ and $P_{c,max}^v = f^{-1}(P_{max}^c)$

represent the feasible regions obtained through bisection search over

$$f(P_k^c) \triangleq \frac{\alpha_k P_k^v}{B_k \alpha_{m,k}} \left( \frac{e^{-\frac{B_k \sigma^2}{\alpha_k P_k^v}}}{1 - p_0} - 1 \right) \geq P_m^c \tag{5.39}$$

So far, various requirements of CUEs (i.e., rate) and VUEs (i.e., latency and reliability) have been jointly taken care. It should be noted however that, even with the optimal transmitting powers, if the maximum ergodic capacity, denoted by $C_{m,k}^*$, of the $m$-th CUE when paired with the $k$-th VUE is less than $r_0^c$, then the CUE-VUE pairing remains infeasible. In other words, the CUE-VUE is unable to meet the rate requirement, therefore, the following condition is applied

$$C_{m,k}^* = \begin{cases} C_{m,k}(P_m^{c^*}, P_k^{v^*}), & \text{if } \mathbb{E}_g \left[ \log_2 \left( 1 + \gamma_m^c \right) \right] \geq r_0^c \text{ and } \mathbb{E}_g \left[ \log_2 \left( 1 + \gamma_k^v \right) \right] \geq r_0^v, \\ -\infty, & \text{otherwise} \end{cases} \tag{5.40}$$

Hence, Algorithm 1 details the procedure involved in finding optimal solution to the PASS scheme.

### 5.3.6 Fairness Index

Considering the proposed PASS scheme as a special case of resource allocation technique, the fairness index becomes necessary to evaluate fairness allocation of resources among the CUEs and VUEs. Hence, the Jain's Fairness index (JFI) is employed in the scheme as functions of

**Algorithm 1** Procedures of the proposed Algorithm for PASS Solution

**for** $m = 1, 2, ..., M$ **do**

  **for** $k = 1, 2, ..., K$ **do**

    Calculate $\gamma_m^c$ and $\gamma_k^v$ from (5.9) and (5.10) respectively.

    Calculate $P_c$ and $P_k^o$ according to (5.24) and (5.30).

    Evaluate the optimal power allocation $(P_m^{c^*}, P_k^{v^*})$ for the $m$th CUE and $k$th VUE respectively from (5.38)

    Substitute $(P_m^{c^*}, P_k^{v^*})$ into (5.21a-5.21d) to obtain $\mathbb{E}_g\left[\log_2\left(1+\gamma_m^c\right)\right]$ and $\mathbb{E}_g\left[\log_2\left(1+\gamma_k^v\right)\right]$;

    **if** $\mathbb{E}_g\left[\log_2\left(1+\gamma_m^c\right)\right] \geq r_0^c$, $\mathbb{E}_g\left[\log_2\left(1+\gamma_k^v\right)\right] \geq r_0^v$ **then**

      $C_{m,k}^* = C_{m,k}(P_m^{c^*}, P_k^{v^*})$

      Calculate $\mathbb{E}_{agg} = \sum_{m=1}^{M} \mathbb{E}_g\left[\log_2\left(1+\gamma_m^c\right)\right] + \sum_{k=1}^{K} \mathbb{E}_g\left[\log_2\left(1+\gamma_k^v\right)\right]$;

    **else if** $\mathbb{E}_g\left[\log_2\left(1+\gamma_m^c\right)\right] < r_0^c$, $\mathbb{E}_g\left[\log_2\left(1+\gamma_k^v\right)\right] < r_0^v$ **then**

      $C_{m,k}^* = -\infty$

    **end if**

  **end for**

**end for**

Find the optimal pairing pattern $\{\rho_{m,k}^*\}$ based on $\{C_{m,k}^*\}$ using the Kuhn and Munkres' Assignment Algorithm [147].

Return the optimal pairing pattern $\{\rho_{m,k}^*\}$ and the associated power allocation $(P_m^{c^*}, P_k^{v^*})$.

throughput for both the CUEs and VUEs, expressed as

$$\text{JFI}_{(\text{CUE})} = \frac{\left( \sum_{m=1}^{M} [\log_2 (1 + \gamma_m^c)] \right)^2}{M \cdot \sum_{m=1}^{M} [\log_2 (1 + \gamma_m^c)]^2}, \quad \forall m \in \mathcal{M}. \tag{5.41}$$

Similarly, for VUEs,

$$\text{JFI}_{(\text{VUE})} = \frac{\left( \sum_{k=1}^{K} [\log_2 (1 + \gamma_k^v)] \right)^2}{K \cdot \sum_{k=1}^{K} [\log_2 (1 + \gamma_k^v)]^2}, \quad \forall k \in \mathcal{K}. \tag{5.42}$$

It can be clearly seen from (5.41) and (5.42) that JFI assumes values in the interval $\{\frac{1}{M}, 1\}$ for CUE and $\{\frac{1}{K}, 1\}$ for VUE, so that

$$\text{JFI} = \begin{cases} 1, & \text{if the scheme attains optimal fair resource allocation,} \\ \left\{ \frac{1}{M}, \frac{1}{K} \right\}, & \text{if the scheme attains least fair resource allocation} \end{cases} \tag{5.43}$$

**Table 5.1:** Simulation Parameters

| Parameters | Values |
|---|---|
| Cell radius | 500 m |
| Bandwidth | 10 MHz |
| Carrier Frequency | 2 GHz |
| Vehicle antenna gain | 3 dBi |
| Vehicle antenna height | 1.5 m |
| Vehicle receiver noise figure | 9 dB |
| Vehicle drop model | Spatial Poisson Process |
| Absolute vehicle speed | 70km/h (Freeway), 60km/h (Urban) |
| Vehicle density | Average inter-vehicle distance is 2.5 sec x absolute vehicle speed |
| Lane width | 4.0 m (Freeway), 3.5 m (Urban) |
| Number of lanes | 6 (Freeway), 4 (Urban) |
| Noise figure | 5 dB |
| BS antenna gain | 8dBi |
| BS antenna height | 25m |
| Distance between BS and highway | 25 m |
| AWGN power $\sigma^2$ | -114 dBm |
| SINR threshold for VUE | 5 dB |
| Minimum rate of VUE and CUE ($r_0^v$,$r_0^c$) | 0.5 bps/Hz (Freeway), 0.5 bps/Hz Straight, 0.25 bps/Hz Turning (Urban) |
| Bisection search accuracy | 0.001 |
| Maximum outage probability of VUE $p_0$ | 0.001 |

## 5.4 Results and Discussion

In this section, simulations were performed to evaluate the effectiveness of the proposed resource and power allocation scheme for the urban vehicular network. We compare our approach with the resource allocation algorithm presented in [131] for freeway case where

allocation of resources is based on channel information and slow fading parameters. In our simulation, vehicle UEs are dropped on the road according to Spatial Poisson Process. The vehicle position is updated every 100 ms in the simulation while the vehicle density is determined by the vehicle speed. For urban case, ISD of BSs is given as 500 m and the wrap around model is used according the 3GPP specification [148]. In addition, the channel model follows the WINNER II standard channel model where both V2I and V2V links assume Rayleigh fading and Log-normal shadowing distribution, with 8 dB and 3 dB shadowing standard deviation, respectively. The rest of simulation parameters are listed in Table 5.1 and all parameters set to the values specified therein unless otherwise stated.

Fig. 5.4 illustrates the sum ergodic capacity trend against the feedback time for different values of transmission powers in highway scenario. It can be seen that the capacity is maximized up to $\Upsilon = 0.5$ ms before a gradual decline in the system capacities for the various values of transmit power. In addition, the insensitivity of the capacity to the CSI feedback period at low SNR values as against higher values of SNR can be seen. Hence, it is clearly suggestive in Fig. 5.4 the benefit inherent in periodically varying the feedback time, motivated by joint optimization of the training duration. A closer look at the figure shows feedback period point for optimal capacity to be 0.5 ms after which the system capacity suffers degradation gradually as the feedback period increases. Fig. 5.4 further explains the effect of incessant CSI feedback procedure on the capacity of V2V/V2I links in terms of latency and reliability constraints. Hence, as the feedback time grows, the more uncertainty is introduced into $\alpha_k$ and $\alpha_{m,k}$, being the links between vehicles. This prompts the BS to control the transmit powers of CUEs in order to favour V2V links in meeting

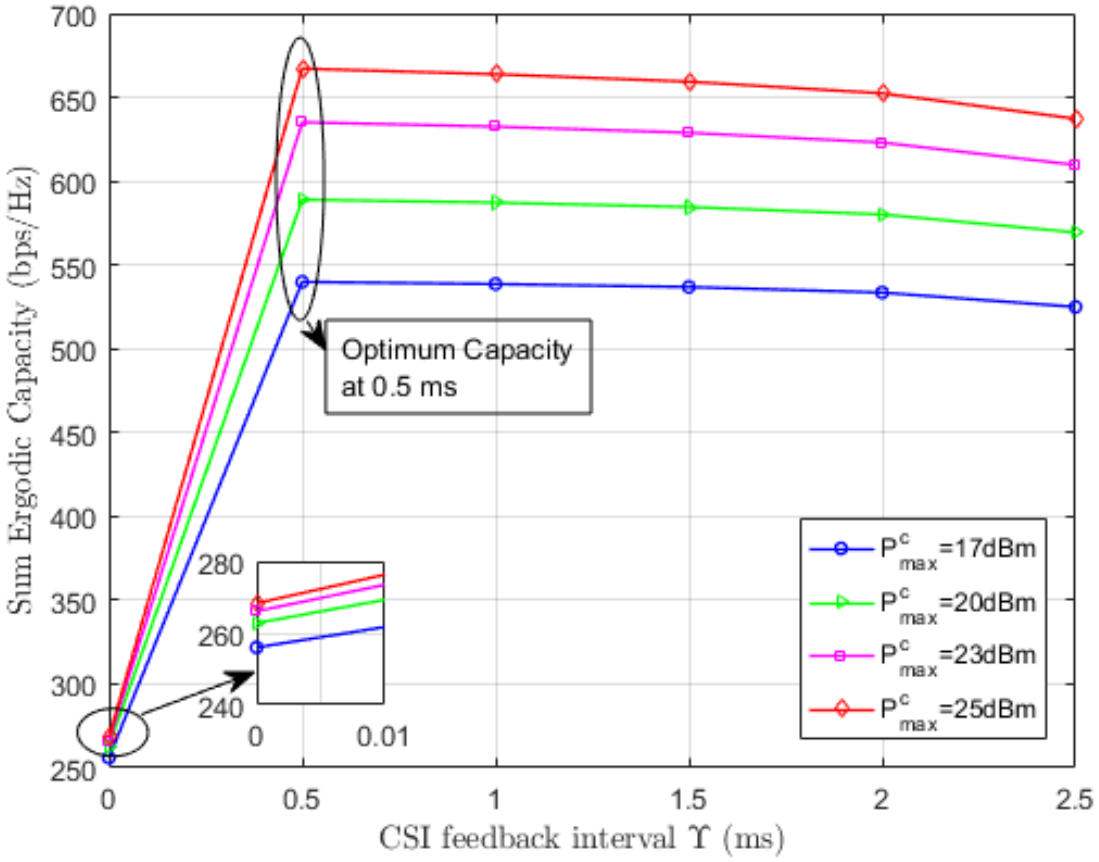


**Figure 5.4:** The effect of feedback time $\Upsilon$ on the sum ergodic capacity with varying values of maximum transmit power for V2V and V2I links.

their reliability requirements, and to protect the V2V against the interference caused by the CUEs. Moreover, at 25 dBm transmit power, the behaviour of the capacity is slightly different from the other three values of transmit power, i.e., 17 dBm, 20 dBm and 23 dBm. While at 17 dBm, the ergodic capacity maintains a relatively constant value after 0.5 ms feedback time when $P^c_{mac} = 23$ dBm. As shown, the capacity starts to fall at $\Upsilon = 2$ ms, particularly for higher transmit power, due to the overhead created by regular exchange of CSI information between CUEs/VUEs and the BS.

Fig. 5.5 shows the effect of average distance on the performance of minimum ergodic capacity of VUEs links. As can be seen, there is a remarkable decrease in the overall capacity of the VUE links with increase in the distance between them, particularly at higher density. This clearly shows that an increase in distance only improves marginally the capacity achieved by both V2I and V2V links, which also brings about reduction in the coverage area of the links. Therefore, to achieve a better capacity when the density of vehicle increases,

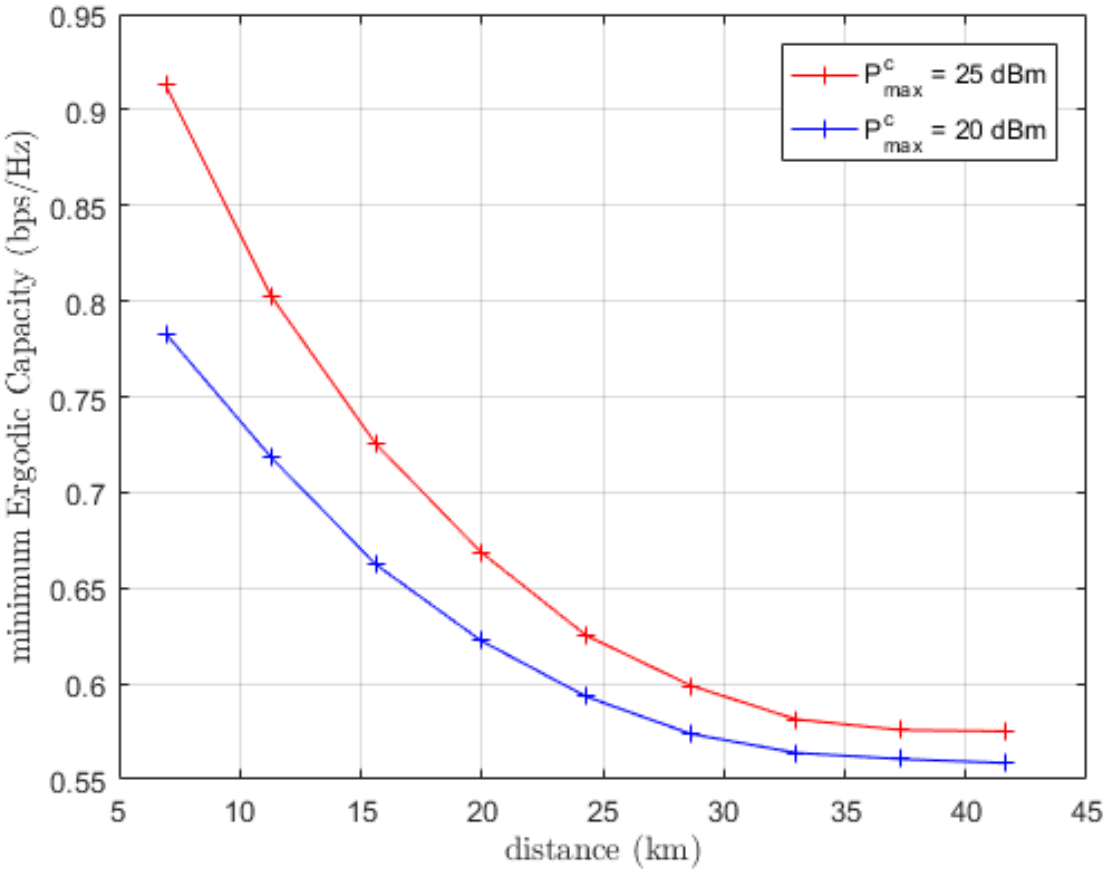


**Figure 5.5:** Minimum path ergodic capacity of VUEs with respect to average distance.

there is need to increase the distance between the associated RSU. This further provides an insight into consideration given to vehicular density when planning the optimal deployment

for V2I networks. To achieve this, cooperative communication can be utilized so as to minimize the number of RSU deployed.

In Fig. 5.6, we compare our approach with the scheme in [131] to demonstrate the superiority when urban vehicular network is stochastically modelled in order to derive the coverage probability when the penetration effect of buildings is considered. In general, the sum ergodic capacity of CUEs decreases as the vehicles speed increases. In other words,

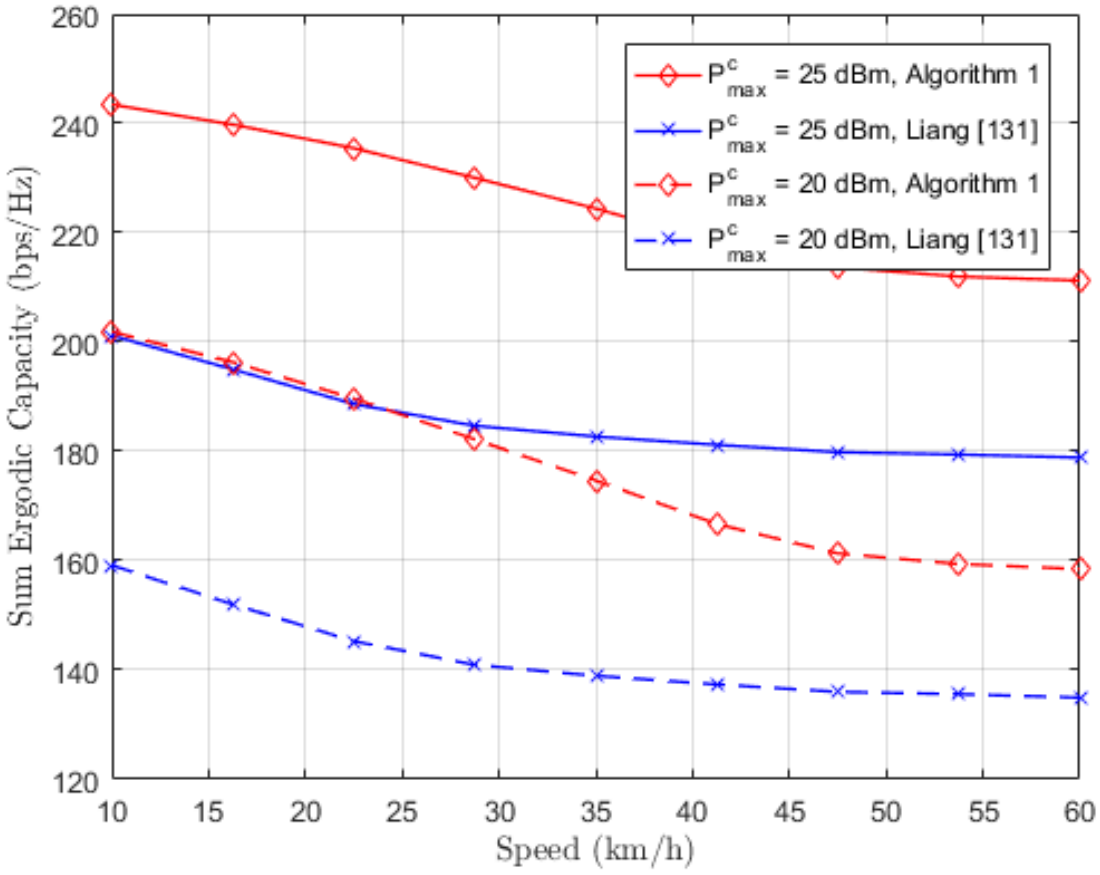


**Figure 5.6:** Sum ergodic capacity of CUE links with varying speed.

less speed implies reduction in the average inter-vehicular distance, which would give rise to higher received power and more reliable V2V link. Although, this will lead to more

interference and therefore reduce the capacity of the network. However, we address this challenge with our pathloss analysis in (5.4) which accounts for street geometry (parallel and cross) in urban environment, with path gain of the LOS and NLOS segments. Hence, the performance of Algorithm 1 remains reasonably better in terms of capacity improvement than the Algorithm in [131]. This is quite noticeable with a capacity increase of 34.63% when $P^c_{max} = 25$ dBm and 27.86% for $P^c_{max} = 20$ dBm, corresponding to gain of about 43 bps/Hz. Also, the performance improvement can be attributed to the consideration given to the unpaired CUEs as shown in (5.14-5.17), contrary to only paired CUEs capacity performance considered in [131]. Thus, the QoS constraints of all the VUEs are satisfied due to continuous access to the network, thereby maximizing the capacity of the unpaired CUEs. Therefore, the superiority of Algorithm 1 is established in terms of performance and complexity, when the capacity of unpaired CUEs are accounted for in our analysis. This validates our results.

Fig. 5.7 shows the CDF of the SINR for V2V links simulated under $\Upsilon = 0.5$ ms and $\Upsilon = 1.0$ ms. The two values are carefully chosen to capture and analyze the capacity at optimum point in Fig. (5.4) and the behaviour beyond this point. The result follows from (5.20) for paired CUE spectrum. As expected, the performance at $\Upsilon = 1$ ms is slightly higher than $\Upsilon = 0.5$ ms by 0.8 dB. The performance gap is due to the availability of CSI at the receiver which enables proper cancellation of interference. Considering the importance of prompt channel feedback on latency and reliability in vehicular networks, the less feedback value is expected to provide enhanced capacity. However, in this case, recurrent exchange of channel information may lead to unnecessary bottlenecks which will reduce the overall system capacity. This challenge is addressed with proper radio resource management scheme

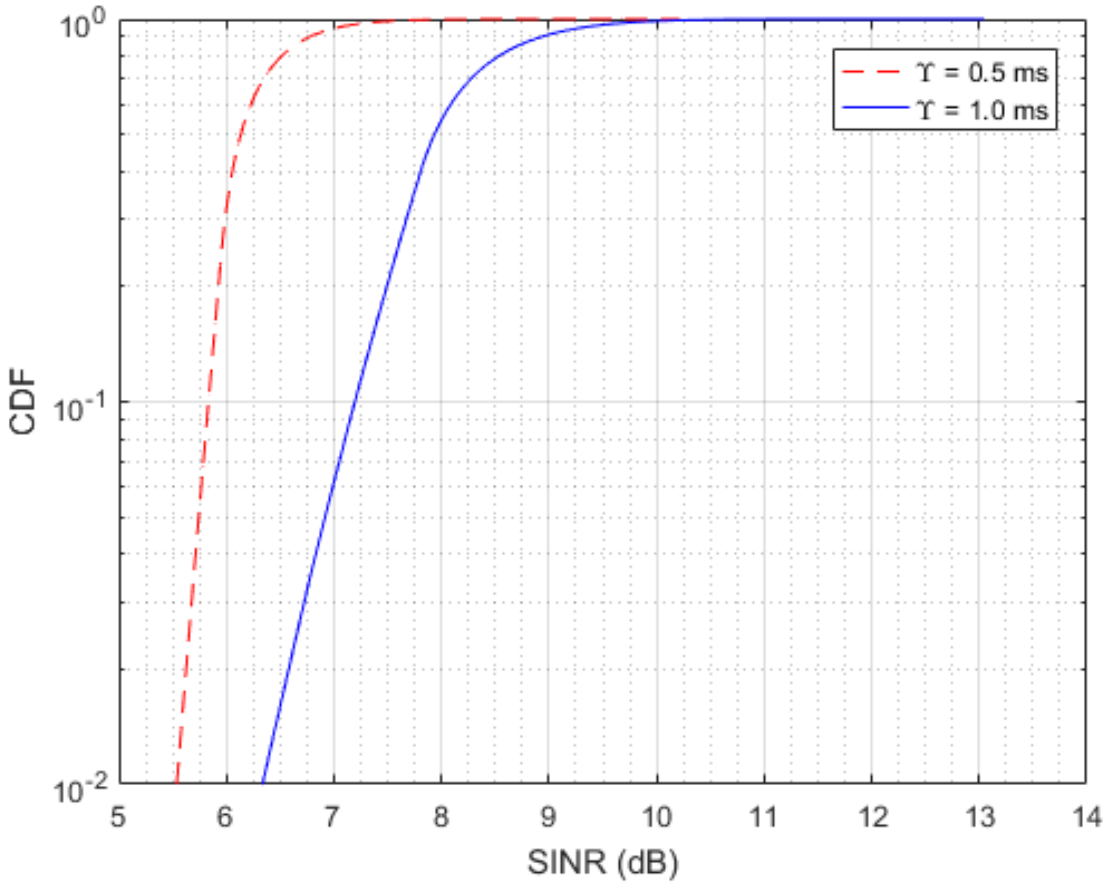


**Figure 5.7:** CDF plot of SINR for V2V links with two values of feedback duration $\Upsilon = 0.5$ ms and $\Upsilon = 1.0$ ms.

that takes into account both small and large scale components of the channel, as expressed in subsections 5.3.1 and 5.3.2.

Fig. 5.8 demonstrates the impact of traffic density and vehicle mobility on successful vehicle connectivity using communication range of 50 m and 100 m from a specific target. The choice of the two range values allows the simulation to capture the freeway car following model and lane changing model in urban settings. As can be seen in the case of 50 m communication range, the average number of vehicle connectivity increases gradually as the traffic density also increases. This is clearly due to the vehicles moving closer to each

other, thereby causing congestion in the traffic. Hence, the average vehicular connectivity increases linearly with the traffic density. However, a slight drop in vehicle connectivity can

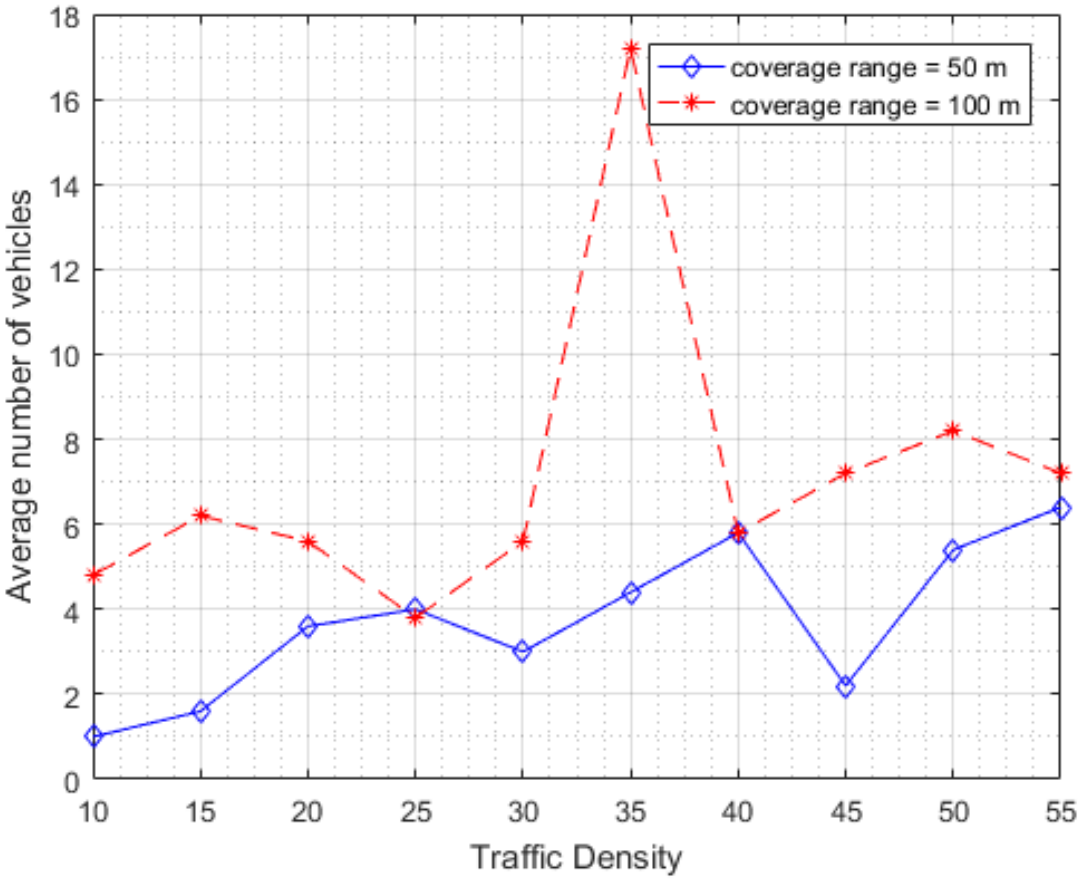


**Figure 5.8:** Connectivity plot for communication range.

still be noticed when the traffic volume is high. This is partly due to the effect of building blockages and change in signal direction along the propagation paths from LoS to NLoS, often experienced in urban environment. The LoS/NLoS segment path gains given in (5.8) and the use of PPP to capture shadowing effect helps to reduce this effect. On the other hand, when the communication range increases to 100 ms, it can be observed that more vehicle connectivity is experienced. There are two possibilities for this observation. Firstly,

in the highway environment, few blockages are common which results in more connectivity, even though the communication range is more. Secondly, increase in traffic density means less speed and possibilities of changing lanes. Therefore, vehicles tend to stay longer on a lane to maintain connectivity as long as the presence of infrastructural blockages is ruled out.

## 5.5 Conclusion and Future Work

In this chapter, we exploit the tractability of Poisson Point Processes and proposed a mathematical framework to model an urban-type vehicular communication network using stochastic geometry. The model takes into account presence of correlated buildings and the resultant shadowing effects, hence providing excellent basis for tractable analysis. In this approach, locations of BSs and cellular users are modeled on a two-dimensional plane as Poisson point processes so as to derive the coverage probability of a cellular user. Thereafter, we derived an expression for the ergodic capacity maximization of different participating cellular users with varying QoS constraints. More specifically, the latency and reliability requirements of V2V/V2I communication are transformed into optimization constraints, involving power allocation and spectrum sharing (PASS), taking into consideration both slow varying and large scale CSI estimation, with the aim of reducing interference to CUEs. Due to non-convex nature of the problem, a robust algorithm that yields optimal resource allocation, with low computational complexity, was proposed to solve the problem. Simulation results showed a better performance in our approach compared to related works. However, the resource management scheme presented in this chapter limits allocation of orthogonal

resource blocks to a single CUE-VUE pair, derived in (5.3.2). In the future, possibility of common RB sharing among multiple VUEs will be an interesting topic for investigation. So far, the last two chapters, i.e., Chapters 4 and 5 presented solutions based on orthogonal multiple access (OMA) principle to allocate resources among users, in user association and vehicular communication scenarios, respectively. However, emerging stringent 5G requirements such as massive connectivity, high reliability, low latency, high throughput and improved bandwidth utilisation require more robust access schemes. The next chapter presents proposed solutions on non-orthogonal multiple access (NOMA), integrated with massive MIMO and carrier aggregation, as promising access scheme to meet high capacity, better sum rate and guaranteed QoS requirements of 5G technology.

# Chapter 6

# Implementation of Non-Orthogonal Multiple Access (NOMA) Techniques for Interference Reduction and Capacity Improvement in 5G UDN

## 6.1 Introduction

The enormous increase in the number of connected devices in the present day communication networks has caused a rapid development in the Internet of Things (IoT). Support for massive connectivity, ultra-reliable and low-latency applications is one of the major goals in 5G UDN. The previous two chapters presented solutions for analyzing and mitigating interference encountered in 5G UDN system. In chapter 4, a model was derived to characterize

SINR in the downlink of cellular network in terms of the data rate and outage/coverage probability. Subsequently, cell selection technique for traffic offloading was incorporated by assigning different bias values for the MBS. Following similar approach, in chapter 5, an accurate expression for the coverage probability was derived, conditioned on the channel gain. Thereafter, the instantaneous SINR distribution was derived for coverage analysis and determination of ergodic capacity of the system.

However, the solution presented in this chapter towards interference coordination in 5G UDN is a blend of traditional and state-of-the-art techniques. In order to satisfy the massive connectivity demands of next generation networks, the 5G radio access technology is expected to achieve high data rate with reduced interference and power consumption, all at considerably minimal equipment cost. The current orthogonal multiple access techniques (OMA) operating in time, frequency and code domains will result in serious spectrum limitation as the number of mobile devices increases. Hence, non-orthogonal multiple access (NOMA) emerges as the candidate access technique for the upcoming 5G networks due to its capability of increasing the system capacity. Specifically, different multiple access techniques such as the frequency division multiple access (FDMA), time divisional multiple access (TDMA), code division multiple access (CDMA) and orthogonal frequency division multiple access (OFDMA) are employed in evolving 1G, 2G, 3G and 4G Long Term Evolution-Advanced (LTE-A) technologies, respectively.

In the traditional orthogonal multiple access (OMA) techniques, multiple mobile users are orthogonally allocated resources in frequency bands, code domain or non-overlapping time slots during a transmission period. One major challenge of OMA schemes is that a user with

poor channel condition can occupy the scarce bandwidth to the detriment of other users with good channel condition. This condition will obviously have negative impact on the spectral efficiency, overall network throughput and fairness among users. Apart from these, OMA may not support the massive connectivity benchmark of IoT envisioned for 5G network. The solutions presented in Chapters 4 and 5 are based on OMA techniques. Although both solutions exploit PPP in the analysis of key performance indices, Chapter 4 employs OMA based approach that operates in time domain to allocate resources orthogonally. Similarly, our solution in Chapter 5 pairs VUEs based on orthogonal allocation of resource blocks. Thus, the OMA scheme in both solutions fails to effectively exploit differences in channels and conditions of users.

Leveraging on the approach used in the last two chapters, this chapter employs capacity analysis, user-pairing, power allocation and user fairness policies of NOMA for interference management in order to meet user's high data rate and network-level requirements of 5G. Unlike OMA, the basic idea behind NOMA is that multiple users are served in the same resource block with the same frequency resources at the same time, but are distinguished by their power levels. Thus, NOMA utilizes superposition coding (SC) at the transmitter side and successive interference cancellation (SIC) at the receiver, which helps to mitigate interference.

Generally, more power is allocated to users located far away from the base station (BS), i.e. weak users, while less power is allocated to users close to the BS, called the strong user. Hence, this research focuses on downlink power-domain NOMA. In this chapter,

we investigate two novel approaches involving combination of NOMA with state-of-the-art schemes namely: massive multiple input multiple output (massive MIMO) and carrier aggregation (CA). The aim is to mitigate interference, enhance network capacity and provide scalable improvement in user throughput.

### 6.1.1 Motivation

Multiple access is among the key technologies employed over the years in wireless communication evolution to distinguish different generations of wireless systems. All the OMA schemes earlier discussed in Section 6.1 allow users to exploit orthogonal resource allocation within a particular frequency band, time slot or code in order to reduce inter-user interference. However, the major drawback in OMA is the limited number of users that can be supported due to scarcity of available orthogonal resources, thereby making it difficult to meet the massive connectivity requirements of 5G. In addition, more boost is also expected in signal quality, bandwidth and transmission latency. Determined to address these challenges is the motivation behind the schemes proposed in this chapter. The chapter focuses on non-orthogonal multiple access (NOMA) as a promising multiple access technique for 5G system. In NOMA, high capacity gains that significantly outperform OMA are achieved by power domain multiplexing at the transmitter and successive interference cancellation (SIC) at the receiver. To mitigate multiple access interference of the received signal and achieve further improvement in spectral and bandwidth efficiency, the NOMA scheme is combined with massive MIMO and Carrier Aggregation (CA) techniques. Generally, the number of users relying on SIC functionality of NOMA should be minimal to avoid performance degradation.

Hence, the introduction of massive MIMO and CA to (1) serve more users while keeping inter-user interference very low and (2) reduce inter-cell interference arising from serving users from multiple BSs, respectively, will be shown to be of great benefit in terms of capacity enhancement.

Generally, the contribution of this chapter can be summarized as follows.

The first part:

- employs massive MIMO technology in conjunction with NOMA concept to improve the sum channel capacity of 5G networks.
- simulates massive MIMO-enabled NOMA technique under perfect and imperfect channel state information (CSI) to evaluate the effect on overall channel capacity, and finally
- aims to minimize the complexity associated with simultaneous use of multiple antennas, transmit antenna selection principle is applied.

The second part:

- investigates a user pairing based on NOMA scheme integrated with CA to achieve enhanced system performance.
- employs the inter-band non-contiguous type of CA to configure the set of component carriers (CCs) and serving cells, through dedicated radio resource control (RRC) signaling functionality of the BS.

– exploits the superiority of proportional fair scheduler to perform resource allocation and maintain fairness between users according to their channel quality.

The rest of this chapter is organized as follows: Section 6.2 discusses related literature while Section 6.3 analyses the performance gains in terms of capacity improvement of the proposed NOMA concept, integrated with massive MIMO technique. Section 6.4 introduces the novel approach based on NOMA, combined with CA techniques for spectrum efficiency and fairness among users. Simulation results and discussion are presented after each approach for validation, while the chapter ends with conclusion and suggestion for future studies in Section 6.5.

## 6.2 Literature Review

A lot of work has been done to investigate various challenges and implementation issues towards the realization of full benefits of NOMA, as a promising access technique for the proposed 5G network. Some of these works focus on integrating NOMA with existing techniques such as massive MIMO [149] and cooperative communication (COMP). In [150], benefits of incorporating massive MIMO, NOMA and Interleave Division Multiple Access (IDMA) in a unified framework are investigated, focusing on multi-user gain. Solution based on iterative processing and time division multiplexing (TDD) are also outlined. As the CSI obtained through pilots at the beginning of transmission is insufficient to establish reliable spatial orthogonality, an IDMA solution with iterative maximum ratio combining (MRC) and data aided channel estimation (DACE) is employed to improve the CSI. The authors in

[151] propose two-user Fair-NOMA approach in the downlink to enable the receiver perform SIC. Analysis of outage capacity is discussed to show individual user and sum capacity improvement over conventional OMA scheme. Two-step approach to mitigate fading and reduce complexity in NOMA signal recovery is implemented in [152]. In this approach, cooperative multi-relay is used to achieve lower bit error rate (BER), better fairness and improved throughput when a set of users relays information for other users in the system, while keeping interference at a relatively low level. Other NOMA schemes under investigation in the literature include bit division multiplexing (BDM) [153] and pattern division multiple access (PDMA) [154]. Nonetheless, NOMA's solutions for 5G-supported technologies such as massive machine type communication (mMTC) [155–157], ultra-reliable and low-latency communication (URLLC) and enhanced mobile broadband (eMBB) [158] are still at infancy. In order to further increase user's data rate, the bandwidth expansion functionality of CA can be exploited in conjunction with NOMA principle. Two or more CCs can be aggregated on the physical layer to increase bandwidth, subject to spectrum availability and user's compatibility. In a more unique manner, the NOMA scheme can be integrated with CA to reasonably increase the data rate and transmission bandwidth of users up to 100 MHz. This will lead to considerable improvement in terms of throughput, energy efficiency and fairness among users. A study in this direction has been accepted for publication in International Journal of Communication Systems (IJCS).

## 6.3 Massive MIMO-integrated NOMA Solution

Radio resource allocation to users in current wireless networks relies on OMA principle. However, increase in the number of users, and strict limitation to modifications for the current communication systems may prevent OMA from meeting demands such as ultra low latency, high spectral efficiency, massive connectivity and improved capacity requirements of 5G networks. NOMA emerges as a promising technique to address these challenges due to its support for more users through inter-user interference cancellation at the receiver. To further improve the sum channel capacity and alleviate the receiver complexity, MIMO technology can be employed. MIMO refers to a technique where multiple transmit and receive antennas are employed, while massive MIMO involves utilisation of larger antennas. In this section, we present a massive MIMO-enabled NOMA techniques, simulated under perfect and imperfect CSI, to evaluate its impact on overall capacity in 5G networks. In addition, transmit antenna selection principle is applied to ease the complexity involved in simultaneous use of multiple antennas. Finally, simulation results are presented to show performance gains of the proposed scheme in terms of capacity enhancement, better spectrum and energy efficiency, in addition to high sum rate compared to traditional OMA schemes. A paper [149] based on this solution has been presented in a reputable conference proceedings.

### 6.3.1 System Model for the proposed Massive MIMO-NOMA Solution

Consider a downlink single-cell NOMA comprising a single BS and $K$ number of UEs with SIC receivers as shown in Fig. 6.1. The BS transmits the superimposed signal which is the combination of signals belonging to multiple users with different power allocation coefficients $\alpha_i$, $i \in \{1, 2, ..., K\}$ according to their channel conditions. The links are assumed to experience independent and identically (i.i.d) Rayleigh fading coupled with additive white Gaussian noise (AWGN). The channel gains are ordered as $0 < |h_1|^2 \leq |h_2|^2 \leq ... \leq |h_k|^2$ where $h_k$ is the channel coefficient of $k$th user, indicating user $k_i$ with $i \in k = \{1, 2, ..., K\}$ to have the $i$th weakest instantaneous channel. Based on NOMA principle, all users are served

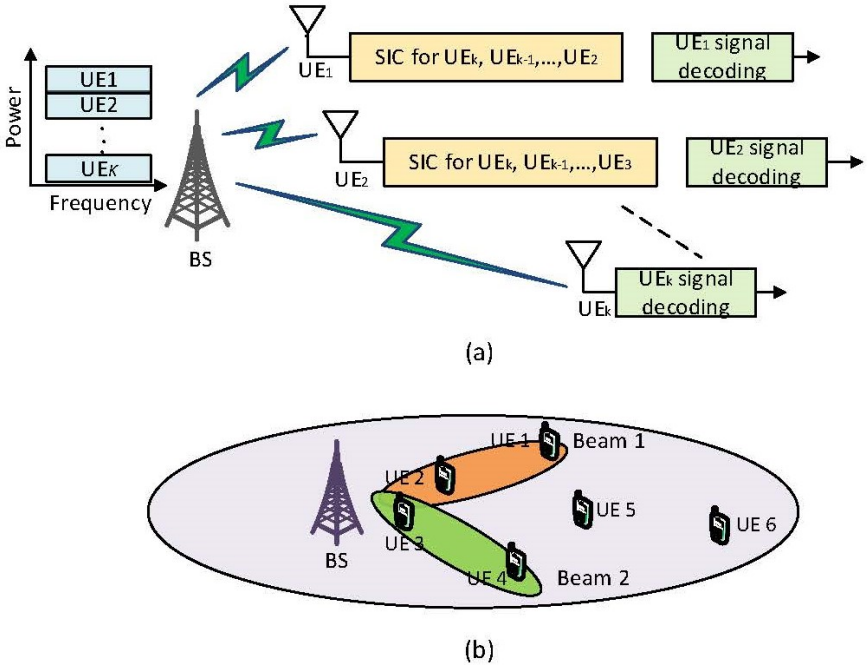


**Figure 6.1:** Downlink NOMA transmission scheme (a) NOMA with $K$ number of users using SIC for signal detection (b) System model of NOMA combined with MIMO architecture.

while utilizing the system bandwidth for data transmission, using SC at the transmitter (i.e. BS) and SIC at the receiver. Unlike OMA techniques, users are multiplexed in the power domain in NOMA. Users with poor channel condition are allocated more power such that $\sum_{i=1}^{K} \alpha_i = 1$ and $\alpha_1 \geq \alpha_2 \geq ... \geq \alpha_K$, subject to the ordering of the channel gains. The fraction of the total power allocated to the $i$th user by the BS at the transmitter end is $P_i = \alpha_i P_x$, where $P_x$ is the BS total transmitted power. At the receiver, the user with the better channel gain first decodes the weaker signal and subtracts it from the received signal through SIC to decode its own signal. On the other side, the weaker user decodes its own signal directly by considering the signal of the strong user as interference. Hence, more power is assigned to the weaker, or farthest user to ensure fairness. This decoding order increases the decoding time for the user nearest to the BS, while the decoding time is lower for the farthest user. The superimposed signal $x(t)$, containing individual information signals for each user transmitted by the BS is

$$x(t) = \sum_{i=1}^{K} \sqrt{\alpha_i P_x} x_i(t) \tag{6.1}$$

where $\alpha_i$ is the power splitting factor assigned to the $i$th user, $x_i(t)$ is the user's individual information-bearing signal with unit energy. The received signal at $i$th user can be expressed as

$$y_i(t) = x(t)h_i + w_i(t) \tag{6.2}$$

where $w_i(t)$ is the zero mean complex additive white Gaussian noise, plus the inter-cell interference, with density $N_0$(W/Hz). If SC at the transmitter and SIC at the receiver are

perfectly carried out, i.e. under perfect CSI, the data rate is optimized. Re-writing (6.2) as

$$y_i(t) = \boldsymbol{H}x(t) + w_i(t) \tag{6.3}$$

where $\boldsymbol{H} \equiv [\boldsymbol{h}_1, \boldsymbol{h}_2, ..., \boldsymbol{h}_k, ..., \boldsymbol{h}_K]$ and $x(t) \equiv [x_1(t), x_2(t), ...x_k(t), ...x_K(t)]$. The expression in (6.3) is very important, as will be seen later when: (1) presenting practical realization of capacity analysis using zero forcing (ZF), and (2) evaluating CSI error. Similarly, the received signal of a MIMO system with $N_t$ and $N_r$ transmit and receive antennas, respectively is given as

$$\mathbf{y}_{MIMO} = \sqrt{\frac{E_x}{N_t}}\mathbf{H}\mathbf{x} + \mathbf{w} \tag{6.4}$$

where $E_x$ is the energy of the transmitted signal, $\mathbf{H} \in \mathbb{C}^{N_r \times N_t}$ represents the narrowband time-variant wireless channel for $N_r \times N_t$ antenna dimensions, $\mathbf{x} \in \mathbb{C}^{N_t \times 1}$ is the transmitted signal vector with $N_t$ independent input symbols $x_1, x_2, ..., x_{N_t}$ and $\mathbf{w} = (w_1, w_2, ..., w_{N_r})^T \in \mathbb{C}^{N_r \times 1}$ denotes the zero-mean complex Gaussian noise vector. Assuming the CSI is known at the transmitter end, and given that the transmit power of the $i$th transmit antenna is $p_i = E|x_i|^2$. One approach to increase the capacity of the network in NOMA, supported by MIMO when interference is taken into account is through ZF and maximum ratio combining (MRC). Since interference is considered, ZF is the preferred option. Although MRC offers lower complexity than ZF due to absence of matrix inversion, interference remains a big challenge and it increases with the number of users. Thus, given a ZF estimator as [150]

$$z(t) = (\boldsymbol{H}^H\boldsymbol{H})^{-1}\boldsymbol{H}^H y_i(t) \tag{6.5}$$

By substituting (6.3) into (6.5), and using $\epsilon(t) = (\boldsymbol{H}^H \boldsymbol{H})^{-1} \boldsymbol{H}^H w_i(t)$, we can write

$$z(t) = x(t) + \epsilon(t) \tag{6.6}$$

Thus, ZF allows allocation of different orthogonal subchannels to a set of users for interference avoidance. In addition, when $\boldsymbol{H}^H \boldsymbol{H}$ is poorly established, the noise term $\epsilon(t) = (\boldsymbol{H}^H \boldsymbol{H})^{-1} \boldsymbol{H}^H w_i(t)$ in (6.6) results in amplification error, which can be corrected using water-filling over different orthogonal subchannels [150]. Therefore, the capacity of the $j$th single input single output (SISO) channel can be expressed as

$$C_i(p_i) = \log_2\left(1 + \frac{E_x p_i}{N_t N_0}\lambda_i\right), \quad i = 1, 2, 3, ..., j \tag{6.7}$$

where $N_0$ denotes the power spectral density of the additive noise $w_{i\,i=1}^{N_r}$ and $\lambda_i$ corresponds to the diagonal elements of the matrix which has a singular value decomposition (SVD). Thus, the capacity of the MIMO-NOMA channel can be expressed as the sum of the capacities of the SISO channels in (6.7), such that,

$$C_{MIMO} = \sum_{i=1}^{j} C_i(p_i) = \sum_{i=1}^{j} \log_2\left(1 + \frac{E_x p_i}{N_t N_0}\lambda_i\right), \quad i = 1, 2, 3, ..., j \tag{6.8}$$

To maximize the capacity in (6.8), the power allocation optimization

$$C_{MIMO} = \max_{\{p_i\}} \sum_{i=1}^{j} \log_2\left(1 + \frac{E_x p_i}{N_t N_0}\lambda_i\right) \tag{6.9}$$

$$\text{s.t.} \quad \sum_{i=1}^{j} p_i = N_t, \quad i = 1, 2, 3, ..., j \tag{6.9a}$$

can be solved. On the other hand, the SINR of downlink (DL) NOMA for the $i$th user without considering MIMO technology is given by

$$SINR_i = \frac{\alpha_i P_x |h_i|^2}{P_x |h_i|^2 \sum_{k=i+1}^{K} \alpha_i + w_k^2} \tag{6.10}$$

Similarly, the SINR of user $k$ when successfully decoded after canceling out signals of other users is

$$SINR_k = \frac{\alpha_i P_x |h_k|^2}{w_k^2} \tag{6.11}$$

When SIC is carried out accordingly, in the increasing order of equivalent channel gains, the intra-beam interference encountered as a result of superposition coding in NOMA can be successfully suppressed [159]. Although, this is based on the assumption of perfect knowledge of the beamspace channel by the BS. In this case, the inter-cell interference could be removed via low complexity zero forcing (ZF) beamforming, which can be actualized by pseudo inversion of the beamspace matrix of all users, on the condition that $N_r \leq N_t$ in a cell. On the other hand, when $N_t = N_r$, ZF beamforming is accomplished through receivers' channel gain inversion, while ZF beamforming is achieved via SVD of the receivers' channel gains when $N_r \leq N_t$ in a cell [160].

However, in MIMO-NOMA system where $N_r >> N_t$, multiuser ZF beamforming may be difficult to implement. In such a case, precoding technique is utilized to form a uniform matrix dimension with the ZF beamforming. Hence, the achievable rate of the $i$th user is given as

$$R_i = \log_2\left(1 + \frac{\alpha_i P_x |h_i|^2}{P_x |h_i|^2 \sum_{k=i+1}^{K} \alpha_i + w_k^2}\right) \tag{6.12}$$

and the achievable rate for user $k$ is

$$R_k = \log_2\left(1 + \frac{\alpha_i P_x |h_k|^2}{w_k^2}\right) \tag{6.13}$$

Based on (6.12) and (6.13), we write the sum rate

$$\begin{aligned} R_{sum} = \log_2\left(1 + \frac{\alpha_i P_x |h_i|^2}{P_x |h_i|^2 \sum_{k=i+1}^{K} \alpha_i + w_k^2}\right) \\ + \log_2\left(1 + \frac{\alpha_i P_x |h_k|^2}{w_k^2}\right) \end{aligned} \tag{6.14}$$

which can be improved by carefully designing the power allocation $P_x$ and power allocation factors $\alpha_i$.

Since the above NOMA technique requires multi-user detection (MUD), it can be categorized as maximum ratio combining (MRC) SIC, while the interference is assumed to be non-negligible. The NOMA MRC-SIC can further be enhanced to guarantee fairness by carefully optimizing the overall system rate and transmission power $p_k = E(|x_k(t)^2|)$, where $x_k(t)$ is the transmitted symbol from $k$th user as in (6.12) and (6.13). These two, i.e. power and rate, constitute gains arising from employing massive MIMO technology. While the power

gain is achieved via beamforming, the rate gain exploits spatial diversity to increase sum-rate with increasing BS antennas [161]. Both gains are quite appreciable under perfect CSI, but can be affected when the CSI encounters error. Let the wireless channel coefficient between the $n$th BS antenna and $k$th user be $H_{n,k}$, then represent $\Delta \boldsymbol{H} = \{\Delta H_{n,k}\}$ and $\tilde{\boldsymbol{H}} = \{\tilde{H}_{n,k}\}$ as two $N_T \times K$ matrices with complex Gaussian entries containing unit variance and zero mean. Thus, the CSI error can be expressed as

$$\boldsymbol{H} = \sqrt{1-\mu}\Delta \boldsymbol{H} + \sqrt{\mu}\tilde{\boldsymbol{H}} \tag{6.15}$$

where $\sqrt{1-\mu}\Delta \boldsymbol{H}$ and $\sqrt{\mu}\tilde{\boldsymbol{H}}$ are the unknown and known parts of $\boldsymbol{H}$ with confidence factor $(0 \leq \mu \leq 1)$ such that $\mu = 0$ indicates no CSI while $\mu = 1$ means perfect CSI [150]. Therefore, the CSI has mean square error (MSE) written as

$$\Gamma_{MSE} = E\left[\left|H_{n,k} - \sqrt{\mu}\tilde{H}_{n,k}\right|^2\right] = 1 - \mu \tag{6.16}$$

Substituting (6.15) into (6.3) to have

$$y_i(t) = \left(\sqrt{1-\mu}\Delta \boldsymbol{H} + \sqrt{\mu}\tilde{\boldsymbol{H}}\right)x(t) + w_i(t) \tag{6.17}$$

By re-arranging, (6.17) becomes

$$y_i(t) = \sqrt{\mu}\tilde{\boldsymbol{H}}x(t) + \tilde{w}_i(t) \tag{6.18}$$

where

$$\tilde{w}_i(t) = \sqrt{1-\mu}\Delta \boldsymbol{H} x(t) + w_i(t) \tag{6.19}$$

corresponds to the Gaussian noise vector in the $t$th time slot. It is noteworthy the dependence of $\tilde{w}_i(t)$ in (6.19) on $x(t)$, which may actually lead to some performance degradation in the system.

### 6.3.2 Results and Discussion

In this section, simulation results are presented to validate the performance of the proposed NOMA scheme when used in conjunction with MIMO technology, taking into consideration instantaneous CSI knowledge at both the transmitter and receiving ends. Specifically, we consider downlink NOMA where the BS communicates with $K$ number of users, while $N_t$ and $N_r$ are varied. In the simulation, ZF precoding is considered for beamspace MIMO to demonstrate higher sum-rate advantage compared to the basic NOMA employing single antenna at the BS. To avoid the difficulty involved in MIMO-NOMA regarding the order in which users are placed, the MIMO-NOMA is decomposed into multiple separate SISO-NOMA subchannels to accord the proposed approach more spatial degrees of freedom. We further employ antenna selection principle for the decomposition to improve maximum diversity gain and compensate for loss in multiplexing gain. The users are ordered by the BS according to their channel quality feedback, treating users with large distances as weak users. This knowledge helps the BS to make good decisions in case of error associated with improper CSI according to (6.19). In addition, we emulate a challenging traffic condition and assume there are 50 users in the network, with $\text{UE}_1$ and $\text{UE}_K$ being the nearest and

farthest users to the BS respectively. The total transmitted power at the BS is taken as $P_x = 1$ Watt, while the noise density $N_0$ is taken as $10^{-15}$ W/Hz. Also, the Okuruma-Hata propagation model is used to obtain the channel gains on 2 GHz carrier frequency. The receiver is assumed to have perfect knowledge of both the channel gains $h_k$ and power splitting factor $\alpha_i$.

Fig. 6.2 shows capacity of the channel with varying antenna number, without CSI knowledge at the transmitter side. In this case, the capacity is maximized when the channel is orthogonal and the total power is evenly allocated to all transmit antennas. Furthermore,

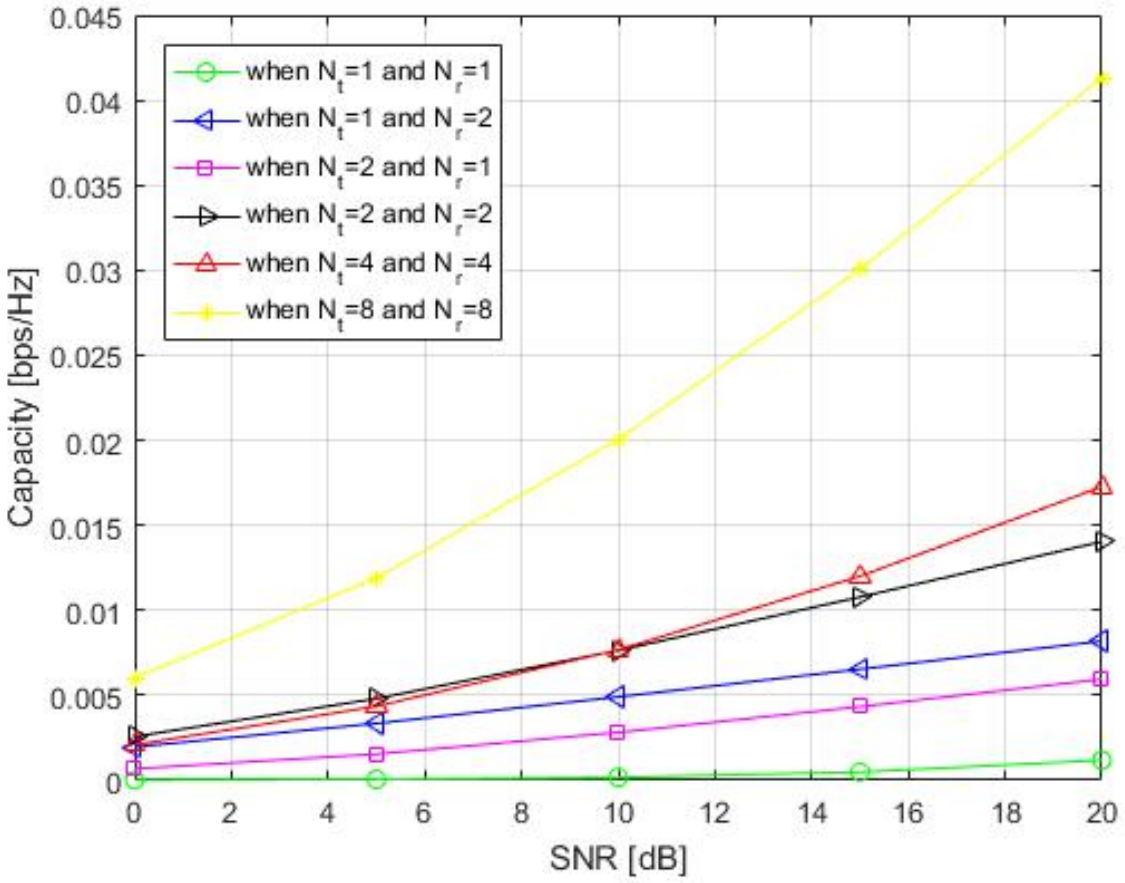


**Figure 6.2:** Channel capacity of the proposed MIMO-NOMA scheme with different antenna configuration.

the capacity of NOMA when MIMO is applied can be seen to be higher as the number of antenna is increased both at the transmit and receive sides. The gain in the beamspace MIMO is remarkably high up to 3dB, which is as a result of NOMA's benefit to serve multiple users in each beam. Therefore, the higher the number of users, the probability that the same beam is selected for the same users becomes relatively high. Also, as the BS performs the precoding in the downlink, the inter-user interference is eliminated according to the available CSI resulting from multi-user MIMO channel matrix $\mathbf{H}$ in (6.3) and (6.4). Note that the capacity when using a single transmit-recieve antenna maintains the least value and remains constant at this value until at SNR = 12dB, when the value gradually rises. This is due to non-orthogonality in the singular values of the channel. In the same vein, in two similar cases when $N_t = 1$ and $N_r = 2$, and when $N_t = 2$ and $N_r = 1$, the channel capacity increases logarithmically with increase in the number of antennas. Thus, knowledge of CSI at the transmitter side has no effect on the channel capacity because only a single data stream can be transmitted. Both capacities follow the same trend as that of SISO, with 50% and $\sim 62\%$ capacity increase for $N_t = 2, N_r = 1$ and $N_t = 1, N_r = 2$, respectively. The overall improvement in rate due to channel precoding is noticeable when $N_t = N_r = 8$, as shown in the figure.

In Fig. 6.3, the impact of decoding under perfect and imperfect CSI, as derived in (6.15-6.19) is presented for $N_t = N_r = 4$. The figure demonstrates that adequate knowledge of CSI at the transmitter achieves higher capacity than when the CSI is not perfectly known. However, it is noteworthy that when MIMO is solely applied, availability of CSI does not have much impact on the capacity when the SNR is very high. The implication of this is

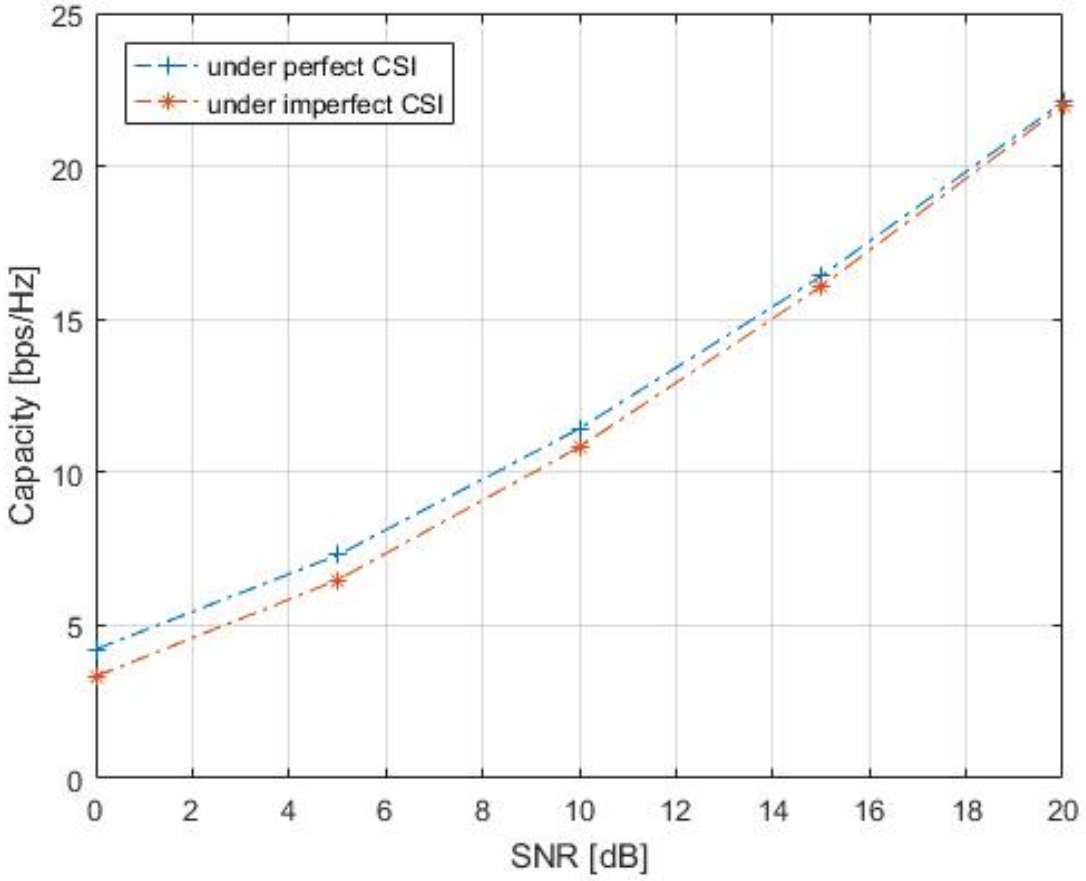


**Figure 6.3:** Channel capacity vs SNR when $N_t = N_r = 4$.

that the same reasonable transmit power allocation can be achieved at lower SNR as when the SNR is high. In the event that the CSI is available at the transmitter, the overall channel capacity is the aggregate capacities of the single antenna configuration (i.e. SISO), given in (6.8) and constrained on solution to the power allocation problem in (6.9). Thus suggesting more power allocation to the farthest user, thereby maintaining fairness and improving the capacity. On the other hand, when the CSI is not available, the total power is allocated equally to all transmit antennas which results in reduced capacity as shown.

Fig. 6.4 compares improvement in achievable rate and robustness to channel error of the proposed MIMO-NOMA scheme under three different precoding techniques. Considering

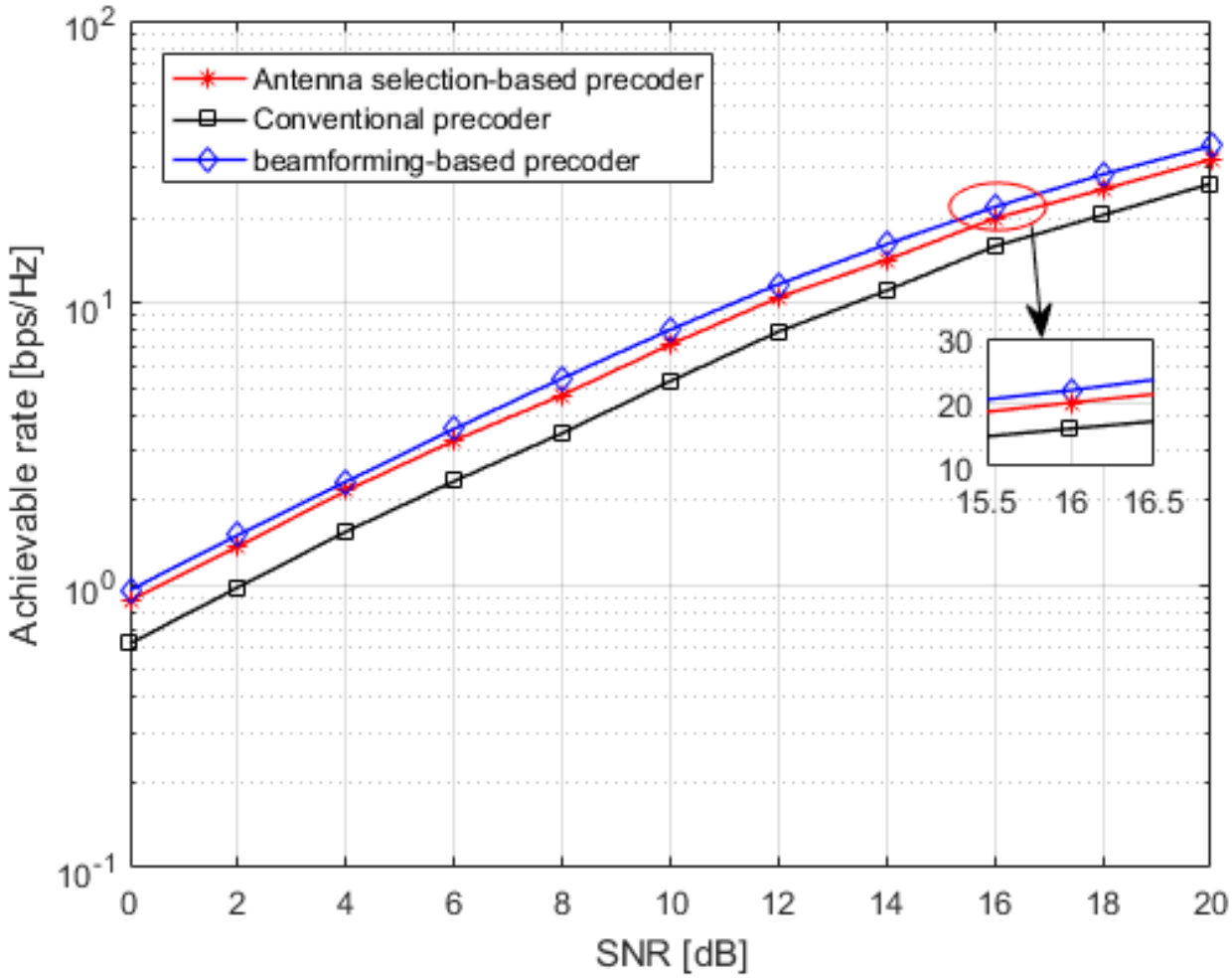


**Figure 6.4:** Performance analysis of the achievable rate of the proposed MIMO-NOMA

that the transmission power is split among 16 users in each cell (for computational simplicity) with a single BS having 256 antennas, it is observed that the achievable rate for the three schemes maintained a considerable growth level. It can be seen that the antenna selection precoding performs better than the conventional precoder. This is partly due to the ability of the ZF to allocate orthogonal sub-channels to different users to avoid

interference. Therefore the inherent error introduced in (6.6) can be corrected via sub-channel water-filling algorithm. In addition, the problem of implementation in multiuser ZF scenario can be avoided, especially when $N_r >> N_t$, hence the marginal performance gap. As expected, the plot shows performance drop with increase in SNR. The drop is noticeable in the three precoders, but more pronounced in the antenna selection precoder at 16 dB. However, the beamforming-based precoder performs best of all the three, with relatively low power consumption and hardware cost. Although, its applicability in multi-cell scenario is subject to further investigations.

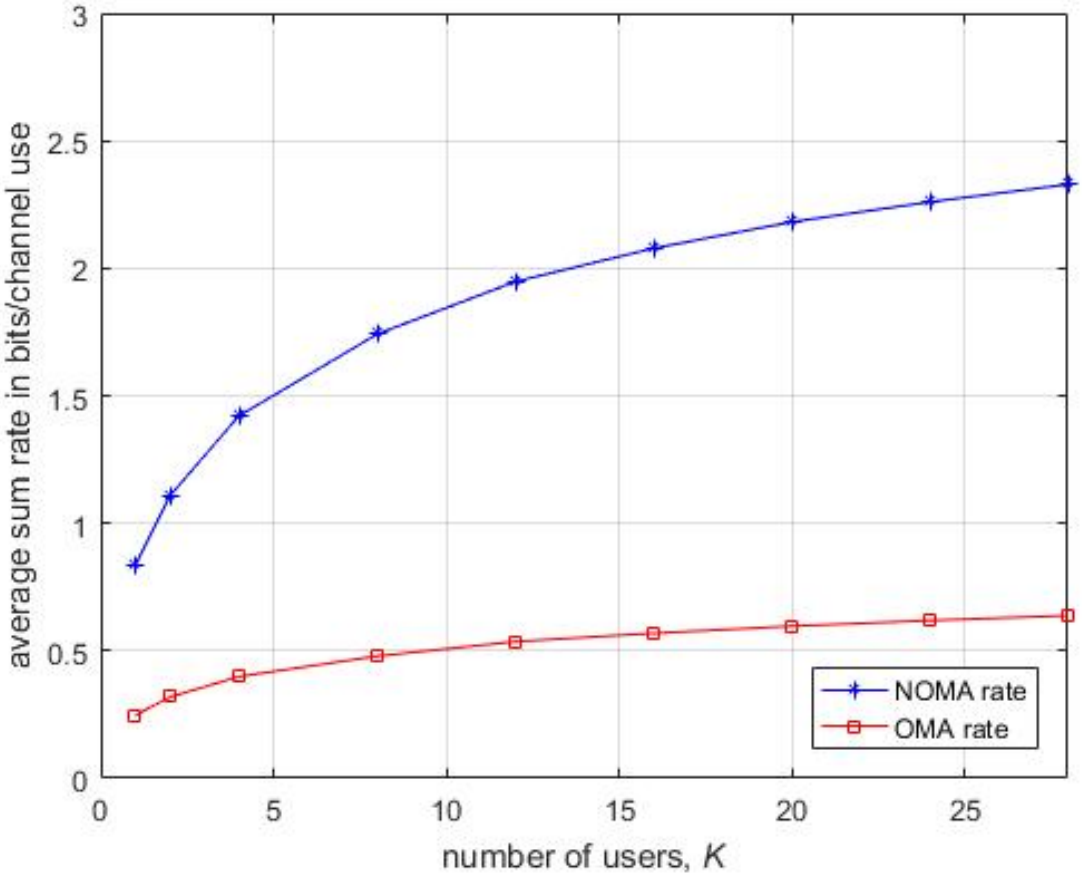


**Figure 6.5:** Comparison of average sum-rate of NOMA with OMA schemes.

Fig. 6.5 demonstrates superiority of NOMA over OMA techniques in terms of sum rate. The less achievable sum rate in OMA compared to NOMA arises from the fact that the total bandwidth and power are equally shared among users in OMA, unlike in NOMA where the available power is split among different users according to their channel conditions. It can be noted that the sum rate of NOMA increases with the number of users. Hence, to further validate this assertion, more users are needed to emulate massive connectivity demands of 5G networks. Although this may come with more receiver complexity when using SIC and some interference avoidance techniques may also be needed to stabilize the network.

## 6.4 CA-enabled NOMA Solution

The need for 5G wireless technology to meet stringent demands on high throughput, ultra low latency, high reliability, massive connectivity and fairness among users has seriously constrained the limited radio spectrum. Hence, NOMA has been identified as one of the promising enabling radio access techniques to solve this problem. The basic principle of NOMA is the ability to serve multiple users in the same time and frequency resources, but differentiated by their power domains. However, the inherent power-domain multiplexing requires channel gain disparity between the strong and weak users, thereby reducing the sum-rate gain of the network. In this section, we propose a solution based on NOMA scheme, integrated with CA to further increase the bandwidth and data rate of users. Simulation results are presented to show considerable improvement in terms of throughput, spectrum efficiency, energy efficiency and fairness among users.

### 6.4.1 System Model for the proposed CA-NOMA Solution

In this section, downlink (DL) transmission is considered in a two-cell scenario with one BS serving two users in each cell as shown in Fig. 6.6. The BSs operate at full duplex mode. The set of DL UE is $\mathcal{I} = \{1, 2, ..., I\}$ and the available CCs are denoted by $\mathcal{N} = \{1, 2, ..., N\}$

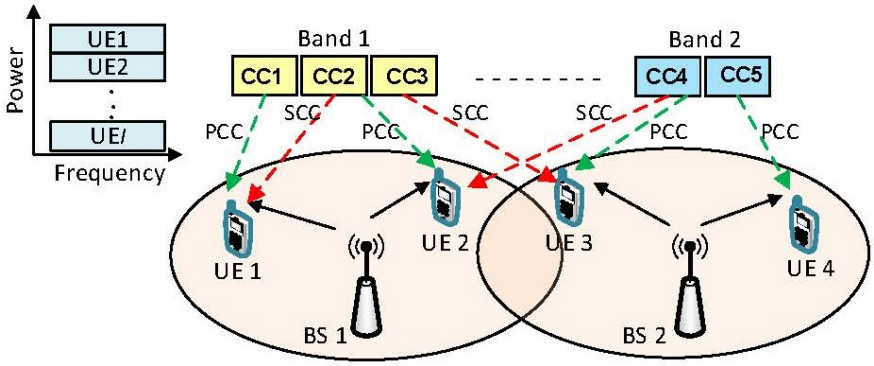


**Figure 6.6:** Illustration of deployment scenarios in CA-enabled NOMA approach.

Since NOMA relies on same band, same time approach to differentiate between each UE's power levels, the interband non-continuous CA is employed so that data can be transmitted over multiple separated carriers across a large frequency for network reliability. Thus, data from all available CCs can be aggregated by each user in the DL. This way, the available CCs are selected by each user so as to estimate the DL bandwidths on each CC for performance enhancement. In NOMA, the transmitted signal by the BS is given by

$$s(t) = \sum_{i=1}^{I} \sqrt{\rho_i P_T} x(t) \tag{6.20}$$

where $x(t)$ denotes the information signal for UE $i$, $P_T$ is the transmission power from the BS, and $\rho_i$ is the power allocation coefficient of UE $i$, such that $\sum_{i=1}^{I} \rho_i = 1$, where $\rho_1 \geq \rho_2 \geq ... \geq \rho_I$ and $|g_1|^2 \leq |g_2|^2 \leq ... \leq |g_I|^2$, since $\rho_i$ is inversely proportional to

the channel condition $g_i$ of the users. The BS then superimposes $s(t)$ that contains UE's information signals with QPSK using superposition coding. The UEs apply SIC to decode the desired signal from the transmitted signal. We assume perfect cancellation at the receiver which means that decoding order at each UE is equal to the user index in the cancellation sequence. At the receiver side, the superimposed signal received by $i$-th UE can be written as

$$z(t) = s(t)g_i + \sigma_i^2(t) \tag{6.21}$$

so that

$$z(t) = g_i \sum_{i=1}^{I} \sqrt{\rho_i P_T} x(t) + \sigma_i^2(t) \tag{6.22}$$

where $\sigma_i$ is the additive Gaussian noise with zero mean and density $N_o$. The strongest of the superimposed signal will be decoded first by the SIC receiver, which in most cases, corresponds to the signal of the farthest UE. Ideally, this process relies on perfect knowledge of both phase $g_i$ and amplitude $\rho_i$ information contained in each UE signals at the receiver. Therefore, since more power is allocated to the farthest UE, it decodes its own signal first and treats others as interference which results in lower decoding time. On the other hand, a near UE incurs high decoding time due to repeated cancellation process required to decode its own signal. Denote $g_{i,n}$ explicitly as the channel gain between the BS and $i$-th user on the $n$-th CC such that

$$g_{i,n} = \beta_n h_{i,n} d_i^{\alpha_n} \tag{6.23}$$

where $d_i$ is the distance between BS and $i$-th UE, $\beta_n$ denotes the pathloss constant on $n$-th CC, and $h_{i,n}$ represents a quantity that captures the fading components of the link between

the BS and $i$-th UE on the $n$-th CC. Ideally, quantity $\beta_n$ depends on the carrier frequency and $\beta_n \cong (\lambda_n/4\pi)^2$ [162], where $\lambda_n$ is the wavelength. Thus, the SINR of the $i$-th user can be expressed as

$$\gamma_{i,n} = \frac{p_{i,n}|g_{i,n}|^2}{\sum_{i=1}^{I-1} I + B_{i,n}\sigma^2}, \quad \forall i, n \tag{6.24}$$

where $I$ is the interference from other cells and $B_{i,n}$ is the bandwidth allocated to the $i$-th UE on the $n$-th CC. In practice, since UE closest to the BS experiences higher channel gain, it will decode its own signal last. Thus the throughput of the $i$-th user can be written as

$$R_{i,n} = B_{i,n} \log_2 (1 + \gamma_{i,n}), \quad \forall i, n \tag{6.25}$$

The aggregate throughput is given by

$$R_{agg} = \sum_{i=1}^{I} \sum_{n=1}^{N} B_{i,n} \log_2 \left( 1 + \frac{p_{i,n}|g_{i,n}|^2}{\sum_{i=1}^{I-1} I_i + B_{i,n}\sigma^2} \right) \tag{6.26}$$

In CA, multiple CCs are combined or aggregated across the available bandwidth to provide higher channel bandwidth for improved network throughput and spectral efficiency. Hence, a UE can be scheduled on multiple or a single CC simultaneously and up to five 20-MHz CCs can be supported to realize a total 100-MHz channel bandwidth. Since we consider the inter-band non-contiguous CA, the spacing between two adjacent CCs for optimized network performance is adjusted according to [19]

$$C_{spacing} = 0.3 \left\lfloor \frac{B_{ch1} + B_{ch2} - 0.1|B_{ch1} - B_{ch2}|}{0.6} \right\rfloor \tag{6.27}$$

where $B_{ch1}$ and $B_{ch2}$ are the channel bandwidths of the two CCs, respectively. A UE is first configured by the serving BS on each CC. Several serving cells are activated in RRC_CONNECTED state to form Primary Cell (PCell) and Secondary Cell (SCell). The PCell operates on the primary frequency and enables UE to perform RRC connection. On the other hand, the SCell operates on the secondary frequency and configured after RRC connection is established. Both PCell and SCell represent a group of configured CCs referred to as Primary CC (PCC) and Secondary CC (SCC), respectively. In the DL, cell selection and information acquisition processes are conducted on the PCC. Hence, SCC is only activated in the connected mode and requires backward compatible mobile device to perform extended generic access schemes. The BS therefore configures the DL SCC usage by the UE for each SCell, while the PCell is specifically assigned by the UE and can vary for different UEs served by the same BS. Unlike the user pairing in a basic two-user NOMA approach where a NOMA user is paired with another NOMA user, such that two users are assigned one carrier based on channel condition, the CA-integrated NOMA is configured for a single user paired with multiple different users at the same time based on channel conditions. Also, the participating BSs are effectively coordinated via resource partitioning to avoid inter-cell interference (ICI). In a multi-cell ultra-dense scenario where better coverage is desired, the CC of the macro BS provides dedicated coverage to macro users, while the small cells complement coverage extension through another CC overhaul. Thus, aggregation of CCs is achieved between the macro BS and the small cells using the same CA arrangement for clustered users. This framework leads to improved system throughput considerably as shall be seen in the result section. To analyze the effect of power consumption on the CA design, we model the total

power consumed by the BS as

$$P_{agg} = \sum_{i=1}^{I}\sum_{n=1}^{N}\eta_n p_{i,n} + \hat{P} + \sum_{n=1}^{N} P_n^{amp}\sum_{i=1}^{I} B_{i,n} \tag{6.28}$$

The first term in (6.28) denotes the transmit power consumption, $\eta_n$ is the inverse of the power amplifier efficiency on $n$-th CC, $\hat{P}$ is the circuit power consumption which constitutes the static power consumed in the BS circuitry, while the third term generally refers to the CC-dependent circuit power consumption which is the combination of the static power consumed in the circuit on $n$-th CC (i.e. $P_n^{amp}$) and used bandwidth $B_{i,n}$ on each CC. Consequently, the total Energy Efficiency (EE) of the network can be expressed as

$$E^e = \frac{R_{agg}}{P_{agg}} \quad \text{(Bits/Joule)} \tag{6.29}$$

Since NOMA aims to achieve trade-off between user fairness and channel conditions in resource allocation, the proportional fairness (PF) scheduler is implemented. Although the PF scheduler can either be independently scheduled per CC or jointly scheduled across CC [163], the latter is adopted in this research, based on different channel quality experienced by users in NOMA concept. When jointly scheduled, the throughput is averaged sequentially in each CC to capture the scheduling outcome of the previous CCs. Let $J$ be the total number of CCs configured for a particular user, the subcarrier allocation is performed according to [163]

$$m = \arg\max\left\{\frac{R_{i,j}(t,k)}{\Phi_{i,j}(t-1)}\right\} \tag{6.30}$$

where $R_{i,j}(t,k)$ represents the throughput of $i$-th user at scheduling interval $t$ of $j$-th CC on subcarrier $k$, and $\Phi_{i,j}(t-1)$ is the average throughput of selected user $m$ to be scheduled in the same CC. Subsequently, the procedure for the update is given as

$$\Phi_{i,1}(t) = (1 - \frac{1}{\Phi_c})\Phi_{i,J}(t-1) + \frac{1}{\Phi_c} \begin{cases} \sum\limits_{k \in \phi_1} R_{i,1}(t,k) & i = m \\ 0, & i \neq m \end{cases} \tag{6.31}$$

so that

$$\Phi_{i,j}(t) = (1 - \frac{1}{\Phi_c})\Phi_{i,j-1}(t) + \frac{1}{\Phi_c} \begin{cases} \sum\limits_{k \in \phi_j} R_{i,j}(t,k) & i = m \\ 0, & i \neq m \end{cases} \tag{6.32}$$

where $\phi_j$ is the set of all RBs in $j$-th CC and $\Phi_c$ represents the sliding window size. It is noteworthy that the results obtained from (6.31) and (6.32) are reflections of the outcome of a specific user in other CCs. As a result, scheduling quantity in CCs with poor channel condition is reduced to compensate for higher average throughput in better CCs, for users with different channel conditions in the configured CCs. In addition to the widely covered throughput analysis of the network involving NOMA, the EE performance is of utmost importance, especially in high network density. In the EE analysis, static power consumption of the network from power amplifiers is incorporated with the power consumed for the information-bearing waveform as contained in (6.20). Thus, the total power consumption at the transmitter side can be expressed as the sum of the information waveform power and

the static power consumed in the circuitry. Mathematically,

$$P_{aggregate} = P_T + P_{amp} \tag{6.33}$$

Consequently, the total EE of the network can be represented as

$$E^e = \frac{R_T}{P_{aggregate}} \qquad \text{(Bits/Joule)}. \tag{6.34}$$

where $R_T$ denotes the sum capacity of the network given as $\sum_{i=1}^{I} R_i$. The EE expression in (6.34) apparently considers the effect of circuit power consumption, contrary to the Shannon's information theory expression, thereby monotonically yielding lower EE when the spectral efficiency (SE) is high. Nonetheless, Shannon theorem shows that achieving dual objectives of maximizing SE, while minimizing EE simultaneously is infeasible, thus suggesting a trade-off. However, in this letter, the key focus in the simulation is on EE, due to the importance of maintaining green communications by reducing energy consumption, which forms one of the major KPIs targeted for 5G.

In an attempt to balance the EE among users in the DL via bandwidth and NOMA-enabled power allocation, different weights are assigned to the EEs of both the BS and users. Let $\varrho_n$ represent the bandwidth of each CC which is not the same for all CCs, and $\mu_i$ be the DL weight factor, then denote $\mathbf{P}_{I\times 2N} = [\mathbf{p}]$ and $\mathbf{B}_{I\times 2N} = [\mathbf{b}]$ such that $\mathbf{p}$ and $\mathbf{b}$ are all $I \times N$ matrices having elements $P_{i,n}$ and $B_{i,n}$, respectively. Consequently, the EE optimization

problem can be formulated as

$$\max_{\mathbf{P,B}} \sum_{i=1}^{I} \mu_i E_i^e \tag{6.35}$$

s.t.

$$\sum_{i=1}^{I}\sum_{n=1}^{N} p_{i,n} \leq p^{max} \tag{6.35a}$$

$$\sum_{i=1}^{I} B_{i,n} \leq \varrho_n, \quad \forall n \tag{6.35b}$$

$$\sum_{i=1}^{I} B_{i,n} \log_2 (1 + \gamma_{i,n}) \geq R_i^{min}, \quad \forall i \tag{6.35c}$$

$$B_{i,n} \geq 0, \, \forall i, n \tag{6.35d}$$

$$p_{i,n} \geq 0, \, \forall i, n \tag{6.35e}$$

The constraints in (6.35a) represent the maximum power demands for BS and each user, (6.35b) is the bandwidth constraints imposed on each CC, (6.35c) ensures that minimum rate requirements for the $i$-th user are met, while the allocated bandwidth and transmit power requirements of the $i$-th user are ensured in constraints (6.35d) and (6.35e), respectively.

### 6.4.2 Problem Transformation and Joint Resource Allocation

The objective function in (6.35) is a non-convex optimization problem which is difficult to solve using conventional optimization methods. Hence, the first approach to solving the problem is to transform it into equivalent convex optimization after which a low complexity iterative algorithm will be developed to solve it. Therefore, the following Theorem details the

process involved in transforming the optimization problem (*Note:* the proof of the theorem is beyond the scope of this work due to space limitation).

*Theorem 1:* Assume $(\mathbf{P}^*, \mathbf{B}^*)$ to be the optimal solution to (6.35), then there exist $\mathbf{u}^* = (u_1^*, u_2^*, ..., u_I^*)$ and $\boldsymbol{\varphi}^* = (\varphi_1^*, \varphi_2^*, ...\varphi_I^*)$ where $(\mathbf{P}^*, \mathbf{B}^*)$ yields a solution

$$\max_{\mathbf{P},\mathbf{B}} \sum_{i=1}^{I} u_i(\mu_i R_{agg} - \varphi_i P_{agg}) \tag{6.36}$$

for $\mathbf{u} = \mathbf{u}^*$ and $\boldsymbol{\varphi} = \boldsymbol{\varphi}^*$, under constraints (6.35a-6.35e).

In addition to $(\mathbf{P}^*, \mathbf{B}^*)$ being an optimal solution to (6.35), it also satisfies

$$u_i = \frac{1}{P_{agg}}, \quad i = 1, 2, ..., I \tag{6.37}$$

and

$$\varphi_i = \mu_i E_i^e, \quad i = 1, 2, ..., I \tag{6.38}$$

Easily, the optimization can be solved by finding the optimal power and bandwidth allocation from (6.36) that satisfies $(\mathbf{u}, \boldsymbol{\varphi})$, and then design an algorithm for its global optimal solution. Thus, substituting (6.26) and (6.28) into (6.36) allows the objective function to be re-written as

$$u_i \left[ \mu_i \sum_{i=1}^{I} \sum_{n=1}^{N} B_{i,n} \log_2 \left( 1 + \frac{p_{i,n}|g_{i,n}|^2}{\sum_{i=1}^{I-1} I_i + B_{i,n}\sigma^2} \right) - \varphi_i \left( \sum_{i=1}^{I} \sum_{n=1}^{N} \eta_n p_{i,n} + \hat{P} + \sum_{n=1}^{N} P_n^{amp} \sum_{i=1}^{I} B_{i,n} \right) \right] \tag{6.39}$$

The transformed objective function in (6.39) exhibits joint concavity over $(\mathbf{P}, \mathbf{B})$, including constraints (6.35c). Ultimately, problem (6.39) has become convex and can be solved by Lagrangian dual method. Re-arranging terms, the Lagrangian becomes

$$\begin{aligned}
&\boldsymbol{\mathcal{L}}(\boldsymbol{\delta}, \boldsymbol{\theta}, \boldsymbol{\vartheta}, \mathbf{P}, \mathbf{B}) \\
&= u_i \left[ \mu_i \sum_{i=1}^{I} \sum_{n=1}^{N} B_{i,n} \log_2 \left( 1 + \frac{p_{i,n} |g_{i,n}|^2}{\sum_{i=1}^{I-1} I_i + B_{i,n} \sigma^2} \right) \right] - u_i \varphi_i \left( \sum_{i=1}^{I} \sum_{n=1}^{N} \eta_n p_{i,n} \right. \\
&\left. + \hat{P} + \sum_{n=1}^{N} P_n^{amp} \sum_{i=1}^{I} B_{i,n} \right) + \sum_{i=1}^{I} \delta_i \left[ \sum_{n=1}^{N} B_{i,n} \log_2 \left( 1 + \frac{p_{i,n} |g_{i,n}|^2}{\sum_{i=1}^{I-1} I_i + B_{i,n} \sigma^2} \right) - R_i^{min} \right] \\
&- \theta \left( \sum_{i=1}^{I} \sum_{n=1}^{N} p_{i,n} - p^{max} \right) - \sum_{n=1}^{N} \vartheta_n \left( \sum_{i=1}^{I} B_{i,n} - \varrho_n \right)
\end{aligned} \tag{6.40}$$

where $\theta$ is the Lagrange multiplier attached to the maximum DL transmit power of constraint (6.35a), $\vartheta$ is the Lagrange multiplier vector imposed on constraint (6.35b) for the bandwidth allocation on each CC with elements $\vartheta_n$ such that $n \in \{1, 2, ..., N\}$, and $\delta$ constitutes Lagrange multiplier vector responsible for the minimum data requirement $R_i^{min}$ presented in constraint (6.35c) for each user.

Given the dual problem as

$$\min_{\boldsymbol{\theta} \geq \mathbf{0}, \boldsymbol{\vartheta}, \boldsymbol{\delta} \geq \mathbf{0}} \quad \max_{\mathbf{P}, \mathbf{B}} \boldsymbol{\mathcal{L}}(\boldsymbol{\delta}, \boldsymbol{\theta}, \boldsymbol{\vartheta}, \mathbf{P}, \mathbf{B}) \tag{6.41}$$

which can be iteratively solved through decomposition into both inner and outer loops. The inner loop maximizes over (**P**,**B**) for given $\boldsymbol{\delta}, \boldsymbol{\theta}$ and $\boldsymbol{\vartheta}$, while the outer loop constitutes the master dual problem and maximizes (**P**,**B**) for $\boldsymbol{\delta}, \boldsymbol{\theta}$ and $\boldsymbol{\vartheta}$.

The inner loop solution follows that the Karush-Kuhn-Tucker (KKT) conditions can be

applied to solve for optimality in $\max_{\mathbf{P},\mathbf{B}} \boldsymbol{\mathcal{L}}(\boldsymbol{\delta}, \boldsymbol{\theta}, \boldsymbol{\vartheta}, \mathbf{P}, \mathbf{B})$ which constitutes a standard concave form for $\boldsymbol{\delta}, \boldsymbol{\theta}$ and $\boldsymbol{\vartheta}$. Thus, the first order derivative Lagrange duality functions for power and bandwidth allocation can respectively be obtained as

$$\frac{\partial \mathcal{L}}{\partial p_{i,n}} = \frac{B_{i,n}|g_{i,n}|^2(u_i\mu_i + \delta_i)}{\ln 2\left(\sum_{i=1}^{I-1} I_i + B_{i,n}\sigma^2 + p_{i,n}|g_{i,n}|^2\right)} - (u_i\varphi_i\eta_n + \theta), \quad \forall i, n \tag{6.42}$$

and

$$\frac{\partial \mathcal{L}}{\partial B_{i,n}} = (u_i\mu_i + \delta_i)\left\{\log_2\left(1 + \frac{p_{i,n}|g_{i,n}|^2}{\sum_{i=1}^{I-1} I_i + B_{i,n}\sigma^2}\right) - \frac{B_{i,n}|g_{i,n}|^2(u_i\mu_i + \delta_i)}{\ln 2\left(\sum_{i=1}^{I-1} I_i + B_{i,n}\sigma^2 + p_{i,n}|g_{i,n}|^2\right)}\right\} - (u_i\varphi_i\hat{P} + \vartheta_n), \quad \forall i, n \tag{6.43}$$

Therefore, equating the derivative $\frac{\partial \mathcal{L}}{\partial p_{i,n}} = 0$ yields the optimal power allocation

$$p_{i,n}^* = \left[\left(\frac{B_{i,n}^*(u_i\mu_i + \delta_i)}{\ln 2\,(u_i\varphi_i\eta_n + \theta)} - \frac{(\sum_{i=1}^{I-1} I_i + B_{i,n}^*\sigma^2)}{|g_{i,n}|^2}\right)\right]^+, \forall i, n \tag{6.44}$$

where $[a]^+ = \max\{a, 0\}$. It is evident in (6.44) the increase of $p_{i,n}^*$ with both the bandwidth $B_{i,n}^*$ and channel gain $g_{i,n}$, which further shows improved CC utilization and fairly high power consumption as a result of high channel gain and bandwidth, respectively. Thus, it can be deduced that for $\left(\frac{B_{i,n}^*(u_i\mu_i+\delta_i)}{\ln 2\,(u_i\varphi_i\eta_n+\theta)} - \frac{(\sum_{i=1}^{I-1} I_i+B_{i,n}^*\sigma^2)}{|g_{i,n}|^2}\right) \leq 0$, $p_{i,n}^* = 0$ and $B_{i,n}^* = 0$. Therefore, by substituting (6.44) into (6.43) results in the KKT condition for the optimal bandwidth

allocation $B^*_{i,n}$ expressed as

$$\begin{aligned}
&\frac{\partial \mathcal{L}}{\partial B^*_{i,n}} \\
&= (u_i\mu_i + \delta_i)\left(\log_2\left(\frac{|g_{i,n}|^2\left(u_i\mu_i+\delta_i\right)}{\ln 2 \cdot \sum_{i=1}^{I-1} I_i + B^*_{i,n}\sigma^2\left(u_i\varphi_i\eta_n+\theta\right)}\right)\right. \\
&\left. - \frac{|g_{i,n}|^2\left(u_i\mu_i+\delta_i\right) - \ln 2 \cdot \sum_{i=1}^{I-1} I_i + B^*_{i,n}\sigma^2\left(u_i\varphi_i\eta_n+\theta\right)}{\ln 2 \cdot |g_{i,n}|^2\left(u_i\mu_i+\delta_i\right)}\right) \\
&- \left(u_i\varphi_i\hat{P} + \vartheta_n\right), \quad \forall i, n
\end{aligned} \tag{6.45}$$

Close observation of (6.45) shows the Lagrangian $\mathcal{L}$ to be an affine function of $B_{i,n}$ with a value set on the vertex of a feasible solution produced by the constraints. Hence, substituting (6.44) into (6.39) to obtain $B^*_{i,n}$ yields the optimization

$$\begin{aligned}
&\max_{B_{i,n}} \sum_{i=1}^{I}\sum_{n=1}^{N}\left\{u_i\mu_i \log_2\left(1 + \frac{Q_{i,n}}{\sum_{i=1}^{I-1} I_i + B_{i,n}\sigma^2}\right)\right. \\
&\left. - \frac{u_i\varphi_i\eta_n Q_{i,n}}{|g_{i,n}|^2} - u_i\varphi_i\hat{P} - u_i\varphi_i P_n^{amp} B_{i,n}\right\}
\end{aligned} \tag{6.46}$$

s.t.

$$\sum_{i=1}^{I}\sum_{n=1}^{N} Q_{i,n}B_{i,n} \le p^{max} \tag{6.46a}$$

$$\sum_{i=1}^{I} B_{i,n} \le \varrho_n, \quad \forall n \tag{6.46b}$$

$$\sum_{i=1}^{I} B_{i,n}\log_2\left(1 + \frac{Q_{i,n}}{\sum_{i=1}^{I-1} I_i + B_{i,n}\sigma^2}\right) \ge R_i^{min}, \quad \forall i \tag{6.46c}$$

$$B_{i,n} \ge 0, \forall i, n \tag{6.46d}$$

where $Q_{i,n} = \left[\frac{B^*_{i,n}|g_{i,n}|^2\,(u_i\mu_i+\delta_i)}{\ln 2\cdot\,(u_i\varphi_i\eta_n+\theta)} - (\sum_{i=1}^{I} I_i + B^{*\sigma^2}_{i,n})\right]^+$.

The problem formulation in (6.46) is clearly a linear programming (LP) optimization which is NP-hard and can be solved using the simplex method.

Contrary to the KKT inner loop solution to the Lagrangian duality problem derived in (6.42), the outer loop solution relies on the differentiable property of the dual function of subgradient method, to obtain power and bandwidth allocation solution for $\boldsymbol{\delta}, \boldsymbol{\theta}$ and $\boldsymbol{\vartheta}$, leading to the subgradient equations

$$\theta^{t+1} = \left[\theta^t - s_1 \times \left(p^{max} - \sum_{i=1}^{I}\sum_{n=1}^{N} p_{i,n}\right)\right]^+, \tag{6.47}$$

$$\vartheta_n^{t+1} = \left[\vartheta_n^t - s_2 \times \left(\varrho_n - \sum_{i=1}^{I} B_{i,n}\right)\right]^+ \forall n \tag{6.48}$$

$$\delta_i^{t+1} = \left[\delta_i^t - s_3 \times \left(\sum_{n=1}^{N} B_{i,n}\log_2\left(1 + \frac{p_{i,n}|g_{i,n}|^2}{\sum_{i=1}^{I-1} I_i + B_{i,n}\sigma^2}\right) - R_i^{min}\right)\right]^+ \forall i \tag{6.49}$$

where $t$ is the iteration index, and $s_k$, $k \in \{1, ..., 3\}$ represents the positive step sizes. For convergence, the power and bandwidth allocation process and updating of $\boldsymbol{\delta}, \boldsymbol{\theta}$ and $\boldsymbol{\vartheta}$ are repeated until the dual optimal value is attained. Algorithm 2 summarizes the detailed procedures involved in the power and bandwidth allocation processes.

**Algorithm 2** Optimal Solution to Power and Bandwidth Allocation for $(\boldsymbol{\varphi}, \mathbf{u})$

Initialize the maximum tolerance $\Delta^{'}$ and the maximum number of iterations $M^{'}_{max}$.
Set the iteration index $t = 0$
  **do while** *convergence*=**false** and $t < M^{'}_{max}$.
  Solve (6.44) and (6.45) for optimal power allocation.
  Solve (6.46) for optimal bandwidth allocation.
  $t = t + 1$.
  Use (6.47)-(6.49) to update the dual variables $\boldsymbol{\delta}, \boldsymbol{\theta}$ and $\boldsymbol{\vartheta}$.
  **if** $|\boldsymbol{\epsilon}^{t+1} - \boldsymbol{\epsilon}^{t}| < \Delta^{'}, \forall \boldsymbol{\epsilon} \in \{\boldsymbol{\delta}, \boldsymbol{\theta}, \boldsymbol{\vartheta}\}$
   *convergence*=**true**.
  **else**
  *convergence*=**false**.
  **end** if
**end** for

**Table 6.1:** Simulation Parameters

| Parameters | Values |
|---|---|
| AWGN power $\sigma^2$ | -114 dBm |
| UE noise figure | 9 dB |
| BS noise figure | 5 dB |
| BS antenna gain | 15 dBi |
| UE antenna gain | 1.5 m |
| 5 CCs Bandwidth, B | [2 4 6 8 10] MHz |
| 5 CCs wavelength | [0.14 0.18 0.22 0.32 0.35] |
| 5 CCs pathloss exponent | [2 3 4 5 6] |
| 5 $p^{amp}$ | [-22 -23 -24 -25 -26] dBm/Hz |
| $\hat{P}$ | 46 dBm |
| $p^{max}$ | 46 dBm |
| Iteration number, $M^{'}_{max}$ | 100 |
| $R_i$ | 15 Mbit/s |
| $\mu_n$, $n = 1, 2, ..., 5$ | 0.5 |
| $\Delta^{'}$ | $10^{-4}$ |

### 6.4.3 Results and Discussion

This section presents simulation results to demonstrate the performance of the proposed NOMA technique integrated with CA schemes. In the simulation, maximum of five inter-band CCs of 20 MHz each are aggregated in the two cells with radius of 500 m for better throughput and overall network capacity. All the five CCs are assigned different bandwidth, power consumption and pathloss. The rest of the simulation parameters are stated in Table 6.1. Although continuous addition of CCs leads to increase in scheduling procedures for resource allocation which impacts on the user's fairness, the fairness index is analyzed in the simulation to determine the trade-off between scheduler's complexity and user's satisfaction.

In Fig. 6.7, the simulated throughput without CA enabled and with different values of CCs aggregated are plotted against the number of users. It can be seen that with

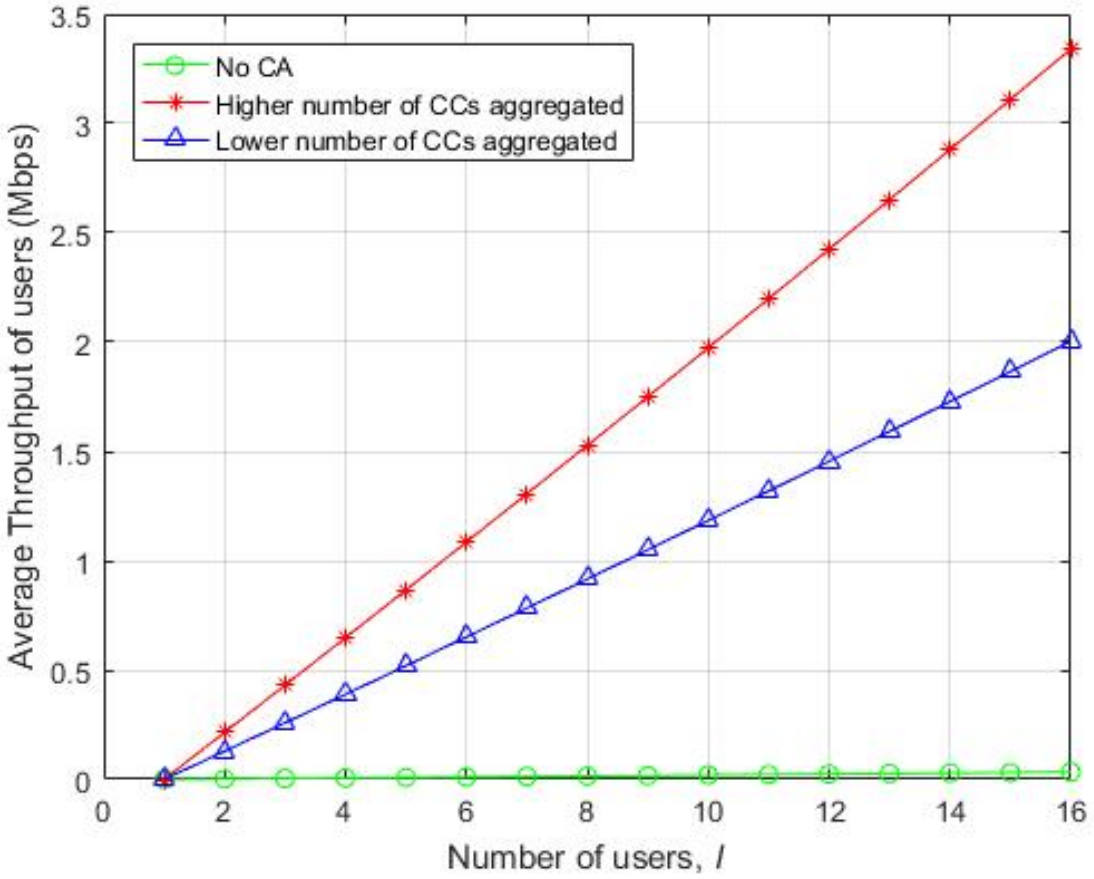


**Figure 6.7:** Improved Throughput for different values of aggregated CCs.

higher number of CCs aggregated, the throughput achieved a remarkably better performance compared to when lower number of CCs are aggregated. This is not surprising because more aggregated CCs means more bandwidth, which in turn yields increased data rate of users. It can also be noticed that higher throughput is achieved with large number of users. For example, when $i = 2$, the percentage improvement in throughput is 0.83%, compared to when $i = 4$, which is 2.50%. The trend is more obvious when $i = 8$ (5.83%), $i = 12$ (9.17%)

and $i = 16$ (12.50%), resulting in approximately average throughput increment of 2.92% per every added user. This suggests that the scheme will perform efficiently well in ultra dense network (UDN), envisioned for 5G. However, proper care must be taken to control the number of aggregated CCs when the number of users becomes large, in order to prevent high implementation complexity and eventual drop in the throughput. This is partly addressed here by using (6.31) and (6.32) to prioritize scheduling users according to their channel quality. On the contrary, with no CA enabled, the throughput is remarkably low as can be seen in the figure.

Fig. 6.8 shows the performance comparison of EE against the number of users. It can be shown that when CA is adopted, irrespective of the number of CCs configured, the EE is higher than basic NOMA scheme without CA. As more CCs are assigned to users to optimize the system performance, the terminal power consumption is minimized, hence the significant improvement in the EE of the network. However, proper observation of Fig. 6.8 shows that with certain number of users, there exists a point where the optimal value of EE is attained, after which a gradual drop is experienced as the number of users increases. In this case, maximum EE performance can be achieved with appropriate power allocation between users, by varying the total power $P_T$ via the use of suitable power control techniques.

Fig. 6.9 shows performance of the weighted sum EE for the CCs when simulated under varying values of transmit power. For all the CCs, the EE is seen to increase with increasing transmit power under NOMA. Also, CC5 shows higher EE than the rest of the CCs, which suggests more bandwidth allocation to CC5. Generally, the improvement in overall EE can be attributed to EE optimization in (6.35) under the total transmit power constraint (6.35a),

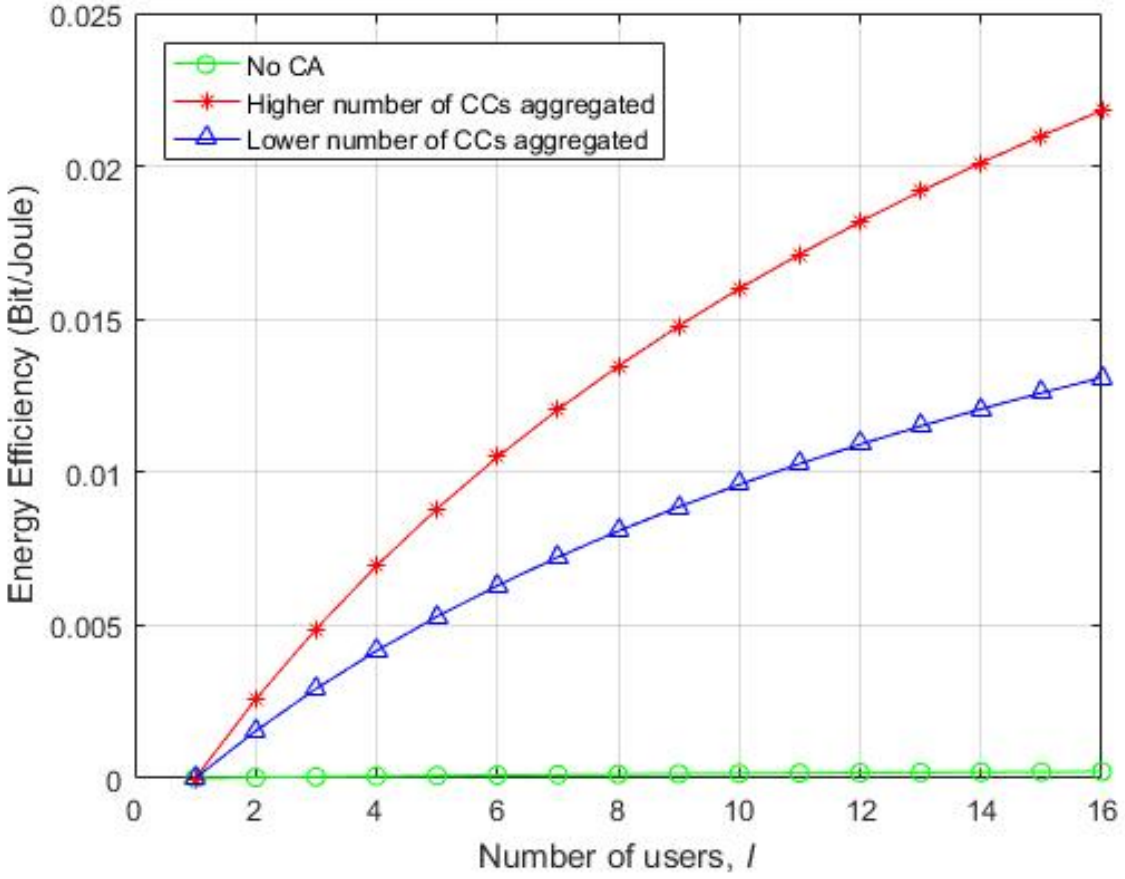


**Figure 6.8:** Plot of Energy Efficiency against number of users. $P_{amp} = 100$ Watts

and the NOMA-supported minimum rate of the farthest user constraint in (6.35c). Although, constraint (6.35b) maintains bandwidth conservation as an important condition for spectrum efficiency (SE) analysis. The need to maintain green communication via reduction in energy consumption is of higher importance for the envisioned 5G network. Therefore, a trade-off between SE and EE is often advocated, since obtaining optimal solutions simultaneously for both is not achievable. Hence, when plotted together, their performances are affected by high SNR values. Also, the result implies that the choice of CA type, non-continuous in this case, makes implementation and management of resource allocation algorithm easier, due

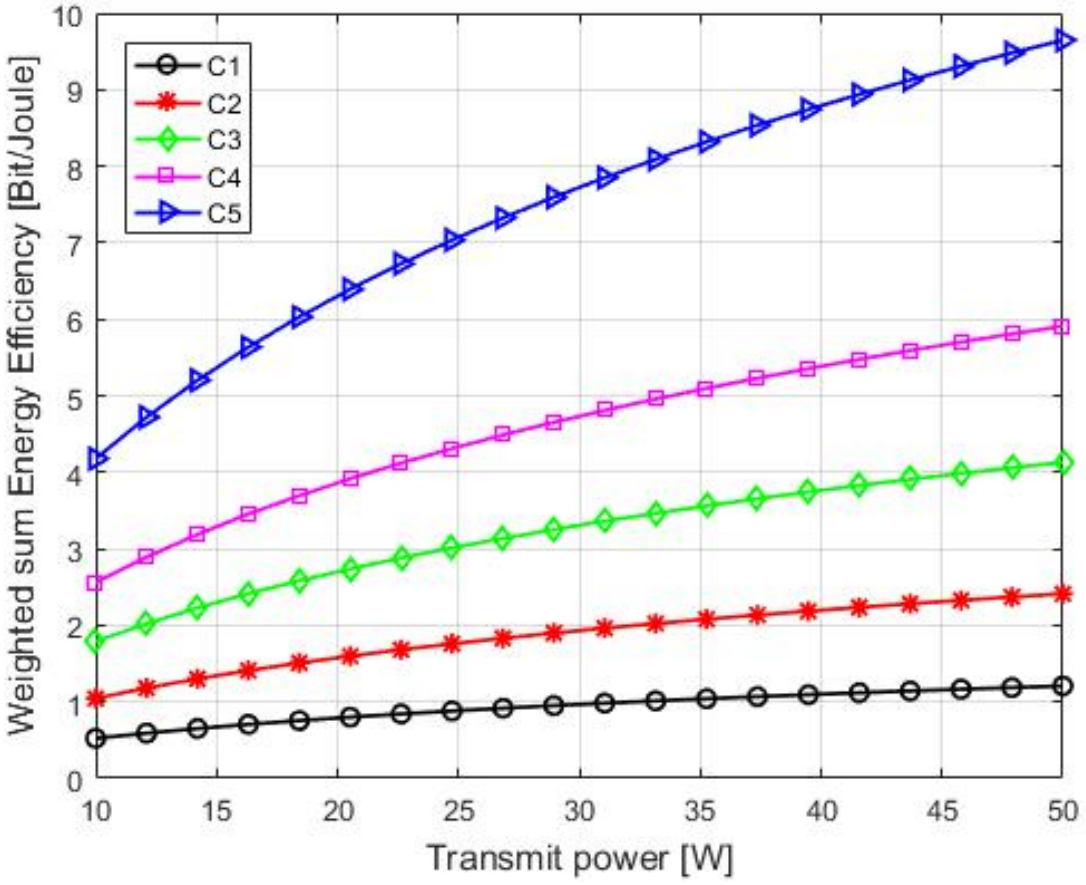


**Figure 6.9:** Weighted sum EE analysis of the proposed CA-NOMA scheme

to support for data transmission at broad frequency range over multiple separated carriers. Hence, the overall improvement in the EE arises from the consideration given in Algorithm 2 to variation, at different frequency bands, in the transmission performance and channel characteristics, such as the Doppler shift and pathloss. Consequently, it is obvious that Algorithm 2 can adaptively adjust the transmission power, coding schemes and modulation for different CCs for EE enhancement. Finally, it is worth mentioning that variation in the channel condition of UEs in adjacent cells under NOMA scheme often leads to measurement complexity for a given UE to estimate the performance of a CC.

## 6.5 Conclusion and Future Work

This chapter first presents massive MIMO-enabled NOMA technique as a promising scheme to enhance capacity, support massive connectivity and provide guaranteed Quality of Service (QoS) in 5G networks. As demonstrated, NOMA is capable of improving the system throughput and achieve low latency requirements, while serving multiple users by eliminating waiting time for orthogonal resource block availability. Furthermore, it was shown that integrating NOMA with massive MIMO can achieve significant improvement on the network performance, especially in terms of capacity. Specifically, this research shows the impact of CSI and error decoding on the system performance. We justify the implementation of massive MIMO with NOMA technique to reduce the decoding error and increase network reliability accordingly, since in fading channels, SIC receivers can be sensitive to cancellation errors.

Also in this chapter, a novel approach involving NOMA scheme, integrated with CA technology was presented to leverage on the benefits that both schemes offer. Specifically, scalable bandwidth expansion of the scarce spectrum resources provided by CA technique is complemented with power-variant resource allocation functionality of NOMA principle to boost the peak user throughput envisioned for 5G systems. Based on the QoS and traffic load requirements of the network, the BS employs dedicated RRC signaling to configure a CA-NOMA user with additional serving cells. Since the deployment scenario in 5G system requires massive connectivity of devices, with different UE's capability, the inter-band non-contiguous type of CA is considered in this approach to configure the set of CCs and serving cells. In addition, we use proportional fair scheduler to perform resource allocation and

maintain fairness between users according to their channel quality. Due to the importance of maintaining green communication in 5G, we follow this up by extending our analysis to EE. We formulate an optimization problem that aims to maximize the EE weighted sum through joint power and bandwidth allocation on each aggregated CC. The optimization is transformed into a convex problem due to its non-convexity, while an iterative Algorithm is designed to solve it for global optimum. Simulation results show improvement in the CA-NOMA scheme in terms of sum rate and EE compared to the conventional OMA scheme. In our future work, we will investigate the compatibility of other CA types on NOMA to determine which one is best suitable for network improvement in 5G systems.

# Chapter 7

# Conclusions and Recommendations

With the proliferation of smart devices in recent times, users' expectations are focussed on ubiquitous and plethora of numerous data-driven and bandwidth-demanding applications. The demand for high data rate, ultra-reliability and low latency from the present and future wireless communication systems, such as 4G-LTE, LTE-A and the envisioned 5G technologies, requires robust optimization to dynamically allocate the available radio resources. Undoubtedly, over the years, efficient resource allocation algorithms, either distributed or centralized, have played important role in the management of various challenges, such as interference coordination in wireless networks. This thesis focused on radio resource and interference management in 5G UDN, with particular attention to user association, user pairing, power control, carrier aggregation and partitioning, covered explicitly in three chapters. In this chapter, the thesis is concluded with brief description of the work done towards achieving the thesis main objectives, split between summary of main conclusions and contributions made. The first section summarises the research carried out

in each chapter, and the second section opens up areas in each chapter that are potential candidates for further improvement and research extension in the future.

## 7.1 Conclusions

Throughout the thesis, a lot of conclusions were drawn from the proposed solutions which are highlighted below:

**Chapter 4** discusses enhanced inter-cell interference coordination (eICIC) technique considered by 3GPP LTE-A standardization as one of the major techniques to mitigate interference in dense network. The eICIC is time-domain coordination, intended to improve spectral efficiency and cell-edge throughput in DL co-channel deployment scenario. It involves two approaches that can either be independently or jointly optimized - biased cell range expansion (CRE) used to offload users from macro BS to small cells, and almost blank subframe (ABS) used to address inter-cell interference caused by neighbouring cell to offloaded cell-edge users. The latter operates at the data-plane level only, hence the introduction of further eICIC (FeICIC) which operates at both the data and control plane levels. Existing literature have considered in detail, solutions based on eICIC and FeICIC under some key performance indices such as spectral efficiency (SE) and proportional fairness (PF). However, the major contribution of this chapter was the exploitation of stochastic geometry - based Poisson Point Processes (PPP), as a tractable tool for system performance evaluation. The aim is to derive closed form expressions for total interference and to encompass coverage and outage probability in our analysis. In addition, rather than completely mute the subframes which leads to performance degradation in spectral

efficiency, we adopted a reduced-power subframe (RSF) approach, in conjunction with CRE, to maintain seamless coverage and improve traffic offloading gains. Since different users may require distinct bias value and ABS ratio based on their location, we further optimized our formulations to dynamically select these two parameters accordingly. Simulation results validated our approach to guarantee fairness among users, improve coverage/outage probability and overall network throughput, while consuming less power.

**Chapter 5** presents a solution for performance analysis of vehicular communication taking into consideration the effects of building blockages and channel fading. Again, we exploit the tractability of stochastic geometry on PPP as a realistic model for urban street to analyse the coverage of cellular and vehicular UEs, termed CUEs and VUEs. The PPP helps to characterize correlated shadowing effects in urban buildings. Based on the realisation that transition between line of sight (LoS) and non line of sight (NLoS) is common in urban setting, due to high density of streets and skyscrapers, a model to capture and address the effect of LOS and NLoS interference resulting from co-located infrastructure was developed. Most literature use Euclidean distance for pathloss model to determine transition between Los and NLoS in vehicular network. This approach only works for randomly oriented buildings, but not vehicle to infrastructure (V2I) links where interference may result from co-located infrastructure on the same street. Equipped sufficiently with these models, series of expressions were derived for the ergordic capacity of vehicle-to-vehicle (V2V)/V2I links, taking into consideration both slow and fast fading information. The benefit of this approach, which is one of our major contributions, is to adequately capture the actual capacity representation of the network and to drive the resource allocation formulation to optimality.

Generally, average capacity can be maximized either by allocation of resources dynamically or through position ergodic scheme. However, in order to analytically compare the performance of urban and freeway scenarios, our solution jointly considered hybrid capacity maximization approach. The aim is to find a trade-off between unrealistic nature of dynamic resource allocation due to channel variability, and achieving low complexity resource allocation in position ergodic scheme. Thereafter, an expression for the outage probability was derived to evaluate the reliability requirements, based solely on the slow fading channel information available at the BS. The individual expressions were therefore aggregated to Power Allocation and Spectrum Sharing (PASS) formulation. Subsequently, we designed an algorithm with reduced complexity to solve the PASS optimization problem. Simulation results showed 36.67% increase in sum capacity when maximum transmit power $P^c_{max} = 25$ dBm and 43.44% when $P^c_{max} = 20$ dBm, compared to existing work. Other results showed improvement in ergodic capacity when simulated against the feedback interval, average distance between the VUEs and traffic density.

**Chapter 6** illustrates the superiority of non-orthogonal multiple access (NOMA) scheme as a promising radio access technology for the envisioned 5G network. The exponential growth in mobile devices and services imposes stringent constraints on the current wireless networks, such that conventional orthogonal multiple access (OMA) schemes brings about spectrum limitation. Since next generation wireless network is expected to be multi-cell ultra dense networks, inter-cell interference (ICI) will form a major challenge. The chapter addressed this challenge in two novel ways. The first part proposed a solution for joint implementation of NOMA with massive MIMO technique to improve network capacity in 5G UDN. Since

imperfect CSI forms one of the major drawbacks to the successful implementation of NOMA, an investigation about power allocation problem was first conducted. This was intended to analyse fairness when target data rate of users are fixed, conditioned on the average CSI. It also supports the knowledge that maximizing sum rate does not fully translate to effective power allocation in MOMA, since both fairness and data rate are seen as a unit. We presented a solution based on low complexity zero-forcing (ZF) beamforming to remove ICI introduced through superposition coding in NOMA, especially under the assumption that the BS has perfect knowledge of the beamspace channel. However, through extensive analysis, suppressing ICI using this method in MIMO-NOMA, when the number of receive antenna is far greater than transmit antenna (as shown in Fig. (6.2)) proved difficult to implement. In such a case, precoding technique was used to improve the achievable rate. Finally, solutions to power consumption redundancy and hardware complexity associated with concurrent use of multiple antennas in MIMO were presented. It was revealed through simulations the improvement in capacity and achievable rate when simulated against various numbers of antennas and SNR values, respectively. The second part of the chapter presented a carrier aggregation (CA) based NOMA solution towards enhanced capacity in 5G UDN. The two main benefits of CA and NOMA, namely, bandwidth expansion functionality provided for the scarce spectrum in CA, and power-variant resource allocation property of NOMA were complemented to increase the peak user throughput of the network. To temporarily answer the research question about the choice of CA type to use for NOMA integration, our solution considered the inter-band non-contiguous to configure CC sets, due to its capability to support massive connectivity of devices, with different UE's requirements in 5G. Maintaining

green communication forms a key requirement of 5G networks. Hence, we formulated an optimization for the energy efficiency of the DL network to quantitatively characterise and further establish the advantages in transmission and circuit power consumption, energy saving, spectrum utilization and different QoS requirements of users. The optimization was formulated as NOMA-based power and CA-tuned bandwidth allocation problem with different weight factors assigned to the EE of the BS and users. The non-convex problem was first transformed to convex equivalence, while an intelligent algorithm was developed for global optimum solution. Lagrangian dual method was then used to solve the power and bandwidth problem iteratively. Numerical results revealed better performance in terms of average throughput and EE (without weight factor) when considerable number of CCs are aggregated, compared to the case without CA. Also, when simulated under varying transmit power levels, the weighted-sum EE showed improved performance, thereby confirming the efficacy of the EE optimization and developed algorithm.

Thus, it can be concluded that the main objectives of the thesis presented in Section 1.4 have been achieved through extensive analyses and simulations carried out in Chapters 4-6. The respective findings produced in this thesis are therefore expected to contribute to the advancement of interference-limited and seamless communication in 5G UDN.

## 7.2 Recommendations and Future Work

Several interesting research areas were invoked during the course of conducting this study, some of which are discussed below.

The success of user association based on FeICIC scheme largely depends on accurate

determination of the bias factor and ABS ratio. Both factors are directly affected by network density, the pathloss model used for analysis and other network-specific factors. However, taking into account these factors simultaneously in high density network, as done in this thesis increased the network overhead. Therefore, possible extensions should seek to dynamically adjust these values in real-time and distributed fashion, with absolutely manageable complexity in heavily loaded network like 5G UDN.

Analysis of vehicular network using stochastic geometry based on PPP has proved to be a tractable model for capturing blockages, spatial configurations and propagation loss. Despite the versatility of the model, expansion of the scope using simple parameters to reflect key features of real-world scenarios, and facilitate more accurate performance metrics, such as latency, at the cost of reduced tractability will be a worthwhile research venture. In addition, the user pairing expression derived in Section 5.3.2 allocates resource block orthogonally among VUEs. Future work that considers multiple VUEs to be paired on a common RB, most importantly, with low implementation complexity so that more VUEs can be accommodated will contribute greatly to research novelty.

The first part of Chapter 6 of this thesis presented NOMA-MIMO based solution, with various design considerations for capacity maximization. As proposed, NOMA-MIMO combination is capable of achieving high throughput gains with large number of users when perfect CSI is available at the transmitter. Also, beamforming techniques, antenna selection principle and utilization of zero-forcing precoding matrix contributed to the maximization of network capacity. However, the above NOMA-MIMO solutions involve high computational complexity. Hence, research activities on how to reduce consumption of extra signaling

overhead and realize physical layer security in NOMA-based networks is of utmost necessity. Second part of Chapter 6 presented solution on CA-NOMA integration, using the interband non-continuous CA type. The choice of this CA type is to achieve network reliability, since in interband non-continuous CA, data can be transmitted over multiple separated carriers across a large frequency, to support differentiated power levels on the same band and time for NOMA UEs. However, ICI issue might be uncontrollable in such situation, especially as the density of BS and connected devices increases. In the future, more in-depth research on compatibility of other CA types for NOMA integration, to promote variability and enhance performance in 5G network will be of notable importance. Finally, integration of NOMA with other state-of-the-art enabling technologies such as mmWave networks, visible light communications (VLC), machine-to-machine (M2M) and massive machine-type communications (mMTC), to support IoT and massive connectivity demands of 5G requires further considerations.

The following section specifically describes possible future perspectives and ongoing work directions related to the contributions of each of the chapters.

### 7.2.1 State-of-the-art research on Interference management in 5G UDN

Interference remains one of the major challenges to the full implementation of 5G technology. This research unveiled the key interference mitigation schemes based on resource partitioning in time domain, frequency domain and spatial domain, as applied in either user side, network side or combination of both. To reduce interference caused by frequency reuse in UDN, joint

cell scheduling on the network side and advanced receivers on the user side has been proposed. However, this approach may not satisfy multiple objectives of energy efficiency, load balance and throughput. Hence, a low cost, joint combination of network side coordinated scheduling and user side advanced interference detection techniques will be desired for enhanced network performance in 5G UDN.

### 7.2.2 Complexity analysis of interference mitigation schemes in 5G UDN

Most proposed solutions presented in this research require complex, frequent exchange of information and cooperation among macro cells, small cells and users. In addition, large volumes of network resources is involved to convey necessary information between the network components and controlling nodes. To reduce signaling overhead with minimal complexity, appropriate interference management scheme executed in a distributed manner is still required for energy conservation and cost reduction.

### 7.2.3 Interference mitigation using multiple access in 5G UDN

In 5G UDN, there is need to explore more robust access technique to handle access collision challenge and support the massive connectivity requirement for improved network capacity. NOMA has been proposed as a replacement to OMA to support more users and enhance spectral efficiency. Co-channel interference remains a big issue in NOMA since multiple users share the same resources in time, frequency and spatial domain. Majority of the existing literature have proposed resource allocation and user association schemes

for unified framework in NOMA. However, only few work has combined NOMA with other technology for improved performance. In this research, we consolidated on the few research on NOMA-MIMO for interference mitigation and capacity enhancement. Subsequently, a novel solution involving NOMA, integrated with carrier aggregation was presented to achieve better performance. In the future, combining NOMA with more state-of-the art techniques, with reduced complexity would help validate superiority of NOMA over OMA.

### 7.2.4 Integration of other techniques for enhanced network performance in 5G UDN

Cell densification undoubtedly improves network capacity by offloading macrocell traffic, reducing congestion and balancing network load. In this research, the enormous benefit offered by utilizing a new multiple access scheme such as NOMA to support massive connectivity goal of 5G was shown through performance analysis. To further strengthen the network against ICI, this work combined two state-of-the art schemes, MIMO and CA to improve capacity and bandwidth efficiency. The resultant resource management challenges in this approach are very serious. Therefore, an open research is developing more robust algorithm that will combine less complexity with performance.

### 7.2.5 Resource allocation for interference management in 5G UDN

Efficient power and spectrum allocation forms a major driver that will impact the system performance of 5G UDN. Spectrum sharing issue arises due to scarcity of spectrum. Although, the current spectrum sharing methods employed in conventional wireless networks is capable of providing efficient spectrum usage. However, this may not produce appreciable result in UDN due to various factors such as co-located building layouts and increased traffic volume which affect the interference dynamics. Joint implementation of power control and spectrum allocation introduced in this research, especially in vehicular application, has proved to be effective in this regard. Nonetheless, further research that will facilitate obtaining full CSI by the BS irrespective of vehicle mobility, and prevent outdated CSI due to rapid variation of small scale fading, in a cost effective manner would be an interesting research direction.

### 7.2.6 Critical application requirement challenges in 5G use cases

Clearly, each new generation wireless network is accompanied by a set of new usage. The envisioned 5G network will not be an exception as it will be focused on use cases such as massive machine-to-machine (M2M) and ultra-low latency IoT critical communications. This requirement will compel the network to provide communication needs for billions of connected devices, taking into cognizance appropriate trade-offs between latency, reliability, speed and cost. In the solution presented in this thesis on vehicular communication as

an important use case for 5G system, simulations are performed in MATLAB for ergodic capacity. In the future, real-life test bed implementation can be performed to obtain more general results.

### 7.2.7 Security and Privacy provisioning in 5G UDN

Although security aspect of 5G UDN was not covered in this research. Nevertheless, a lot of security threats is expected to plague 5G deployment due to extremely high number of information exchanged as a result of network densification. Furthermore, the network is susceptible to serious security and privacy concerns due to data roaming and data computing. Also, introduction of new techniques, multiple diverse network and increased system complexity will increase the exposure rate. Hence, more research is needed to develop low complexity and practical schemes for achieving security, both at the edge (device) and at the core (network) in 5G UDN.

# References


[1] X. Ge, S. Tu, G. Mao, C.-X. Wang, and T. Han, "5g ultra-dense cellular networks," *IEEE Wireless Communications*, vol. 23, no. 1, pp. 72–79, 2016.

[2] K. Samdanis, S. Wright, A. Banchs, A. Capone, M. Ulema, and K. Obana, "5g network slicing–part 2: Algorithms and practice," *IEEE Communications Magazine*, vol. 55, no. 8, pp. 110–111, 2017.

[3] G. Forecast, "Cisco visual networking index: global mobile data traffic forecast update, 2017–2022," *Update*, vol. 2017, p. 2022, 2019.

[4] E. M. Report, "Ericsson mobility report interim update, february, 2018."

[5] C. Zhang, S. L. Ariyavisitakul, and M. Tao, "Lte-advanced and 4g wireless communications [guest editorial]," *IEEE Communications Magazine*, vol. 50, no. 2, 2012.

[6] D. Soldani and A. Manzalini, "Horizon 2020 and beyond: on the 5g operating system for a true digital society," *IEEE Vehicular Technology Magazine*, vol. 10, no. 1, pp. 32–42, 2015.

[7] R. N. Mitra and D. P. Agrawal, "5g mobile technology: A survey," *ICT Express*, vol. 1, no. 3, pp. 132–137, 2015.

[8] X. Foukas, G. Patounas, A. Elmokashfi, and M. K. Marina, "Network slicing in 5g: Survey and challenges," *IEEE Communications Magazine*, vol. 55, no. 5, pp. 94–100, 2017.

[9] G. I. P. Association *et al.*, "5g vision-the 5g infrastructure public private partnership: the next generation of communication networks and services," *White Paper, February*, 2015.

[10] N. Panwar, S. Sharma, and A. K. Singh, "A survey on 5g: The next generation of mobile communication," *Physical Communication*, vol. 18, pp. 64–84, 2016.

[11] H. Zhang, N. Liu, X. Chu, K. Long, A.-H. Aghvami, and V. C. Leung, "Network slicing based 5g and future mobile networks: mobility, resource management, and challenges," *IEEE Communications Magazine*, vol. 55, no. 8, pp. 138–145, 2017.

[12] E. Hossain, M. Rasti, H. Tabassum, and A. Abdelnasser, "Evolution toward 5g multi-tier cellular wireless networks: An interference management perspective," *IEEE Wireless Communications*, vol. 21, no. 3, pp. 118–127, 2014.

[13] E. Hossain and M. Hasan, "5g cellular: key enabling technologies and research challenges," *IEEE Instrumentation & Measurement Magazine*, vol. 18, no. 3, pp. 11–21, 2015.

[14] S. Talwar, D. Choudhury, K. Dimou, E. Aryafar, B. Bangerter, and K. Stewart, "Enabling technologies and architectures for 5g wireless," in *Microwave Symposium (IMS), 2014 IEEE MTT-S International*. IEEE, 2014, pp. 1–4.

[15] S. Abdelwahab, B. Hamdaoui, M. Guizani, and T. Znati, "Network function virtualization in 5g," *IEEE Communications Magazine*, vol. 54, no. 4, pp. 84–91, 2016.

[16] M. Agiwal, A. Roy, and N. Saxena, "Next generation 5g wireless networks: A comprehensive survey," *IEEE Communications Surveys & Tutorials*, vol. 18, no. 3, pp. 1617–1655, 2016.

[17] D. Lopez-Perez, I. Guvenc, G. De la Roche, M. Kountouris, T. Q. Quek, and J. Zhang, "Enhanced intercell interference coordination challenges in heterogeneous networks," *IEEE Wireless Communications*, vol. 18, no. 3, 2011.

[18] B. Soret, K. I. Pedersen, N. T. Jørgensen, and V. Fernández-López, "Interference coordination for dense wireless networks," *IEEE Communications Magazine*, vol. 53, no. 1, pp. 102–109, 2015.

[19] S. Ahmadi, *LTE-advanced: A practical systems approach to understanding 3GPP LTE releases 10 and 11 radio access technologies*. Academic Press, 2013.

[20] M. Kamel, W. Hamouda, and A. Youssef, "Ultra-dense networks: A survey," *IEEE Communications Surveys & Tutorials*, vol. 18, no. 4, pp. 2522–2545, 2016.

[21] D. Darsena, G. Gelli, and F. Verde, "Design of cooperative mimo wireless sensor networks with partial channel state information," *IEEE Access*, vol. 8, pp. 109 677–109 686, 2020.

[22] S. M. Rakshit, S. Banerjee, M. Hempel, and H. Sharif, "Towards an integrated approach for distributed 5g cell association in udn under interference and mobility," in *2018 International Conference on Computing, Networking and Communications (ICNC)*. IEEE, 2018, pp. 810–814.

[23] X. Wang, R. Chen, Y. Xu, and Q. Meng, "Low-complexity power allocation in noma systems with imperfect sic for maximizing weighted sum-rate," *IEEE Access*, vol. 7, pp. 94 238–94 253, 2019.

[24] J. Sangiamwong, Y. Saito, N. Miki, T. Abe, S. Nagata, and Y. Okumura, "Investigation on cell selection methods associated with inter-cell interference coordination in heterogeneous networks for lte-advanced downlink," in *Wireless Conference 2011-Sustainable Wireless Technologies (European Wireless), 11th European*. VDE, 2011, pp. 1–6.

[25] I. Guvenc, "Capacity and fairness analysis of heterogeneous networks with range expansion and interference coordination," *IEEE Communications Letters*, vol. 15, no. 10, pp. 1084–1087, 2011.

[26] J. Oh and Y. Han, "Cell selection for range expansion with almost blank subframe in heterogeneous networks," in *Personal Indoor and Mobile Radio Communications (PIMRC), 2012 IEEE 23rd International Symposium on*. IEEE, 2012, pp. 653–657.

[27] M. Chiang, P. Hande, T. Lan, C. W. Tan *et al.*, "Power control in wireless cellular networks," *Foundations and Trends® in Networking*, vol. 2, no. 4, pp. 381–533, 2008.

[28] N. L. Pradhan and T. Saadawi, "Power control algorithms for mobile ad hoc networks," *Journal of Advanced Research*, vol. 2, no. 3, pp. 199–206, 2011.

[29] G. J. Foschini and Z. Miljanic, "A simple distributed autonomous power control algorithm and its convergence," *IEEE transactions on vehicular Technology*, vol. 42, no. 4, pp. 641–646, 1993.

[30] K.-K. Leung and C. W. Sung, "An opportunistic power control algorithm for cellular network," *IEEE/ACM Transactions on Networking*, vol. 14, no. 3, pp. 470–478, 2006.

[31] M. Rasti, A. R. Sharafat, and J. Zander, "Pareto and energy-efficient distributed power control with feasibility check in wireless networks," *IEEE Transactions on Information Theory*, vol. 57, no. 1, pp. 245–255, 2011.

[32] M. Rasti and A. R. Sharafat, "Distributed uplink power control with soft removal for wireless networks," *IEEE Transactions on Communications*, vol. 59, no. 3, pp. 833–843, 2011.

[33] M. Rasti, A. R. Sharafat, and J. Zander, "A distributed dynamic target-sir-tracking power control algorithm for wireless cellular networks," *IEEE Transactions on Vehicular Technology*, vol. 59, no. 2, pp. 906–916, 2010.

[34] S. Lagén Morancho, "Coordination strategies for interference management in mimo dense cellular networks," 2016.

[35] S.-S. Sun, W. Liao, and W.-T. Chen, "Traffic offloading with rate-based cell range expansion offsets in heterogeneous networks," in *Wireless Communications and Networking Conference (WCNC), 2014 IEEE*. IEEE, 2014, pp. 2833–2838.

[36] F. Liu and M. Petrova, "Traffic load balancing based on user data rate estimation in heterogeneous cellular networks," in *Personal, Indoor, and Mobile Radio Communication (PIMRC), 2014 IEEE 25th Annual International Symposium on*. IEEE, 2014, pp. 1514–1519.

[37] C. Avin, A. Cohen, Y. Haddad, E. Kantor, Z. Lotker, M. Parter, and D. Peleg, "Sinr diagram with interference cancellation," *Ad Hoc Networks*, vol. 54, pp. 1–16, 2017.

[38] I. Atzeni and M. Kountouris, "Full-duplex mimo small-cell networks with interference cancellation," *IEEE Transactions on Wireless Communications*, vol. 16, no. 12, pp. 8362–8376, 2017.

[39] C. Yang and J. Li, *Interference Mitigation and Energy Management in 5G Heterogeneous Cellular Networks*. IGI Global, 2016.

[40] J. Hofmann, V. Rexhepi-van der Pol, G. Sébire, and S. Parolari, "3gpp release 8," *GSM/EDGE: Evolution and Performance*, pp. 63–99, 2011.

[41] S. Parkvall, A. Furuskar, and E. Dahlman, "Evolution of lte toward imt-advanced," *IEEE Communications Magazine*, vol. 49, no. 2, 2011.

[42] B. Soret, H. Wang, K. I. Pedersen, and C. Rosa, "Multicell cooperation for lte-advanced heterogeneous network scenarios," *IEEE Wireless Communications*, vol. 20, no. 1, pp. 27–34, 2013.

[43] K. I. Pedersen, B. Soret, S. B. Sanchez, G. Pocovi, and H. Wang, "Dynamic enhanced intercell interference coordination for realistic networks," *IEEE Transactions on Vehicular Technology*, vol. 65, no. 7, pp. 5551–5562, 2016.

[44] E. U. T. R. Access, "Further enhancements to lte time division duplex (tdd) for downlink-uplink (dl-ul) interference management and traffic adaptation," 2012.

[45] M. Ding and H. Luo, *Multi-point cooperative communication systems: Theory and applications*. Springer, 2013.

[46] G. Nardini, A. Virdis, and G. Stea, "Modeling x2 backhauling for lte-advanced and assessing its effect on comp coordinated scheduling," in *Link-and System Level Simulations (IWSLS), International Workshop on*. IEEE, 2016, pp. 1–6.

[47] Y. Yuan, Z. Yuan, G. Yu, C.-h. Hwang, P.-k. Liao, A. Li, and K. Takeda, "Non-orthogonal transmission technology in lte evolution," *IEEE Communications Magazine*, vol. 54, no. 7, pp. 68–74, 2016.

[48] 3rd Generation Partnership Project, "Network assisted interference cancellation and suppression (naics)," 3GPP TR 36.866, 2013.

[49] N. Zorba and C. Verikoukis, "Energy optimization for bidirectional multimedia communication in unsynchronized tdd systems," *IEEE Systems Journal*, vol. 10, no. 2, pp. 797–804, 2016.

[50] K. Samdanis, R. Shrivastava, A. Prasad, P. Rost, and D. Grace, "Virtual cells: Enhancing the resource allocation efficiency for td-lte," in *Vehicular Technology Conference (VTC Fall), 2014 IEEE 80th.* IEEE, 2014, pp. 1–5.

[51] X. Liu, L. Wang, D. Liu, W. Guo, and Q. Quan, "Energy-efficient algorithm for carrier aggregation and cognitive radio based td-lte system," 2014.

[52] A. V. Kini, M. Hosseinian, P. Sadeghi, and J. Stern-Berkowitz, "A dynamic subframe set power control scheme for interference mitigation in reconfigurable td-lte systems," in *Wireless and Optical Communication Conference (WOCC), 2014 23rd.* IEEE, 2014, pp. 1–6.

[53] H. Li, L. Han, R. Duan, and G. M. Garner, "Analysis of the synchronization requirements of 5g and corresponding solutions," *IEEE Communications Standards Magazine*, vol. 1, no. 1, pp. 52–58, 2017.

[54] L. Zhao, K. Liang, G. Cao, R. Qian, and D. López-Pérez, "An enhanced signal-timing-offset compensation algorithm for coordinated multipoint-to-multiuser systems," *IEEE Communications Letters*, vol. 18, no. 6, pp. 983–986, 2014.

[55] N. Bhushan, J. Li, D. Malladi, R. Gilmore, D. Brenner, A. Damnjanovic, R. Sukhavasi, C. Patel, and S. Geirhofer, "Network densification: the dominant theme for wireless evolution into 5g," *IEEE Communications Magazine*, vol. 52, no. 2, pp. 82–89, 2014.

[56] E. G. Larsson, O. Edfors, F. Tufvesson, and T. L. Marzetta, "Massive mimo for next generation wireless systems," *IEEE communications magazine*, vol. 52, no. 2, pp. 186–195, 2014.

[57] L. Zhao, H. Zhao, K. Zheng, and W. Xiang, *Massive MIMO in 5G Networks: Selected Applications*. Springer, 2017.

[58] S. Gupta, "Statistical channel knowledge based transmission strategies for energy-constrained ad-hoc wireless relay networks," Ph.D. dissertation, 2016.

[59] R. Bordón, S. M. Sánchez, S. B. Mafra, E. M. Garcia Fernandez, R. D. Souza, and J. L. Rebelatto, "Energy-efficient outage-constrained power allocation based on statistical channel knowledge for dual-hop cognitive relay networks," *International Journal of Communication Systems*, vol. 30, no. 3, 2017.

[60] P. Marsch and G. P. Fettweis, *Coordinated Multi-Point in Mobile Communications: from theory to practice*. Cambridge University Press, 2011.

[61] B. Dai and W. Yu, "Sparse beamforming and user-centric clustering for downlink cloud radio access network," *IEEE Access*, vol. 2, pp. 1326–1339, 2014.

[62] J. Zhang, R. Chen, J. G. Andrews, A. Ghosh, and R. W. Heath, "Networked mimo with clustered linear precoding," *IEEE Transactions on Wireless Communications*, vol. 8, no. 4, 2009.

[63] M. Hong, R. Sun, H. Baligh, and Z.-Q. Luo, "Joint base station clustering and beamformer design for partial coordinated transmission in heterogeneous networks," *IEEE Journal on Selected Areas in Communications*, vol. 31, no. 2, pp. 226–240, 2013.

[64] M. Sanjabi, M. Hong, M. Razaviyayn, and Z.-Q. Luo, "Joint base station clustering and beamformer design for partial coordinated transmission using statistical channel state information," in *Signal Processing Advances in Wireless Communications (SPAWC), 2014 IEEE 15th International Workshop on*. IEEE, 2014, pp. 359–363.

[65] L. B. Le, V. Lau, E. Jorswieck, N.-D. Dao, A. Haghighat, D. I. Kim, and T. Le-Ngoc, "Enabling 5g mobile wireless technologies," 2015.

[66] D. H. Dobyns, "Proximity based social networking," Jan. 31 2017, uS Patent 9,560,505.

[67] A. Merwaday and I. Guvenc, "Uav assisted heterogeneous networks for public safety communications," in *Wireless Communications and Networking Conference Workshops (WCNCW), 2015 IEEE*. IEEE, 2015, pp. 329–334.

[68] I. Butun, M. Erol-Kantarci, B. Kantarci, and H. Song, "Cloud-centric multi-level authentication as a service for secure public safety device networks," *IEEE Communications Magazine*, vol. 54, no. 4, pp. 47–53, 2016.

[69] J. Chen, G. Mao, C. Li, A. Zafar, and A. Y. Zomaya, "Throughput of infrastructure-based cooperative vehicular networks," *IEEE Transactions on Intelligent Transportation Systems*, vol. 18, no. 11, pp. 2964–2979, 2017.

[70] K. C. Dey, A. Rayamajhi, M. Chowdhury, P. Bhavsar, and J. Martin, "Vehicle-to-vehicle (v2v) and vehicle-to-infrastructure (v2i) communication in a heterogeneous wireless network–performance evaluation," *Transportation Research Part C: Emerging Technologies*, vol. 68, pp. 168–184, 2016.

[71] D. Liu, L. Wang, Y. Chen, M. Elkashlan, K.-K. Wong, R. Schober, and L. Hanzo, "User association in 5g networks: A survey and an outlook," *IEEE Communications Surveys & Tutorials*, vol. 18, no. 2, pp. 1018–1044, 2016.

[72] T. Kudo and T. Ohtsuki, "Cell range expansion using distributed q-learning in heterogeneous networks," *EURASIP Journal on Wireless Communications and Networking*, vol. 2013, no. 1, p. 61, 2013.

[73] S. Deb, P. Monogioudis, J. Miernik, and J. P. Seymour, "Algorithms for enhanced inter-cell interference coordination (eicic) in lte hetnets," *IEEE/ACM transactions on networking*, vol. 22, no. 1, pp. 137–150, 2014.

[74] S. Singh and J. G. Andrews, "Joint resource partitioning and offloading in heterogeneous cellular networks," *IEEE Transactions on Wireless Communications*, vol. 13, no. 2, pp. 888–901, 2014.

[75] W. Bao and B. Liang, "Structured spectrum allocation and user association in heterogeneous cellular networks," in *INFOCOM, 2014 Proceedings IEEE*. IEEE, 2014, pp. 1069–1077.

[76] H. S. Dhillon, R. K. Ganti, F. Baccelli, and J. G. Andrews, "Modeling and analysis of k-tier downlink heterogeneous cellular networks," *IEEE Journal on Selected Areas in Communications*, vol. 30, no. 3, pp. 550–560, 2012.

[77] H. S. Dhillon, R. K. Ganti, and J. G. Andrews, "Load-aware modeling and analysis of heterogeneous cellular networks," *IEEE Transactions on Wireless Communications*, vol. 12, no. 4, pp. 1666–1677, 2013.

[78] S. Sadr and R. S. Adve, "Tier association probability and spectrum partitioning for maximum rate coverage in multi-tier heterogeneous networks," *IEEE Communications Letters*, vol. 18, no. 10, pp. 1791–1794, 2014.

[79] Y. Lin, W. Bao, W. Yu, and B. Liang, "Optimizing user association and spectrum allocation in hetnets: A utility perspective," *IEEE Journal on Selected Areas in Communications*, vol. 33, no. 6, pp. 1025–1039, 2015.

[80] M. Hajir, "Resource management and interference mitigation for dense heterogeneous small-cell networks," Ph.D. dissertation, École de technologie supérieure, 2017.

[81] D. Kimura, Y. Harada, and H. Seki, "De-centralized dynamic icic using x2 interfaces for downlink lte systems," in *Vehicular Technology Conference (VTC Spring), 2011 IEEE 73rd*. IEEE, 2011, pp. 1–5.

[82] D. González, M. García-Lozano, S. Ruiz, and D. S. Lee, "A metaheuristic-based downlink power allocation for lte/lte-a cellular deployments," *Wireless Networks*, vol. 20, no. 6, pp. 1369–1386, 2014.

[83] X. Jiang, H.-C. Chao, G.-M. Muntean, G. Ghinea, and C. Xu, "Green communication for mobile and wireless networks," *Mobile Information Systems*, vol. 2016, 2016.

[84] Z. Wang, B. Hu, X. Wang, and S. Chen, "Cooperative game-theoretic power control with a balancing factor in large-scale lte networks: an energy efficiency perspective," *The Journal of Supercomputing*, vol. 71, no. 9, pp. 3288–3300, 2015.

[85] S. Shuang, L. Zhuoming, W. Peng, Z. Wanjun, W. Wei, and W. Xuanli, "Power control for self-organizing network in lte-advanced system," in *Instrumentation and Measurement, Computer, Communication and Control (IMCCC), 2014 Fourth International Conference on*. IEEE, 2014, pp. 836–839.

[86] X. Wang, B. Liu, and X. Su, "A power allocation scheme using non-cooperative game theory in ultra-dense networks," in *Wireless and Optical Communication Conference (WOCC), 2018 IEEE 27th International Conference on*. IEEE, 2018, pp. 1–5.

[87] D. T. Ngo, S. Khakurel, and T. Le-Ngoc, "Joint subchannel assignment and power allocation for ofdma femtocell networks," *IEEE Transactions on Wireless Communications*, vol. 13, no. 1, pp. 342–355, 2014.

[88] V. N. Ha and L. B. Le, "Distributed base station association and power control for heterogeneous cellular networks," *IEEE Transactions on Vehicular Technology*, vol. 63, no. 1, pp. 282–296, 2014.

[89] X. Jiang, X. Li, and H. Ji, "Service-driven resource allocation based on energy efficiency in uudn," in *Communication Technology (ICCT), 2017 IEEE 17th International Conference on*. IEEE, 2017, pp. 498–502.

[90] M. Ali, S. Qaisar, M. Naeem, and S. Mumtaz, "Joint user association and power allocation for licensed and unlicensed spectrum in 5g networks," in *GLOBECOM 2017-2017 IEEE Global Communications Conference*. IEEE, 2017, pp. 1–6.

[91] S. Islam, M. Zeng, and O. A. Dobre, "Noma in 5g systems: Exciting possibilities for enhancing spectral efficiency," *arXiv preprint arXiv:1706.08215*, 2017.

[92] J. He and Z. Tang, "Low-complexity user pairing and power allocation algorithm for 5g cellular network non-orthogonal multiple access," *Electronics Letters*, vol. 53, no. 9, pp. 626–627, 2017.

[93] J. He, Z. Tang, and Z. Che, "Fast and efficient user pairing and power allocation algorithm for non-orthogonal multiple access in cellular networks," *Electronics Letters*, vol. 52, no. 25, pp. 2065–2067, 2016.

[94] A. Marcano, S. Mumtaz, R. V. Prasad, H. Christiansen *et al.*, "Unveiling capacity gains in ultradense networks using mm-wave noma: A system-level performance evaluation

shows the power-efficient benefits of directional antennas," *IEEE Vehicular Technology Magazine*, 2018.

[95] X. Zhang and J. Wang, "Joint heterogeneous statistical-qos/qoe provisionings for edge-computing based wifi offloading over 5g mobile wireless networks," in *Information Sciences and Systems (CISS), 2018 52nd Annual Conference on.* IEEE, 2018, pp. 1–6.

[96] M. Sinaie, D. W. K. Ng, and E. A. Jorswieck, "Resource allocation in noma virtualized wireless networks under statistical delay constraints," *IEEE Wireless Communications Letters*, 2018.

[97] S. R. Islam, M. Zeng, O. A. Dobre, and K.-S. Kwak, "Resource allocation for downlink noma systems: Key techniques and open issues," *IEEE Wireless Commun*, 2018.

[98] S. Lee, M. Yang, T. W. Kim, and D. K. Kim, "Low complexity user pairing algorithm for in-band full-duplex networks with power control," in *Communications (APCC), 2017 23rd Asia-Pacific Conference on.* IEEE, 2017, pp. 1–5.

[99] Z. Zhang, G. Yu, D. Wen, and R. Liu, "Joint user pairing, resource block allocation, and power control for full-duplex cellular networks," in *Communications in China (ICCC), 2016 IEEE/CIC International Conference on.* IEEE, 2016, pp. 1–6.

[100] R. Sultan, L. Song, K. G. Seddik, Y. Li, and Z. Han, "Mode selection, user pairing, subcarrier allocation and power control in full-duplex ofdma hetnets," in

*Communication Workshop (ICCW), 2015 IEEE International Conference on*. IEEE, 2015, pp. 210–215.

[101] X. Chai, S. Zhang, T. Zhang, and Z. Zhang, "A user-pairing power control algorithm in two-tier hetnet," in *Vehicular Technology Conference (VTC Spring), 2015 IEEE 81st*. IEEE, 2015, pp. 1–5.

[102] M. Susanto, H. Fitriawan, A. Abadi *et al.*, "On the reduction of interference effect using power control for device-to-device communication underlying cellular communication network," in *Electrical Engineering and Computer Science (ICECOS), 2017 International Conference on*. IEEE, 2017, pp. 28–32.

[103] Y. Wang, Z. Yang, Y. Pan, and M. Chen, "Joint power control and user pairing for ergodic capacity maximization in v2v communications," in *Wireless Communications and Signal Processing (WCSP), 2017 9th International Conference on*. IEEE, 2017, pp. 1–6.

[104] X. Liu, Y. Li, L. Xiao, and J. Wang, "Performance analysis and power control for multi-antenna v2v underlay massive mimo," *IEEE Transactions on Wireless Communications*, 2018.

[105] D. T. Ngo and T. Le-Ngoc, "Architectures and interference management for small-cell networks," in *Architectures of Small-Cell Networks and Interference Management*. Springer, 2014, pp. 11–31.

[106] J. Boccuzzi and M. Ruggiero, *Femtocells: design & application.* McGraw Hill Professional, 2010.

[107] N. Saquib, E. Hossain, L. B. Le, and D. I. Kim, "Interference management in ofdma femtocell networks: Issues and approaches," *IEEE Wireless Communications*, vol. 19, no. 3, 2012.

[108] M. Al-Omari, A. R. Ramli, A. Sali, and R. S. Azmir, "Deployment of femtocell and its interference management approaches in lte heterogeneous networks." *Journal of Theoretical & Applied Information Technology*, vol. 87, no. 1, 2016.

[109] M. Aldababsa, M. Toka, S. Gökçeli, G. Karabulut, and O. K. Kurt, "A tutorial on non-orthogonal multiple access (noma) for 5g and beyond."

[110] S. M. Al-Shehri, P. Loskot, T. Numanoglu, and M. Mert, "Common metrics for analyzing, developing and managing telecommunication networks," *arXiv preprint arXiv:1707.03290*, 2017.

[111] 3rd Generation Partnership Project, "General packet radio service (gprs) enhancements for evolved universal terrestrial radio access network (e-utran) access," *Release 12, 3GPP Technical Specification, TS 23.401 V12.1.0*, June, 2013.

[112] ——, "Evolved universal terrestrial radio access network (e-utran) access," *Stage 2, Release 11, 3GPP Technical Specification, TS 36.300 V11.6.0*, June, 2013.

[113] E. Hossain, L. B. Le, and D. Niyato, *Radio resource management in multi-tier cellular wireless networks.* John Wiley & Sons, 2013.

[114] L. Song and J. Shen, *Evolved cellular network planning and optimization for UMTS and LTE*. CRC press, 2010.

[115] J. Acharya, L. Gao, and S. Gaur, *Heterogeneous Networks in LTE-advanced*. John Wiley & Sons, 2014.

[116] M. Tören and C. Çiflikli, "Peak-to-average-power-ratio (papr) reduction methods with wavelet transform in mimo-ofdm," *IETE Journal of Research*, pp. 1–7, 2017.

[117] R. C. Kizilirmak, "Non-orthogonal multiple access (noma) for 5g networks," in *Towards 5G Wireless Networks-A Physical Layer Perspective*. InTech, 2016.

[118] S. R. Islam, N. Avazov, O. A. Dobre, and K.-S. Kwak, "Power-domain non-orthogonal multiple access (noma) in 5g systems: Potentials and challenges," *IEEE Communications Surveys & Tutorials*, vol. 19, no. 2, pp. 721–742, 2017.

[119] K. Pahlavan and P. Krishnamurthy, *Principles of wireless networks: A unified approach*. Prentice Hall PTR, 2011.

[120] H. ElSawy, E. Hossain, and M. Haenggi, "Stochastic geometry for modeling, analysis, and design of multi-tier and cognitive cellular wireless networks: A survey," *IEEE Communications Surveys & Tutorials*, vol. 15, no. 3, pp. 996–1019, 2013.

[121] A. He, "Performance evaluation and enhancement in 5g networks: A stochastic geometry approach," Ph.D. dissertation, Queen Mary University of London, 2017.

[122] A. Omri, M. O. Hasna, and M. Nafie, "Effective area spectral efficiency for wireless communication networks with interference management," *EURASIP Journal on Wireless Communications and Networking*, vol. 2015, no. 1, p. 205, 2015.

[123] F. Capozzi, G. Piro, L. A. Grieco, G. Boggia, and P. Camarda, "Downlink packet scheduling in lte cellular networks: Key design issues and a survey," *IEEE Communications Surveys & Tutorials*, vol. 15, no. 2, pp. 678–700, 2013.

[124] R. D. Trivedi and M. Patel, "Comparison of different scheduling algorithm for lte," *International Journal of Emerging Technology and Advanced Engineering*, vol. 4, no. 5, pp. 334–339, 2014.

[125] A. Merwaday, S. Mukherjee, and I. Güvenç, "Capacity analysis of lte-advanced hetnets with reduced power subframes and range expansion," *EURASIP Journal on Wireless Communications and Networking*, vol. 2014, no. 1, p. 189, 2014.

[126] M. Al-Rawi, J. Huschke, and M. Sedra, "Dynamic protected-subframe density configuration in lte heterogeneous networks," in *Computer Communications and Networks (ICCCN), 2012 21st International Conference on*. IEEE, 2012, pp. 1–6.

[127] A. Morimoto, N. Miki, and Y. Okumura, "Investigation of inter-cell interference coordination applying transmission power reduction in heterogeneous networks for lte-advanced downlink," *IEICE transactions on communications*, vol. 96, no. 6, pp. 1327–1337, 2013.

[128] A. Merwaday, S. Mukherjee, and I. Güvenç, "Hetnet capacity with reduced power subframes," in *Wireless Communications and Networking Conference (WCNC), 2014 IEEE*. IEEE, 2014, pp. 1380–1385.

[129] H.-S. Jo, Y. J. Sang, P. Xia, and J. G. Andrews, "Heterogeneous cellular networks with flexible cell association: A comprehensive downlink sinr analysis," *IEEE Transactions on Wireless Communications*, vol. 11, no. 10, pp. 3484–3495, 2012.

[130] M. Ali, "Simulation and analysis of vehicular network capacity," Master's thesis, Institutt for telematikk, 2013.

[131] L. Liang, G. Y. Li, and W. Xu, "Resource allocation for d2d-enabled vehicular communications," *IEEE Transactions on Communications*, vol. 65, no. 7, pp. 3186–3197, 2017.

[132] R. Zhang, X. Cheng, and L. Yang, "Cooperation via spectrum sharing for physical layer security in device-to-device communications underlaying cellular networks," *IEEE Transactions on Wireless Communications*, vol. 15, no. 8, pp. 5651–5663, 2016.

[133] W. Wang, F. Xie, and M. Chatterjee, "Small-scale and large-scale routing in vehicular ad hoc networks," *IEEE Transactions on Vehicular Technology*, vol. 58, no. 9, pp. 5200–5213, 2009.

[134] S. Guo and X. Zhou, "Robust power allocation for noma in heterogeneous vehicular communications with imperfect channel estimation," in *2017 IEEE 28th Annual*

*International Symposium on Personal, Indoor, and Mobile Radio Communications (PIMRC)*. IEEE, 2017, pp. 1–5.

[135] C. Perfecto, J. Del Ser, and M. Bennis, "Millimeter-wave v2v communications: Distributed association and beam alignment," *IEEE Journal on Selected Areas in Communications*, vol. 35, no. 9, pp. 2148–2162, 2017.

[136] X. Wang, M. Tao, J. Mo, and Y. Xu, "Power and subcarrier allocation for physical-layer security in ofdma-based broadband wireless networks," *IEEE Transactions on Information Forensics and Security*, vol. 6, no. 3, pp. 693–702, 2011.

[137] B. Di, L. Song, Y. Li, and G. Y. Li, "Noma-based low-latency and high-reliable broadcast communications for 5g v2x services," in *GLOBECOM 2017-2017 IEEE Global Communications Conference*. IEEE, 2017, pp. 1–6.

[138] T. E. Bogale and L. B. Le, "Massive mimo and mmwave for 5g wireless hetnet: Potential benefits and challenges," *IEEE Vehicular Technology Magazine*, vol. 11, no. 1, pp. 64–75, 2016.

[139] Y. Wang, K. Venugopal, A. F. Molisch, and R. W. Heath, "Mmwave vehicle-to-infrastructure communication: Analysis of urban microcellular networks," *IEEE Transactions on Vehicular Technology*, vol. 67, no. 8, pp. 7086–7100, 2018.

[140] O. Afolalu and N. Ventura, "Robust power allocation for capacity maximization in 5g ultra-dense vehicular communication networks," in *2018 Southern Africa*

*Telecommunication Networks and Applications Conference (SATNAC)*. SATNAC, 2018, pp. 2–7.

[141] L. Wang, J. Yan, K. Yu, and D. Deng, "Research of d2d communications mode for 5g vehicular networks," in *2019 IEEE International Conference on Communications Workshops (ICC Workshops)*. IEEE, 2019, pp. 1–6.

[142] W. Sun, D. Yuan, E. G. Ström, and F. Brännström, "Cluster-based radio resource management for d2d-supported safety-critical v2x communications," *IEEE Transactions on Wireless Communications*, vol. 15, no. 4, pp. 2756–2769, 2015.

[143] L. Liang, J. Kim, S. C. Jha, K. Sivanesan, and G. Y. Li, "Spectrum and power allocation for vehicular communications with delayed csi feedback," *IEEE Wireless Communications Letters*, vol. 6, no. 4, pp. 458–461, 2017.

[144] T. Izydorczyk, F. M. Tavares, G. Berardinelli, M. Bucur, and P. Mogensen, "Performance evaluation of multi-antenna receivers for vehicular communications in live lte networks," in *2019 IEEE 89th Vehicular Technology Conference (VTC2019-Spring)*. IEEE, 2019, pp. 1–6.

[145] I. Gradshteyn and I. Ryzhik, "Table of integrals, series, and products. ed. by d. zwillinger and v. moll," 2015.

[146] W. Sun, E. G. Ström, F. Brännström, K. C. Sou, and Y. Sui, "Radio resource management for d2d-based v2v communication," *IEEE Transactions on Vehicular Technology*, vol. 65, no. 8, pp. 6636–6650, 2015.

[147] D. B. West *et al.*, *Introduction to graph theory*. Prentice hall Upper Saddle River, NJ, 1996, vol. 2.

[148] S. 3GPP, "3rd generation partnership project: Technical specification group radio access network: Study lte-based v2x servics: (release 14)," *TR 36.885 V2.0.0*, June. 2016.

[149] O. Afolalu and N. Ventura, "Joint implementation of massive mimo and noma techniques for improved capacity in 5g networks," in *2019 Southern Africa Telecommunication Networks and Applications Conference (SATNAC)*. SATNAC, 2019, pp. 26–31.

[150] C. Xu, Y. Hu, C. Liang, J. Ma, and L. Ping, "Massive mimo, non-orthogonal multiple access and interleave division multiple access," *IEEE Access*, vol. 5, pp. 14 728–14 748, 2017.

[151] J. A. Oviedo and H. R. Sadjadpour, "A new noma approach for fair power allocation," in *2016 IEEE Conference on Computer Communications Workshops (INFOCOM WKSHPS)*. IEEE, 2016, pp. 843–847.

[152] A. Gendia, M. Elsabrouty, and A. A. Emran, "Cooperative multi-relay non-orthogonal multiple access for downlink transmission in 5g communication systems," in *2017 Wireless Days*. IEEE, 2017, pp. 89–94.

[153] J. Huang, K. Peng, C. Pan, F. Yang, and H. Jin, "Scalable video broadcasting using bit division multiplexing," *IEEE Transactions on Broadcasting*, vol. 60, no. 4, pp. 701–706, 2014.

[154] J. Zeng, D. Kong, X. Su, L. Rong, and X. Xu, "On the performance of pattern division multiple access in 5g systems," in *2016 8th International Conference on Wireless Communications and Signal Processing (WCSP)*. IEEE, 2016, pp. 72–76.

[155] "3gpp-r1-162332 tsg ran, overview of new radio interface," CATT, Busan, Korea, 11-15, Apr. 2016.

[156] S. Parkvall, E. Dahlman, A. Furuskar, and M. Frenne, "Nr: The new 5g radio access technology," *IEEE Communications Standards Magazine*, vol. 1, no. 4, pp. 24–30, 2017.

[157] "3gpp tsg ran r1-162305, multiple access for 5g new radio interface," CATT, Busan, Korea, 11-15, Apr. 2016.

[158] "3gpp tsg ran r1-162306, candidate solution for new multiple access," CATT, Busan, Korea, 11-15, Apr. 2016.

[159] B. Wang, L. Dai, Z. Wang, N. Ge, and S. Zhou, "Spectrum and energy-efficient beamspace mimo-noma for millimeter-wave communications using lens antenna array," *IEEE Journal on Selected Areas in Communications*, vol. 35, no. 10, pp. 2370–2382, 2017.

[160] S. Ali, E. Hossain, and D. I. Kim, "Non-orthogonal multiple access (noma) for downlink multiuser mimo systems: User clustering, beamforming, and power allocation," *IEEE access*, vol. 5, pp. 565–577, 2016.

[161] X. Liu and X. Wang, "Efficient antenna selection and user scheduling in 5g massive mimo-noma system," in *2016 IEEE 83rd Vehicular Technology Conference (VTC Spring)*. IEEE, 2016, pp. 1–5.

[162] X. Lin, J. G. Andrews, and A. Ghosh, "Modeling, analysis and design for carrier aggregation in heterogeneous cellular networks," *IEEE Transactions on Communications*, vol. 61, no. 9, pp. 4002–4015, 2013.

[163] L. Liu, M. Li, J. Zhou, X. She, L. Chen, Y. Sagae, and M. Iwamura, "Component carrier management for carrier aggregation in lte-advanced system," in *2011 IEEE 73rd Vehicular Technology Conference (VTC Spring)*. IEEE, 2011, pp. 1–6.